Republic of Iraq
Ministry of Higher Education and Scientific Research
University of Baghdad/College of Engineering
Civil Engineering Department

PUNCHING SHEAR STRENGTH OF REACTIVE POWDER CONCRETE SLABS REINFORCED WITH CFRP BARS

A THESIS

SUBMITTED TO THE COLLEGE OF ENGINEERING OF

BAGHDAD UNIVERSITY IN PARTIAL FULFILLMENT OF

THE REQUIREMENTS FOR THE DEGREE OF DOCTOR

OF PHILOSOPHY IN CIVIL ENGINEERING

(STRUCTURES)

BY

SAMIR MOHAMMED CHASSIB

M.Sc. CIVIL ENGINEERING,2010

2016

بِسْمِ اللَّهِ الرَّحْمَنِ الرَّحِيمِ

﴿يَرْفَعِ اللَّهُ الَّذِينَ آمَنُوا مِنْكُمْ وَالَّذِينَ أُوتُوا الْعِلْمَ دَرَجَاتٍ﴾ ﴿11﴾

سورة المجادلة

Certification

I certify that this thesis entitled "***PUNCHING SHEAR STRENGTH OF REACTIVE POWDER CONCRETE SLAB REINFORCED WITH CFRP BARS***" was prepared by **Samir Mohammed Chassib** under my supervision at University of Baghdad / College of Engineering – Department of Civil Engineering, in partial fulfillment of the requirements for the Degree of Doctor of Philosophy in Civil Engineering (Structures).

Signature:

Name: ***Prof. Dr. Abdul Muttalib I. Said***

(Supervisor)

Date: / / 2016

In view of the available recommendation, I forward the thesis for debate by the examining committee.

Signature:

Name: ***Asst. Prof. Dr. Amir Farouk Izzet***

Head of the Civil Engineering Department

University of Baghdad

Date: / / 2016

Examination Committee Certificate

We certify that we have read the thesis titled **(*PUNCHING SHEAR STRENGTH OF REACTIVE POWDER CONCRETE SLABS REINFORCED WITH CFRP BARS*)** and as an examining committee, we examined the student **(Samir Mohammed Chassib**) in its contents and what is connect with it and that in our opinion it meets standards of a thesis for the Degree of Doctor of Philosophy in Civil Engineering (Structures).

Signature:
Name: Prof. Dr. Nazar K. Oukaili
Date: / /
(Chairman)

Signature:
Name: Asst. Prof. Dr. Ihsan A. S. Al- Shaarbaf
Date: / /
(Member)

Signature:
Name: Asst. Prof. Dr. Abbas A. Allawi
Date: / / 2016
(Member)

Signature:
Name: Asst. Prof. Dr. Alaa H. Al-Zuhairi
Date: / / 2016
(Member)

Signature:
Name: Asst. Prof. Dr. Hadi Nasir Ghadhban Al-Maliki
Date: / / 2016
(Member)

Signature:
Name: Prof. Dr. Abdul Muttalib I. Said
Date: / / 2016
(Supervisor)

Approved by the Dean of College of Engineering

Signature:

Name: *Prof. Dr. Ahmed A. M. Ali*

Acting Dean, Collage of Engineering / University of Baghdad

Date: / / 2016

To my parents …

To my wife . . .

To my sons …

With the best invocations and best wishes

To my brothers …

With entire my honorary and my respect

.

.

.

.

.

ACKNOWLEDGEMENTS

First and foremost, So much thanks to God for many graces and blessings.

The author would like to express grateful and deepest indebtedness to his supervisor **Prof. Dr. Abdul Muttalib I. Said**, for the considerable assistance, constructive suggestions, tireless guidance, and enduring patience throughout this work.

I would also like to express my superior gratefulness to my **parents** and my **wife** and my **brothers** for their great support during the period of this work.

An expression of gratitude is presented to the staff of engineering collage of misan university, **Asst. Prof. Dr. Addel Abdula Shuhaib , Dr. Abas Oda**, **Dr. Abdul Kaliq , Dr. Saad**, **Dr. Mustafa Shareef** for their assistance in preparing the work.

The author expresses greetings to my uncle **Prof. Dr. Majeed Chassib Hussain.**

Samir Mohammeh Chassib

2016

Abstract

New reinforcement type (carbon fiber reinforce polymer bars) with very high strength and advanced mechanical properties material have appeared in the last few decades. Reactive powder concrete (RPC) is a high strength, low porosity material with high cement and silica fume contents and steel fibers.

The present research can be divided into two parts as follow:

The first part is to study punching shear strength of reactive powder concrete reinforced by carbon fiber reinforced polymer bars. Fourteen reactive powder concrete slabs reinforced by CFRP bars were tested. The studied variables were CFRP bars as a flexural reinforcement, slab thickness, column area(loading area), and the arrangement of flexural reinforcement. The effect of the above mentioned parameters on deformation characteristics of tested slabs including deflection, concrete strains, failure angle, and ultimate loads are elaborately covered in this study. Tests illustrate that 8% increasing in flexural reinforcement (ρ_f), the ultimate punching shear capacity of RPC slab reinforced by CFRP bars increased by mean 18%, and by increasing the area of column about 20% the ultimate punching shear capacity of RPC slab is increased by average 14.5%

The second part is to analyze the slabs which are tested using nonlinear finite element program ANSYS Ver.11. RPC slabs are represented as smeared layers within the concrete elements (solid 65 element) depending on the volume fraction in the mortar. An acceptable agreement with the experimental tests is obtained in analysis of the tested slabs by ANSYS program. It is founded that, the ratio of numerical failure

load to experimental failure load is ranging from (0.82-1.04) and the ratio of maximum experimental deflection to maximum numerical deflection is (1.178). A numerical parametric study is conducted on the effect of increasing compressive strength of reactive powder concrete on the load-deflection behavior of slabs reinforced by CRFP bars.

LIST OF CONTENT

List of Tables

Notation

Most commonly used symbols are listed below, these and others are defined where they appear in the research.

SYMBOLS:-

Symbol	Description
b	*Perimeter of the loaded area*
b_o	*Perimeter of critical section*
c or r	*Side length of the square column*
d	*Effective depth of the slab*
Ec	*Modulus of elasticity of concrete*
Es	*Modulus of elasticity of steel*
f'c	*Concrete cylinder compressive strength*
fy	*Yield stress of steel reinforcement*
f_{cu}	*Concrete cube compressive strength*
Gs	*Strain gage factor*
Ks	*Size effect term*
L	*The span between centre to centre of column*
P	*Applied load*
p	*Applied pressure on the structure.*
P	*Applied force on the structure.*
R1	*Strain gage resistance*
Sp	*Superplasticizer*
Vu	*Ultimate punching strength of the slab*

W/C	*Water to cement ratio*
N.C.	*Normal Strength Concrete*
H.C.	*High Strength Concrete*
D5 , D7	*Two Depth Effecte (50 and 70) mm*
$ß_C$	*Ratio of long side to short side of the column*
eo	*Bridge voltage*
ε	*Strain*
ε_o	*Strain of maximum compressive strength of concrete*
ϕ	*Strength reduction factor*
ρ	*Steel reinforcement ratio*
ρ_b	*Balanced steel ratio*
ρ_{max}	*Maximum steel ratio at insure tension failure*
υ	*Poisson's ratio.*
$\Delta R1$	*Change in strain resistance*
ΔV	*change in voltage (reading of the increment of voltage*

ABBREVIATIONS:-

ACI	*American Concrete Institute.*
AFRP	*Aramid Fiber Reinforced Polymer.*
ANSYS	*Analysis System.*
ASTM	*American Society for Testing and Materials.*
B.S	*British Standards*
CFRP	*Carbon Fiber Reinforced Polymer.*
FRP	*Fiber Reinforced Polymer.*
FEM	*Finite Element Method*
GFRP	*Glass Fiber Reinforced Polymer.*
HM	*High Modulus of elasticity.*
HS	*High Strength.*
HSC	*High Strength Concrete*
NSM	*Near Surface Mounted.*
NSC	*Normal Strength Concrete*
RC	*Reinforced Concrete.*

Chapter One

INTRODUCTION

1.1 General

Reinforced concrete flat plates are chosen by architects and engineers because they provide an elegant form of construction. In addition, they simplify and speed up site operation, allow easy and flexible partitioning of space and reduce the overall height of building **[1]**.

A flat plate is a reinforced concrete floor which is usually with or without drops, supported generally without beams or girders **[2]**, plate(1-1)**[3]**. It acts as a plate and is divided into column strips and middle strips. The steel reinforcement runs continuously in both directions in order to bring its load directly to the supporting columns[4].

One of the major problems in such slabs is the punching shear failure at the connection between slab and column. Punching shear failure takes place when a plug of concrete is pushed out from the slab immediately above the column **[5]**.

Punching shear failure of plates is usually sudden and leads to progressive failure of flat plate structures. Therefore, caution is needed in the design of slabs and attention should be given to avoid the sudden failure condition. The catastrophic nature of the failure exhibited at the connection between slab and column has taken engineers attention. This area, Figure (1-2), becomes the most critical area as far as the strength of flat slabs is concerned due to the concentration of high bending moments and shear forces**[6]**, see plate (1-2)

plate(1-1): Flat Plate Construction[3].

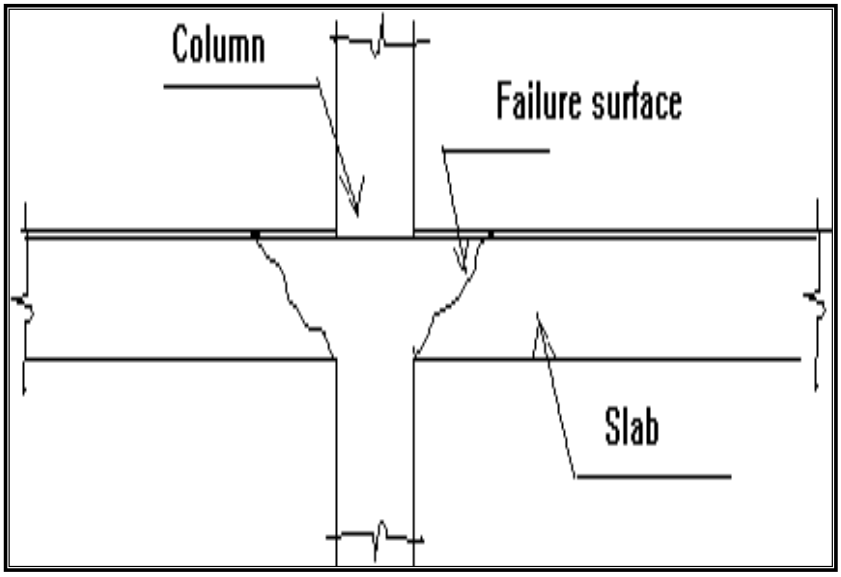

plate(1-2): Punching Failure Surfaces of Flat plate[6].

plate (1-3) shows a typical punching shear failure in Piper's Row Car Park, Wolverhampton, UK, 1997 (built in 1965).

Plate(1-3): Punching Shear Failure in Piper's Row Car Park, Wolverhampton, UK, 1997 (built in 1965)[7].

Punching shear failure can also occur during construction, when the weight of the fresh concrete and shoring are transferred to the adjacent lower stories. These construction loads are sometimes larger than the designed live loads. If the shoring is removed too early, the concrete strength of the lower story may not be sufficient, resulting in lower punching shear capacity **[7].**

1.2 Fiber Reinforced Polymer (FRP)

Recently, composite materials made of fibers embedded in a polymeric resin, also known as FRPs, have become an alternative to steel reinforcement for concrete structures. Because FRP materials are nonmagnetic and noncorrosive, the problems of electromagnetic interference and steel corrosion can be avoided. Additionally, FRP

materials exhibit several properties, such as high tensile strength, that make them suitable for use as structural reinforcement [8].

Fiber Reinforced Polymer (FRP) composite reinforcement was accepted in the construction industry as a promising substitute for conventional steel reinforcement in the past decade. In the early 1990's, the deteriorating state of the US infrastructure, particularly highway bridges due to corrosion, forced structural engineers to find alternative reinforcement types. The use of FRP composites as a replacement to steel reinforcement proved to be a promising solution to this problem. FRP found an increasing number of applications in construction either as internal or as external reinforcement for concrete structures [9].

As the name implies, FRP composites are materials made of fiber reinforcements, resin, fillers, and additives. The fibers exhibit high tensile strength and stiffness and are the main load carrying element. The resin offers high compressive strength and binds the fibers into a firm matrix. The additives help to improve the mechanical and physical properties as well as the workability of composites. The most common types of fibers used in advanced composites for structural applications are the glass (GFRP), aramid (AFRP), and carbon (CFRP). The GFRP is the least expensive but has lower strength and significantly lower stiffness compared to other alternatives. CFRP is the stiffest, most durable, and the most expensive one. AFRP has improved durability and excellent impact resistance. FRP reinforcement is available in different forms such as: bars, grids, pre-stressing tendons, and laminates to serve a wide range of purposes [9].

In relation to steel reinforcement, FRP bars show limited applicability due to the bending difficulties when producing either stirrups or shaped pieces. Such elements can be manufactured through molding in specific machineries. FRP bars are currently used as straight bars or grids to build slabs, walls and diaphragms [10].

1.2.1 Applications and Use

The material characteristics of FRP reinforcement need to be considered when determining whether FRP reinforcement is suitable or necessary in a particular structure. Table (1-1) lists some of the advantages and disadvantages of FRP reinforcement for concrete structures when compared with conventional, steel reinforcement.

1.2.2 Commercially Available FRP Reinforcing Bars

Commercially available FRP reinforcing materials are made of continuous aramid FRP (AFRP), carbon FRP (CFRP), or glass FRP (GFRP) fibers embedded in a resin matrix[9]. The bars have various types of cross-sectional shapes (square, round, solid, and hollow) and deformation systems (exterior wound fibers, sand coatings, and separately formed deformations). A sample of distinctly different FRP reinforcing bars is shown in Plate(1-4).

Table (1-1): Advantages and disadvantages of FRP reinforcement

Advantages of FRP reinforcement	**Disadvantages of FRP reinforcement**
High longitudinal tensile strength	No yielding before brittle rupture
Corrosion resistance (not dependent on a coating)	Low transverse strength
Nonmagnetic	Low modulus of elasticity (varies with type of reinforcing fiber)
High fatigue endurance (varies with type of reinforcing fiber)	Susceptibility of damage to polymeric resins and fibers under ultraviolet radiation exposure
Lightweight (about 1/5 to 1/4 the density of steel)	Low durability of glass fibers in a moist environment
Low thermal and electric conductivity (for glass and aramid fibers)	Low durability of some glass and aramid fibers in an alkaline environment
	High coefficient of thermal expansion perpendicular to the fibers, relative to concrete. May be susceptible to fire depending on matrix type and concrete cover thickness

1.2.3 History of Use

Up to the mid of 1990, the Japanese had the most FRP reinforcement applications, with more than 100 demonstration or commercial projects. FRP design provisions were included in the design and construction recommendations of the JSCE (1997b). In Asia, China has recently become the largest user of composite reinforcement for new construction in applications that span from bridge decks to underground works [9].

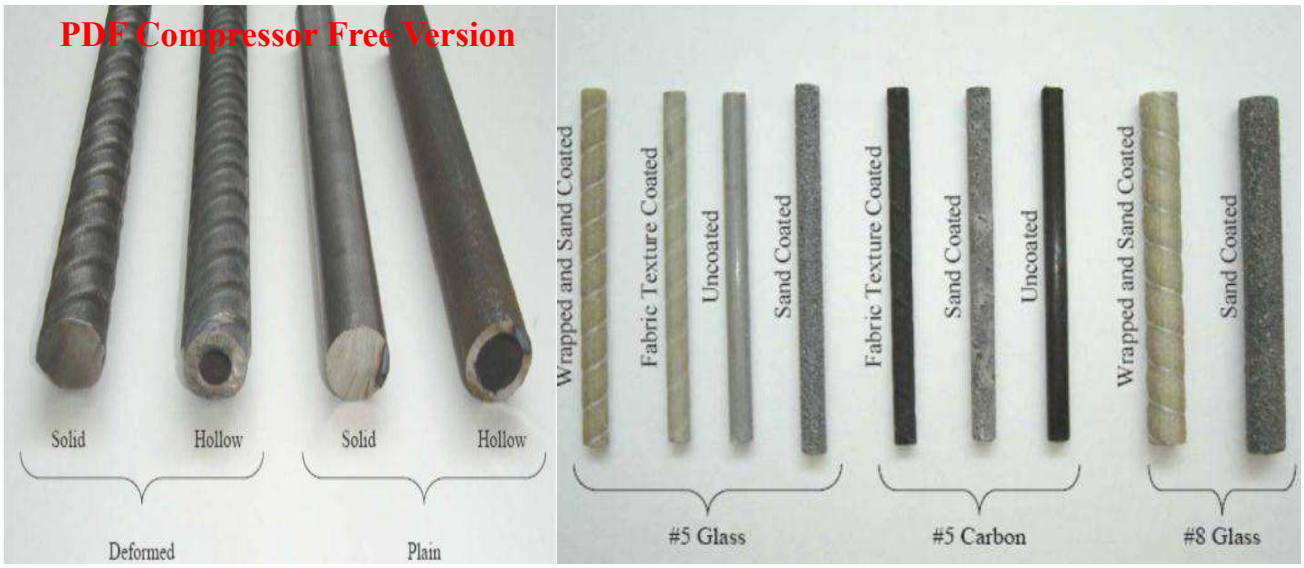

Plate (1-4) : Sample FRP Reinforcement Configurations[9]

The use of FRP reinforcement in Europe began in Germany with the construction of a prestressed FRP highway bridge in 1986. Since the construction of this bridge, programs have been implemented to increase the research and use of FRP reinforcement in Europe. The European BRITE/EURAM Project, "Fiber Composite Elements and Techniques as Nonmetallic Reinforcement," conducted extensive testing and analysis of the FRP materials from 1991 to 1996. More recently, EUROCRETE has headed the European effort to research and demonstration projects.

Canadian civil engineers had developed provisions for FRP reinforcement in the Canadian Highway Bridge Design Code and have constructed a number of demonstration projects. The Headingley Bridge in Manitoba included both CFRP and GFRP reinforcement. Additionally, the Kent County Road No. 10 Bridge used CFRP grids to reinforce the negative moment regions [9].

1.2.4 Carbon Fiber Reinforced Polymers (CFRP)

CFRP has become an increasingly notable material used in structural engineering applications over the past two decades. Studied in an academic context, CFRP has proved itself cost-effective in a number of field applications strengthening concrete, masonry, steel, cast iron, and timber structures. Its use in industry can be either for retrofitting to strengthen an existing structure or as an alternative reinforcing (or prestressing material) instead of steel from the outset of a project. Applied to reinforced concrete structures for flexure, CFRP typically has a large impact on strength, but only a moderate increase in stiffness (perhaps a 10% increase), because the material used in this application is typically very strong (3000 MPa ultimate tensile strength, more than 10 times mild steel) but not particularly stiff (150 to 250 GPa, a little less than steel, is typical). As a consequence, only small cross-sectional areas of the material are used. Small areas of very high strength but moderate stiffness material will significantly increase strength, but not stiffness [10].

CFRP can also be applied to enhance the shear strength of reinforced concrete by wrapping fabrics or fibers around the section to be strengthened. Wrapping around sections (such as bridge or building columns) can also enhance the ductility of the section, greatly increasing the resistance to collapse under earthquake loading. Such 'seismic retrofit' is the major application in earthquake-prone areas, since it is much more economic than alternative methods [11].

Much researches continue to be done on using CFRP both for retrofitting and as an alternative to steel as a reinforcing or prestressing material. Some are concerned about the brittle nature of CFRP, in contrast to the ductility of steel. Though design codes have been drawn up by institutions such as the American Concrete Institute, there remains some hesitation among the engineering community about implementing these alternative materials. In part, this is due to a lack of standardization and the proprietary nature of the fiber and resin combinations on the market [11].

1.3 Objective of the Study

CFRP systems have been increasingly used as materials for strengthening or main reinforcement of concrete structures, and the development which is happened in concrete such as reactive powder concrete for these reason, it is become necessary to study these materials. Punching shear strength of reactive powder concrete slab reinforced with CFRP bars is studied.

The main objectives of the present study are:

1-Experimental study and comparing the performance of reactive powder concrete slab reinforced with CFRP bars with the ACI 440-1R provision and other research works .

2- Study the effect of CFRP bars as a flexural reinforcement, slab thickness, column dimensions, and the arrangement of flexural reinforcement on punching shear strength of the RPC slabs.

The establishment of a methodology is required for applying computer modeling of reactive powder concrete slab reinforced by CFRP bars. So,

finite element models will be utilized to simulate the behavior of these slabs by using three-dimensional finite element analysis, (ANSYS-11) program.

1.4 Thesis Layout

In order to get an overview of this thesis the chapters are listed below with a short description of the content:

Chapter one, includes introduction and some general knowledge about punching shear of reactive powder concrete slab reinforced with CRFP bars. Chapter two, presents literature survey and a brief review of available related researches and works that deal with the study and analysis of punching shear of slab. Chapter three present the experimental work of reactive powder concrete and the parameters which are studied and the tested slabs with the mechanism of test and the instrumentation. Chapter four explains and discusses the results of tested slab. Chapter five presents the finite element model for the tested slab. Chapter six presents a modeling and analysis methodology and discussion of theoretical results and compared one case of study with the same case of experimental results. Chapter seven presents a conclusions of this work and recommendations for future work.

Chapter Two

REVIEW OF LITERATURE

2.1 General

Reinforced concrete slabs on columns were initially developed in U.S. and Europe at the beginning of the 20th century. Their designs typically included large mushroom-shaped column capitals to facilitate the local introduction of forces from the slab to the column. In 1950s, flat slabs without capitals started to become prevalent. Because of their simplicity, both for construction and for use (simple formwork and reinforcement, flat soffit allowing an easy placement of equipment, and installation underneath the slab), they have become very common for medium height residential and office buildings as well as for parking garages[12] .

Flat plate slabs exhibit higher stress at the column connection and most likely fail due to punching shear rather than flexural failure, especially when a high reinforcement ratio is used. The punching shear failure is characterized by the crushing of concrete in the column periphery before the steel reinforcement reaches the yield strain. This type of failure is not desired for structural engineering systems and should be avoided in the design of concrete structures [13].

An essential problem in the design of flat plate reinforced concrete floors is the slab-column connection, a region where the stress concentration due to high moment and shears is very high. But away from the column vicinity, the stress concentration decreases rapidly due to the decrease of the radial moments until they become zero at a distance of (0.2 L to 0.22L) from the column where (L) denotes the span length between the columns[14].

Reinforcing against shear failure is traditionally accomplished by providing reinforcement either at an angle or laterally to the main flexural reinforcement.

This chapter is concerned with the literature related to the behavior of slabs

failing by punching, factors that affect shear strength of slab-column connections in flat plate construction, types of punching shear failure, methods of increasing the punching shear strength, and researches concerning the punching shear strength with and without shear reinforcement. Punching shear and flexural strengths of fiber reinforced concrete flat slabs.

2.2 Types of Slabs:

In reinforced concrete construction, slabs are used to provide flat, useful surfaces. A reinforced concrete slab is a broad ,flat plate, usually horizontal, with top and bottom surfaces parallel or nearly so. It is supported by reinforced concrete beams (and is usually cast monolithically with such beams), by masonry or reinforced concrete walls, by structural steel members, directly by columns, or continuously by the ground[15].

Slabs may be supported on two opposite sides only ,Figure(2-1-a) in which case, the structural action of the slab is essentially one-way, and the loads carried by the slab are in the direction perpendicular to the supporting beams. There may be beams on all four sides, as shown in Figure(2-1-b), so that two-way slab action is obtained. Intermediate beams may be provided, as shown in Figure(2-1-c). If the ratio of length to width of one slab panel is larger than about (2), most of the load is carried in the short direction to the supporting beams and one-way action is obtained in effect, even though supports are provided on all sides[15].

Concrete slabs may in some cases be carried directly by columns, as shown in Figure(2-1-d), without the use of beams or girders. Such slabs are described as Flat plates[16]. Flat slab construction, shown in Figure(2-1-e), is also beamless but incorporates a thickened slab region in the vicinity of the column and often employs flared column tops.

Both are means to reduce stresses due to shear and negative bending around the columns. They are referred to as drop panels and column capitals, respectively. Closely related to the flat plate slab is the two-way joist, also known as a grid or

waffle slab, Figure(2-1-f). To reduce the dead load of solid-slab construction, voids are formed to resist moments and shears better in these areas.

In addition to the column-supported types of construction, many slabs are supported continuously on the ground, as for highways, airport runways and warehouse floors. In such cases, a well-compacted layer of crushed stone or gravel is usually provided to ensure uniform support and to allow for proper sub-grade drainage.

Reinforcing steel for slabs is primarily parallel to the slab surfaces. Straight bar reinforcement is generally used, although in continuous slabs, bottom bars are sometimes bent up to serve as negative reinforcement over the supports. Welded wire reinforcement is commonly employed for slabs on the ground. Bar or rod mats are available for the heavier reinforcement sometimes needed in highway slabs and airport runways. Slabs may also be prestressed using high tensile strength strands.

Reinforced concrete slabs of the types shown in Figure(2-1) are usually designed for loads assumed to be uniformly distributed over one entire slab panel and bounded by supporting beams or column centerlines. Minor concentrated loads can be accommodated through two-way action of the reinforcement(Two-way flexural steel for Two-way slab systems or One-way flexural steel plus lateral distribution steel for One-way flexural steel plus lateral distribution steel for One-way systems). Heavy concentrated loads generally require supporting beams.

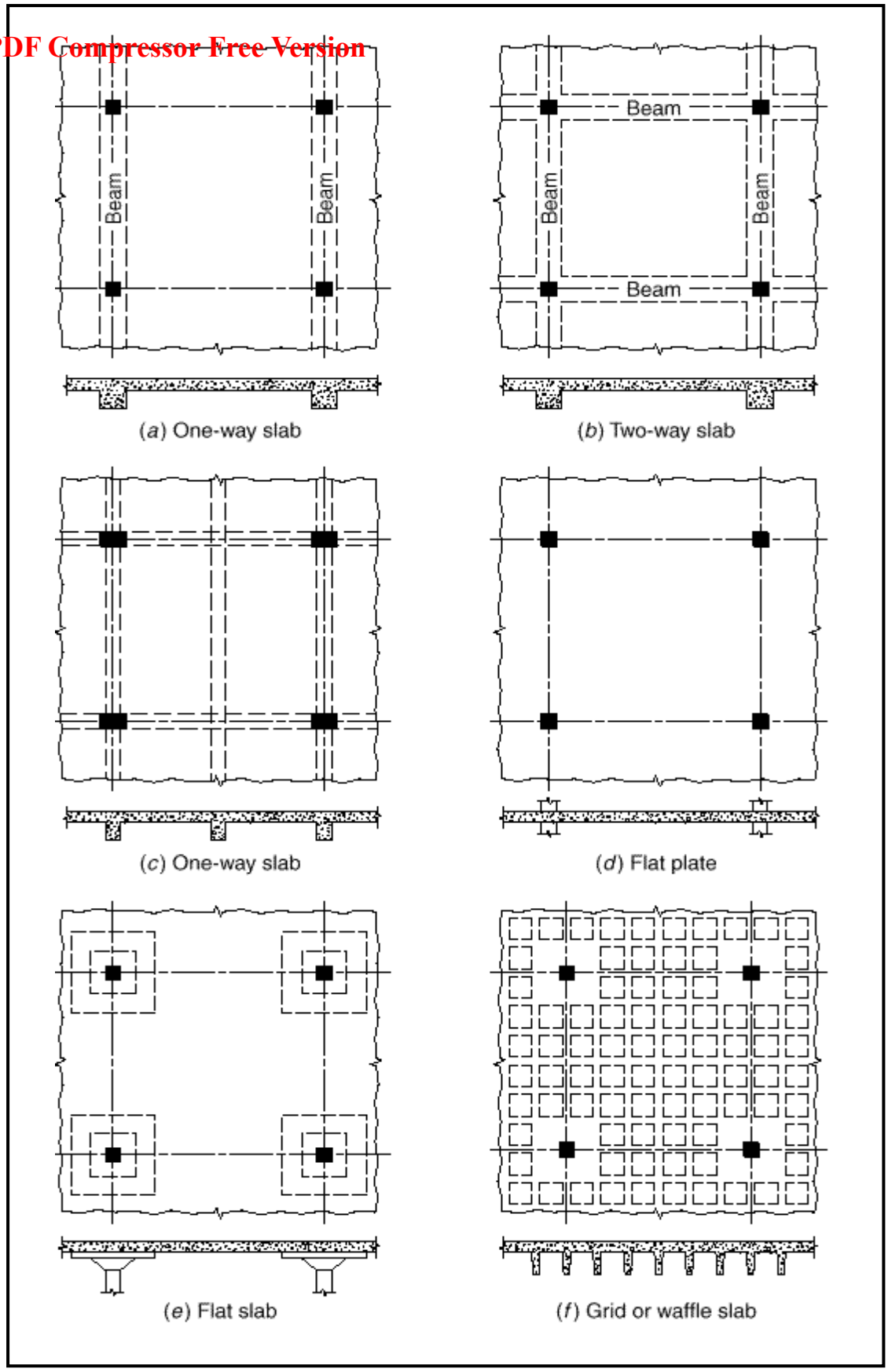

Fig.(2-1):Types of structural slabs[15].

2.3 Flexural Failure Mechanism

Yield line theory was developed primarily by Johansen[16] in 1948 and used for the ultimate flexural strength of reinforced concrete slabs. This theory can be applied to slabs subjected to concentrated loads, provided that the flexural capacity is reached before a punching shear failure can take place. Plate (2-2) shows the typical slab failing in flexural.

This predication has been verified later by many experimental tests. Test results show that the calculated flexural load by the yield line analysis is normally underestimated by about (10-20%) because of the effects of the tensile membrane action accompanying the large slab deflections and extension of the slab past the supporting columns. For this reason, designers can use the yield line theory in calculating the ultimate flexural strength of slab-column connections with good confidence as it gives a conservative estimate of strength.

The critical factors that must be considered when using yield line analysis are the distribution of the slab reinforcement, the ductility of the slab, and the conditions at the ultimate load[17].

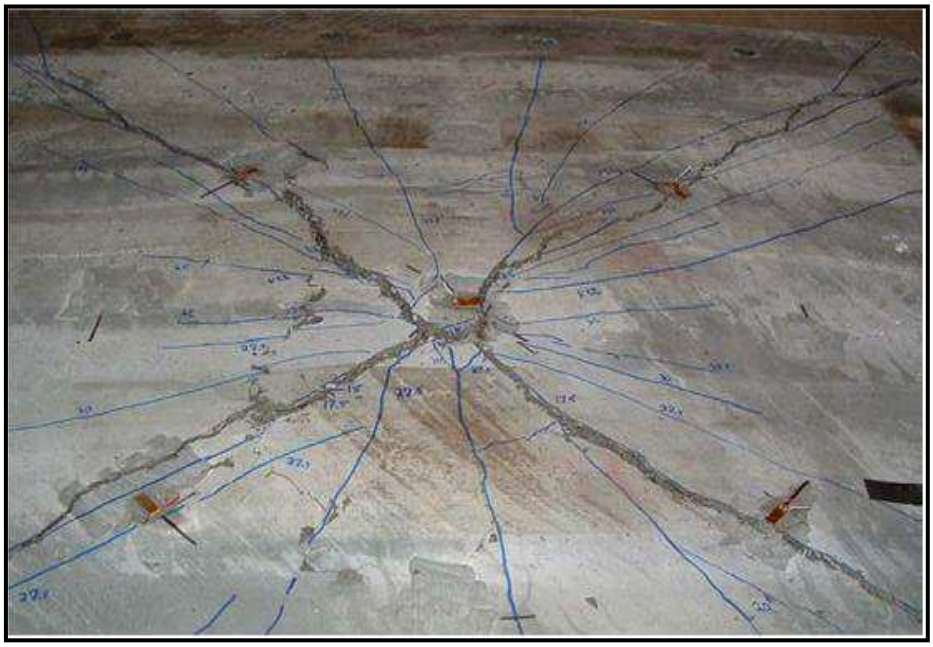

Plate (2-2): Typical slab failing in flexure[16].

2.4 Previous Researches on Punching Shear Resistance of Two-Way Slab

In the early 1900's, *Morsch* [18] of Germany made significant contributions to the understanding of the behavior of reinforced concrete structures with his work on shear. In his 1906 and 1907 papers, Morsch presented an explanation of diagonal tension and proposed the following expression for the nominal shearing stress, v:

$$v = \frac{V}{bd} \qquad \text{.....Eq.(2-1)}$$

where

V : is the applied shear force.

b : is the perimeter of the loaded

d : is the effective depth.

The shear stress from Morsch′s equation is calculated along the perimeter,(b). of the loaded area. Hence, for a uniformly loaded slab, the shear stress was evaluated around the perimeter of the column.

In (1913) *Talbot* [19], published a report of 114 wall footings and 83 column footings tested to failure. Twenty of these footings failed in shear. They exhibited failure surfaces that were at an angle of approximately 45° to the vertical and that extended from the bottom face of the slab at its intersection with the column, reaching the level of the reinforcement at a distance d from the column face. From these test findings, Talbot concluded that it would be reasonable to take the vertical section located at a distance (d) from the face of the column as the critical shear section. He proposed the following expression for the nominal shearing stress, v. which is similar to Morsch's equation, except that the critical section was moved from the face of the column to a distance (d) from the face.

Therefore, b is now equal to 4(c+2d).. giving:

$$v = \frac{V}{4(c+2d)jd} \quad \text{..... (psi) Eq.(2-2)}$$

where c = side dimension of square column.

jd = internal moment arm of slab.

Harris, [20], also recognized that increased percentages of flexural reinforcement resulted in an increase in the shear strength of the slabs.

In (1933), *Graf* [21], studied the shear strength of slabs loaded by concentrated loads near the supports. From the test findings, he concluded that the shear capacity decreases as the load is moved away from the supports and that flexural cracking has some influence on shear strength.

In (1948), *Richart* [22], presented a report on a number of reinforced concrete footing tests. He concluded that the high tensile stresses in the flexural reinforcement lead to extensive cracking in the footings. This cracking reduces the shear strength resulting in the footings failing at lower shearing stresses than expected.

In the years(1952-1954), *Elstner* and *Hognestad* [23], reported tests of 34 slabs, (1.83m) square slab and (152.4mm) thick which were supported along all four edges. They exhibited punching shear modes of failure. In two of these slabs, 50%of the flexural reinforcement was concentrated over the column. They then compared these two slabs with two others that were similar except that the flexural reinforcement was uniformly distributed throughout the width of the slabs. They concluded that concentrating the flexural reinforcement near the column does not result in any increase in the punching shear strength of the slab specimens. Also, increasing compression reinforcement has little effect on ultimate capacity. An increase in column size is found to increase the stiffness and decrease deflection and here, increase the ultimate capacity.

The major variables were concrete strength, amount of flexural tension and compression reinforcement and size of column. The following empirical formula was derived from test result:

$$vu = \frac{Vu}{7/8 b_o d} = \left(0.035 + \frac{0.07}{Vu/V_{flex}}\right) f'c + 130 \quad \ldots\ldots\ldots\ldots \text{(psi)} \quad \text{Eq.(2-3)}$$

where: Vu and Vflex are the ultimate shear and flexural capacity; f'c is the cylinder compressive strength, (b_o) is the perimeter of the loaded area and (d) is effective depth of the slabs.

In 1957,*Whitney* [24], concluded that the main important variables which influence the ultimate shear strength are size and spacing of bars, strength of steel reinforcement and concrete, column size, position of loading and depth to span ratio of the slab.

In 1961 *Moe* [5], tested forty-three (1.83m) square slabs of (150mm) thickness. Moe's principal variables are: effect of opening near the face of the column, effect of concentration of tensile reinforcement in narrow bands across the column, column size, eccentricity in applied load and effectiveness of special types of shear reinforcement. Some of the most important conclusions obtained by Moe are:

1. The shear strength of slabs and footings depend on flexural strength.
2. Inclined cracks develop in the slabs at loads as low as 50% of the ultimate.
3. Concentration of flexural reinforcement in narrow bands across the column does not increase the shear strength. However, such reinforcement increases the flexural rigidity of the test slab, and also decreases deflections.
4. The ultimate shear strength of slabs and footings is predicted with a good accuracy by the formula:

$$vu = \frac{Vu}{b_o d} = [15(1 - 0.075\frac{c}{d}) - 5.25\phi^\circ]\sqrt{f'c} \quad \ldots\ldots\ldots\ldots\ldots\ldots \text{(psi)} \quad \text{Eq. (2-4)}$$

where:

b_o = perimeter of the loaded area

d= effective depth of slab

c= side length of square loaded area

V_u= ultimate shear force

V_{flex}= ultimate shear force if flexural failure has occurred

$\phi^o = V_u/V_{flex}$

5. The critical section governing the ultimate shear strength of slabs and footings should be measured along the diameter of the loaded area.
6. Some increase in shear strength can be obtained by shear reinforcement.
7. Concentration of flexural reinforcement in narrow bands across the column does not increase the flexural rigidity of the tests slabs, and also increase the load at which yielding begins in the tension reinforcement.

In 1966, *Yitzhaki* [6], presented a correlation between the punching resistance and flexural strength of slabs. He showed that punching strength depends mainly on the flexural reinforcement strength (fy) and concrete strength (f'c). The nominal shearing stress at a distance (d) from the face of the column can be calculated from the following equation in (imperial units):

$$\frac{Vu}{b_o d} = (149.3 + 0.164\rho fy)\left(1 - 1/2\rho\frac{fy}{f'c}\right) \quad \text{.....Eq. (2-5)}$$

where: b_o : perimeter of critical section = 4c + 8d

The constants of the above equation are evaluated from available test data.

In 1967, *Long* and *Bond* [25], tested 5 square slabs. A theoretical analysis of the punching shear problem for round slabs with no shear reinforcement was made.

They concluded that punching strength in slab is strongly dependent on the flexural strength especially for slabs with a realistic amount of reinforcement. Another conclusion was reached in which the concentration of flexural

reinforcement within the column strip has no effect on increasing the punching shear capacity of slab-column connection.

In 1970, *Herzog* [26], derived a simple empirical formula to estimate the punching shear strength of slabs. He analyzed the results of fourteen previous investigations, and the main variables taken into consideration were flexural reinforcement ratio (ρ), steel reinforcement characteristics (fy) and the concrete compressive strength (f'c). The results of all tested slabs led up to the following equation:-

$$\frac{V}{\sqrt{f'c}} = (2.64 + 0.00477\rho fy) \leq 6.3 \quad \text{.....(psi) Eq. (2-6)}$$

The nominal shearing stress was calculated as a distance d/2 from face of column, as follows:-

$$v = \frac{Vu}{4(c+d)d} \quad \text{.....Eq. (2-7)}$$

In 1975, *Long* [27], derived formula to predict the punching shear capacity of slabs at interior column. The derived formula represented a significant improvement over previously reported formula which was mostly empirically based. The predicted load for a slab is taken from the following equation (in imperial units):

$$Vu = \frac{16(c+d)d(100\rho)^{0.25}}{(0.75+4\frac{c}{L})}\sqrt{f'c} \quad \text{.....Eq.(2-8)}$$

where: L is the span between center to center of column in the above equation and the critical section was assumed to be at distance (d/2) from column face.

In 1979, *Hawkins and Mitchell* [28], reported that in a punching shear failure, the shear strength is dependent on the flexural capacity of the slab and that it will decrease if there has been significant yielding of the flexural reinforcement.

In 1981, *Regan* [29], developed an equation to calculate the punching shear capacity of reinforced concrete slabs. *Regan's* shear perimeter for rectangular column was a rounded rectangle located (1.25d) out from the column face, for circular column it was the circular perimeter located (1.25d) from the column face.

$$Vu = KaKscKs(\rho \times f'c)^{\frac{1}{3}} \times d\left(\sum c + 7.85d\right) \quad \text{.....Eq.(2-9)}$$

where:

Vu: ultimate shear force (kN)

Ka: 0.13 for normal density

Ksc: 1.15× [4π×column area /(column perimeter)^2]$^{1/3}$

Ks: size effect term (300/d)$^{1/4}$ (SI unit)

ρ: steel ratio

f'c: concrete strength (MPa or N/mm^2)

d: effective depth of slab (mm)

∑c: perimeter of column

In 1987, *Rankin and Long* [30], proposed a method for determining the punching shear strength of conventional slab-column connections based on rational concepts of the modes of failure of these connections.

They proposed the following punching shear strength expression:

$$p_{vs} = 1.66\sqrt{f'c}\ (c + d)\ d\ \sqrt[2]{100\rho} \quad \text{(N / mm) .....Eq.(2-10)}$$

where:

f′c is the compressive strength in MPa.

c is the dimension of square column.

d is effective depth of slab.

ρ is the reinforcement ratio, As/bd, and,

Pvs is the punching shear strength.

In 1990, *Gardner* [31], reported tests of thirty circular slabs. The variables in Gardener's tests are concrete strength, steel ratio and slab thickness. He also made comparison with some researchers and code provision on punching shear capacity. *Gardener* concluded that the steel ratio in the region (3d) from the column should be of the order of 0.5 percent in each direction, and the spacing should be equal to the effective depth. He also found that the cubic root relationship between shear strength and concrete strength is preferable to the square root relationship

In 1992, *Alexander* and *Simmonds* [32], studied the effects of concentrating the reinforcement near the column on the shear strength of slab specimens. They concluded that all the tests exhibit the classical pyramid shaped punching shear failure, but several tests actually have loss of anchorage. The anchorage failures were not distinguishable from punching shear failures on the basis of external appearances. They suggested that many of the punching shear failures reported in the previous tests were actually bond failures. They believed that investigators such as *Moe [5], EIstner* and *Hognestad* [23],wrongly diagnosed the mode of failure in many of their tests and that it prevented them from observing an improvement in the shear capacity of slabs with the concentration of the flexural reinforcement near the column.

British Standard [33], (BS 8110-1997), the design of punching shear for concrete slab with compressive strength (fcu) not greater than (40 MPa) should be based on:

$$vck = 0.79\sqrt[3]{100\rho}\sqrt[3]{fcu/25}\sqrt[4]{400/d} \quad \text{.....Eq. (2-11)}$$

u=4(c+3d) for square loaded area

$$Vu = vck.u.d \le 1.2\sqrt{fcu}.u.d \quad \text{.....Eq. (2-12)}$$

where: (100ρ) should not be taken as greater than (3);

($\sqrt[4]{400/d}$) should not be taken as less than (0.67) for members without shear reinforcement; and not be taken as less than (1) for members with shear

reinforcement providing a design shear resistance of (0.4 N/mm^2).

In 2001, *Tuan* [7], compared the value of punching shear calculated from Concrete Structure Standard of Australia (AS-3600), 1994, with twenty-nine tests results from four research studies. A considerable variety of concrete strengths, slab reinforcement ratio and slab depth is represented in these four approaches. Tuan concluded that the use of high strength improves the punching shear resistance allowing higher forces to be transferred through the slab-column connection. He also found that the comparison of experimental results shows that AS-3600 formula is applicable up to 100 MPa.

ACI Code (318-11), [34], design of slabs for two-way action without shear reinforcement should be based on:

$Vu < \varphi\ Vc$ ……Eq.(2-13)

$Vu = wu \times A$ ……Eq.(2-14)

where: Vu: Factored shear force at section considered

φ : strength reduction factor(0.85)

wu = 1.2 × (dead load) +1.6(live load)

A: shaded area as in Figure(2-3).

While: Vc: should be the smallest of:

$$Vc = (1 + \frac{2}{\beta c})\frac{\sqrt{f'c}\, b_\circ d}{6} \quad \text{(SI)} \quad \text{…… Eq.(2-15)}$$

$$Vc = (2 + \frac{\alpha_s d}{b_\circ})\frac{\sqrt{f'c}\, b_\circ d}{12} \quad \text{(SI)} \quad \text{……Eq.(2-16)}$$

$$Vc = \frac{1}{3}\sqrt{f'c}\, b_\circ d \quad \text{(SI)} \quad \text{…… Eq.(2-17)}$$

where: b_o: perimeter of the critical section at distance d/2 from face of column, as in plate (2-3).

$\beta_c = \frac{\text{long side of column}}{\text{short side of column}}$

α_s= 40 for interior column

= 30 for edge column

= 20 for corner column

ACI code, (440.1R-06)[35], design of slabs for two-way action reinforced by FRP bars should be based on:

$$Vc = \frac{5K}{2} 0.33\sqrt{fc'}bod \quad \text{..... Eq.(2-18)}$$

where: b_o: perimeter of the critical section, as in Fig. (2-6).

d: effective depth of slab (mm).

K= $\sqrt{2\rho_f n_f + (\rho_f n_f)^2} - \rho_f n_f$

In 2004,El-Gamal et al[36], proposed a new equation for punching shear strength of two way slab reinforced with FRP bars:

$V_c = v_{c,ACI-318} \times \alpha \times (1.2)^N$ .....Eq.(2-19)

where:

N is the continuity factor taken as:

= 0 (for one panel slabs).

= 1 (for slab continuous along one axis).

= 2 (for slabs continuous along their two axes).

α : is a new parameter which is a function of the flexural stiffness of the tensile reinforcement (ρE), the perimeter of the applied load, and the effective depth of the slab was introduced.

$\alpha = 0.5\ (\rho E)^{1/3}\ (1+8d/b_0)$

where: ρ and E are the reinforcement ratio and modulus of elasticity (in GPa) of the main bottom reinforcement, respectively.

In 2003, *Zhang* [3], studied the effect of concrete strength, reinforcement ratio, slab depth and column size on the punching shear strength of 17 high strength

concrete slabs. The test results indicated that shear strength depends on a power of the concrete compressive strength (f'c) that is less than 0.5 and more like a cubic root relationship. The assumption that the critical perimeter is at a distance of 0.5 d from the loaded area is reasonable, and the reinforcement ratio has a considerable effect on the shear strength especially when the slab depth is at a high level. Also, it was concluded that as the column size is increased the punching shear resistance increases too.

In 2005, *Ahmed* [37], studied the punching strength of HSC panels through an experimental program consisting of 27 high and normal strength concrete slabs. The test data from the experiment were analyzed and divided into three series. The three series were primarily concerned with the effects of three variables on the punching strength of HSC slabs: the concrete strength, the slab depth and the column size and shape. He concluded that there is an increase in shear strength with the increase of compressive strength and HSC slabs have reduced deflections at all loading stages over the ordinary concrete slabs. Also, he found that the size of the failure zone decreases by decreasing compressive strength and the size of the failure zone increases by increasing column dimension ratio.

In 2007,*Muhammed N.J.*[38], studied the post – heating behavior of normal strength concrete (NSC), high strength concrete (HSC) and lightweight concrete (LWC) slabs and assessing the residual flexural and punching shear strengths of two-way slab specimens. she tested Twenty two reduced scale reinforced concrete slab specimens with cube compressive strengths of 50, 94 and 37 N/mm^2 representing NSC, HSC and LWC respectively, with two different steel ratios 0.002 and 0.005 for flexure and punching testes respectively. The effects of concrete type and structural failure type when slabs are exposed to different temperature levels are investigated. Results indicate reduction of strengths with exposure to high temperature. The behavior of HSC slab specimens is more brittle than the NSC and LWC slab specimens, and the behavior of LWC slab specimens

is the flattest at all temperature levels. Also, the results show that when the temperature reaches **(700 ^{0}C)**, the type of failure is changed from the expected punching shear failure to flexural failure in both slab specimens of NSC and HSC, but for the LWC slab specimen, the type of failure remains punching shear at this high temperature.

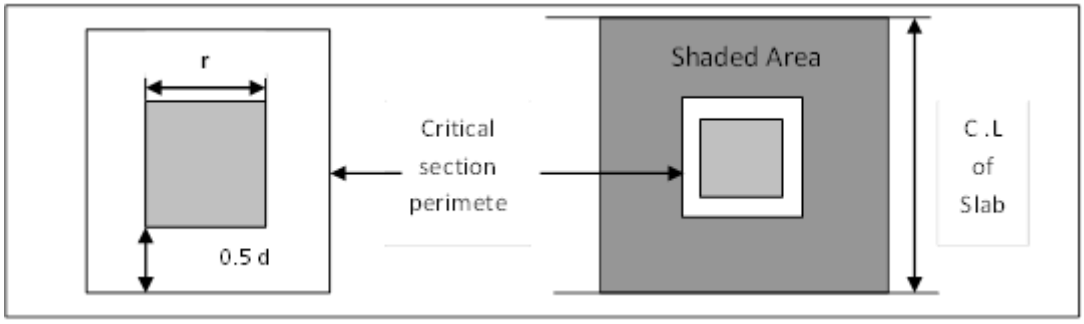

Plate (2-3):Critical section for punching shear and area of shear force [34].

2.5 Factors Influencing the Punching Shear Resistance and Behavior of Flat Plate Systems

2.5.1 Concrete Strength

Research has been done to find the relation between the concrete compressive strength, f'c and the shear strength. *Moe* (1961) [5],was the first to conclude that the shear strength is related not to f'c but to $\sqrt{f'c}$. *Moe* explained that shear strength is primarily affected by concrete tensile splitting strength which is often assumed to be proportional to $\sqrt{f'c}$.

The compressive strength of concrete has a large influence on the punching shear strength and behavior of flat slabs . The shear strength of flat slab was assumed to be proportional either to the square root or to the cubic root of the concrete compressive strength. The former is adopted by *ACI318-11* [34] and *AS3600* [39]while the latter by *BS8110* [33] and *CEB-FIP MC90*[40].

However, this power relation may be higher for slabs with small shear span-to-

depth ratio, implying a large influence of the concrete compressive strength on the punching shear strength. When testing punching shear on a column footing , it was found that the punching shear strength is proportional to concrete compressive strength to the power of (0.76).

Regan and *Braestrup* [41], 1985, concluded that both the cubic and the square root dependencies are adequate since the variability of these predictions is also influenced by differences in the dependence upon other factors such as reinforcement ratio, slab depth and position of shear perimeter.

For normal strength concrete, when a large number of circular flat plates with the concrete strength from 14 to 56 MPa was investigated experimentally, *Gardner*[31], found that the cube-root relationship between shear strength and concrete strength is preferable to the square-root relationship. The former results were in a better correlation with the experimental data. The cube-root relationship between shear strength and concrete strength was also recommended for high strength concrete by *Marzouk* and *Hussein* [42]. Moreover, as the concrete strength increases beyond (40-50 MPa), most current approaches become less conservative and even unsafe in some cases[7]. This is partly because for high strength concrete, the relation between the shear resistance of a member and the strength of concrete depends upon the characteristic of the aggregate [40]. If the aggregate fractures at a crack, leaving smooth cracked surfaces, the shear resistance may be below the predicted values which are based upon results for normal strength concrete. Besides, the increasing strength of concrete also brings about other changes:

1. The ultimate deflection and deformation as well as the rotation capacity and moment capacity increase significantly when high-strength is used, especially for specimens subjected to high moments.
2. The displacement ductility, the rotation ductility, and the energy-absorption capacity increase significantly when high-strength concrete is used.

2.5.2 Slab Depth

The ultimate punching capacity is directly proportional to the square of effective depth[43]. Thus, small absolute variations in effective depth would produce significant differences in punching shear resistance. This highlights the importance of accurate placement reinforcement in practice. However, as increasing the slab thickness will increase the dead load accordingly, net gains in strength, obtained by increasing the slab thickness, might be less than the proportionality to the square of effective depth. Where dead load makes up a substantial portion of the total load, these net gains are only approximately linearly related to effective depth [44].

2.5.3 Size Effect of Slab

Size effect is one of the salient aspects of fracture mechanics. *Bazant* and *Cao* (1987) [45], noted that the load-deflection diagram of a slab without stirrups exhibits a gradual decline rather than a plastic yield plateau. The larger the slab thickness, the steeper the post-peak decline of the load-deflection diagram, thus the punching shear behavior of thinner slabs is closer to plasticity, and that of thicker slabs is closer to linear elastic fracture mechanics.

In (1999), *Ozbolt* and *Vocke* [46],discussed the application of the nonlinear FE-code MASA to the simulation of the punching shear failure of flat slabs without shear reinforcement and it was found that the punching failure exhibits a pronounced size effect, i.e. increasing the slab thickness leads in the calculations to decrease the nominal shear capacity of the slabs.

2.5.4 Flexural Reinforcement

Addition of steel reinforcement increases the ultimate punching capacity, *Marzouk* and *Hussein*[42] ,1991, noticed an increase in the ultimate applied load by 2.4 times as the reinforcement ratio is increased from 0.49% to 2.37% for slab of 120 mm thickness. Similar capacity enhancement of 1.8 times was also

observed for slab thickness of 150 mm when the steel ratio was varied from 0.64% to 2.33%. However, ductility is adversely affected by the increase in steel reinforcement ratio. Increasing the reinforcement ratio from 1.1% to 2.3% and from 1.2% to 2.4% for slab thickness of 150 and 120 mm decreases the ductility by 46% and 22%, respectively.

In 1992, *Kuang* and *Morley*[47], investigated the influence of the addition of steel reinforcement on ultimate punching capacity. It was found that punching shear strength is enhanced significantly as the reinforcement ratio is increased from 0.3% to 1%. The corresponding increases were 51% for slabs of 40 mm thickness and 68% for those of 60 mm thickness. Nevertheless, when the percentage of steel was over 1%, there was a little increase in the nondimensional punching shear strength. This indicates that the steel reinforcement has an important effect on the punching shear strength for lightly reinforced restrained slabs, but little effect on those heavily reinforced.

2.5.5 Boundary Condition

Membrane compressive forces are developed when a slab is restrained against lateral expansion,. Membrane action is generally considered as a secondary effect that occurs after cracking of the concrete or yielding of the reinforcement, and has been found to result in substantial enhancement in the flexural load-carrying capacity of restrained concrete slabs[45] .

Compressive membrane forces also play an important part in the control of slab deflection and cracking. As the degree of slab restraint increases, the value of slab deflection decreases, and the cracks are finer, narrower but larger in number .

2.5.6 Column Size

Marzouk and *Hussein* [42], test results clearly indicated that as the column size increases both ductility and stiffness increase accordingly.

2.5.7 Openings

Openings in the vicinity of column may be required for ducting. They are detrimental to the punching shear capacity of the slab to various extents depending upon location and size. An opening located at the front of the column decreases the punching shear capacity of the connection more than the same size opening located at the side of the column . This may be explained by the fact that the opening at the side face of the column has a smaller effect on the area and inertia of the critical shear section. The ultimate punching shear strength of the slab with the larger opening is less than that with smaller one [48].

2.5.8 Span-to-Depth Ratio

It is expected that the punching strength to be influenced by the span-to-depth ratio if the failure extends to the support, whereas the span-to-depth ratio would be of no consequence if the failure is fully contained within the slab. This has been experimentally demonstrated by *Lovrovich* and *Mclean*[49], While the normalized punching shear strength remains relatively constant for span-to-depth ratios of 6, 8 and 12, it increases significantly as span-to-depth ratios are decreased from 6 to 2. The increases in shear strength were 247% and 102% for specimens without and with shear reinforcement, respectively. Observed during the experiment , was evidence of the formation of compression struts between the point of application of the load and the support as specimens approached failure. Thus, a tied-arch mechanism similar to that observed in deep beams may have developed.

2.5.9 Shear Reinforcement

Shear reinforcement, in general, is intended to make failure to occur at larger load preceded by larger deflections in a more ductile manner. Conventionally, shear reinforcement can be in the form of stirrups or bent-up bars. However, these types of shear reinforcement have proven not to be very effective, especially in thin slabs (150-250 mm in overall thickness) [50]. Structural shear heads have also

been used extensively since mid 1930's and are included in many codes . Stud shear reinforcement was introduced and has become widely-accepted as an effective and efficient measure to improve punching shear strength and ductility[51].

Recently, novel forms of shear reinforcement, such as inclined stirrups, steel plates and steel bolts[52], or the combination of bent bars and stirrups, have produced effective and promising shear reinforcing systems, which not only result in desirable ductile behavior under load, but also are suitable for standard practice usage.

2.5.10 Arrangement of Flexural Reinforcement

Elstner and Hognestad, 1956 and Moe [5], 1961, investigated the punching behavior of column-slab connections with flexural reinforcement concentrated over the column region and compared them to others reinforced with uniformly spaced bars. In the Elstner and Hognestad study[23], slabs 50% of the tensile reinforcement was concentrated within a distanced d (effective depth) of the column, as shown in Figure (2-4). While in Moe's slabs the total amount of steel was held constant and the spacing varied between uniform spacing and an arrangement in which 82% of the total steel was placed within a distance d of the column. Both tests indicated that the concentration of reinforcement does not increase the ultimate load of slab. In some slabs, concentration of the reinforcement even reduced the ultimate load of the slab. This is because the concentration of reinforcement leaves a large radial sector almost unreinforced; see plate (2-4). From these tests results, it could be concluded that concentration of reinforcement causes a slight decrease in strength and a reduction of ductility.

Alexander and Simmonds [32] in 1992 conducted a similar study on the effect of adding extra reinforcement over the column strip. They placed a different amount of steel reinforcement over the column strip of 450mm resulting in spacing's of 50mm, 75mm and 150mm at the column region. All slabs failed in punching, but

they found that decreasing the spacing increases the load capacity but decreases the ductility.

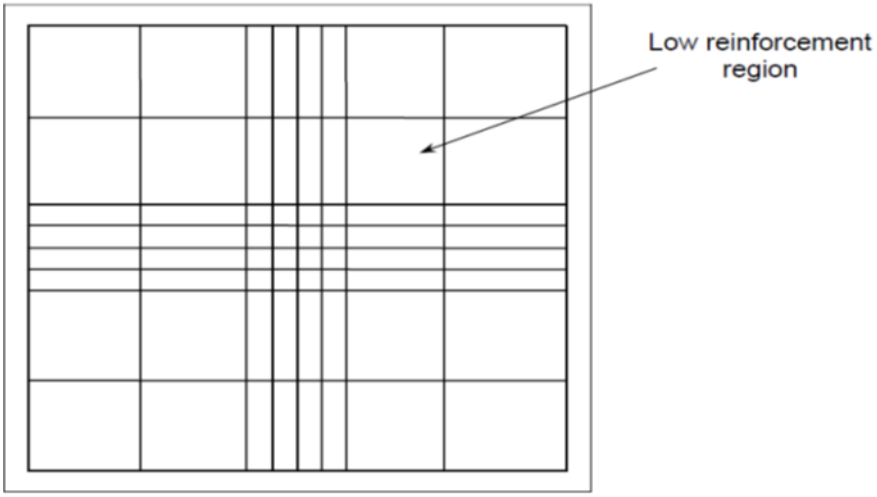

Fig(2-4): distribution of reinforcement.

Also in the slab with a spacing of 50mm, the bar force profiles indicate that anchorage failure occurred in the central bars. Based on this observation, they argued that in those slabs tested by Elstner and Hognestad [23] and Moe [5] failure was actually anchorage failure. They concluded that the above observation may explain why the concentrating of reinforcement through the column region does not increase punching capacity. However, Euro code recommends 50% of flexural reinforcement needed for the negative moment should be placed in the column region at a distance equal to the sum of 0,125 times the panel width on either side of the column because it improves the behavior of the slab in the service load range. Concentration increases the stiffness of the slab, increases the load for the first yielding of the flexural reinforcement, and consequently results in smaller maximum crack widths under the same loading condition.

Ali Hameed Naser,[53] 2014, investigated the punching shear strength and failure behavior of self-compacted concrete (SCC) slabs using carbon fiber reinforced polymer (CFRP) bars as internal strengthening in connection region for slab-column. Seven interior slab-column connections tested including same concrete compressive strength and ratio of the reinforcement. All slabs have been

tested as a simply supported and subjected to punching loading by interior column.

Test results show that the internal strengthening technique by using high tensile strength CFRP bars improves the bearing capacity of RC two-way slabs.

Based on the experimental results, it is possible to increase punching shear capacity by using internally reinforced with CFRP bars concentrated in slab-column zone, this increase is about (33-100%) compared with the unstrengthen (control) slab.

The effectiveness of the CFRP bars is depended substantially on distributed or arrangement manner in slab-column region.

Also, found that, the use of NSM CFRP bars is an effective technique to enhance shear capacity of SCC slab-column models and nearly provided the same efficiency of internal reinforcement.

Even efficient to increase the punching shear load, the top reinforcement of CFRP bars will not change the brittle-type punching shear failure mode compared with bottom CFRP bars reinforcement.

2.6 Types of Punching Shear Failure

Depending on the characteristics of the slabs, several types of punching shear failure can take place . Due to high bending and shear stresses, an interaction between shear and flexure takes place which may result in one of the following types of failure .

2.6.1 Shear-tension Type

The initial flexural cracks progress to form inclined principle tensile cracks, pushing the familiar pyramid out of the slab in this type of failure.

2.6.2 Shear-compression Type

In this type of failure, the extension of the flexural cracks reduces the depth of the compression zone around the column and leads to local crushing of the region and produces the typical punching failure.

Nielsen [54],believed that punching failure is sliding failure because the relative displacement along the failure surface is not perpendicular to the surface as it has to be in a pure tensile failure.

2.7 Method of Increasing the Punching Shear Strength in Flat Plate Construction:

2.7.1 Using Structural Members :

Many shapes of structural members can be used to increase the punching shear strength , by thickening the slabs around the column (drop panel) or by flaring the column under the slab. This method is very satisfactory for heavy loads and long spans. Alternatively, or in combination with drop panels, column capital may be provided to increase the capacity. The column capital geometry should follow a (45^{o}) degree projection. The benefit of using column capital is to reduce the clear span lengths and increase the critical section of the slab-column force transfer.

Researchers found that the shear capital is a good solution to prevent punching shear failure in static and dynamic loads. Different types of structural members were used as structural members called shear capitals to prevent punching shear failure. These types were tested by *Wey* and *Durrani* [55]in 1992.

In 2002, *Patrick* and *Caroline* [56], studied other types of structural members called continuous drop panel, formwork can be simplified by building continuous drops panel between the column lines in the direction parallel to the longer span. This method makes long spans possible in multi-level parking garages and shopping centers as well as in apartment and office buildings. Such a slab system allows for an obstructed span with minimum structural floor depth.

2.7.2 Using Higher Strength Concrete

The use of high-strength concrete improves the punching shear resistance by allowing higher forces to be transferred through the slab-column connection according to *Tuan* [7].

Kaiss F. Sarsam and Hassan F. Hassan[57], 2014, studied the mechanical properties of reactive powder concrete(RPC) and modified reactive powder concrete (MRPC) as a material as well as studied the punching shear behavior of RPC and MRPC slabs. They investigated the effect of steel fiber volumetric ratio (V_f) and absence of coarse aggregates on some important mechanical properties of RPC and MRPC such as compressive strength, modulus of elasticity (E), splitting tensile strength and modulus of rupture. They also conducted to study the effect of V_f, steel reinforcement ratio (ρ) and slab thickness on the failure characteristics of the punching shear (in terms of observation of failure, shape of the failure zone, size of the failure zone, failure angles, critical section perimeters and ultimate punching shear stress) of simply supported reinforced RPC slabs having dimensions of 1000×1000 × 50 or 70 mm under concentrated load at the center of the slab.

2.7.3 Using Steel Fiber Reinforced Concrete

Several investigations have shown the performance improvement of the slab-column connection by using steel fiber concrete. Both strength and ductility enhancement were observed by *Alexander* & *Simmonds*[32]. The combination of high-strength concrete and steel fibers shows interesting results because punching strength can be raised without loss in ductility. Random dispersion of steel fibers to the conventional concrete offers a convenient and practical means of achieving in many of the engineering properties of the concrete such as tensile strength, compressive strength, flexural strength, impact resistance and first crack and ultimate loads.

Ali H. Aziz, Shatha S. Kareem and Ban Sahib [58], 2013, investigated experimentally the punching shear behavior of hybrid flat plate. They tested five slab specimens with (1000x1000x70) mm dimensions, two of which have been made fully with High Strength Concrete and Steel Fiber Reinforced Concrete, while, the others have been made by mixing two types of concrete (Steel Fiber Reinforced Concreter in

the critical zone and High Strength Concrete in the other part of slab specimen). The slab dimensions, main reinforcement have been kept constant in all slab specimens. The variables are concrete type and dimensions of critical area. Experimental results show that the use of SFRC improves the punching shear resistance and allows higher forces to be transferred through the slab-column connection. For slab specimen which made fully with SFRC, the ultimate shear capacity increased by (25%) in comparison with the normal slab. While, for slab specimens which made with hybrid concrete the ultimate shear capacity increased by (5%-13%) in comparison with the normal slab.

2.7.4 Using Vertical Prestressing of Slab-column Connection

The prestressing of flat slabs across the thicknesses near the column faces can prevent or delay the rotation and the widening of the crack which would form the failure surface. It can also provide more effectively the confining effect as stirrups. The prestress can thus provide substantial increase in strength of slabs at their connection with column and increases the ductility of connection.

In 1974, *Ghali, et al*[59], tested ten specimens of (1804.3 mm) square, and (152.4 mm) thickness with column (304.8 mm) square cross-section. The ten specimens were divided into three groups; group (A) consists of two prestressed slab identical in all details except in the distance between the center of the prestress bolt and the column face. These two tests served to determine a location in which the prestressing tendons are more effective. Specimens of group (B) were subjected to moment and supported on either two or four sides. The specimens of group (C) were subjected to axial force, and also supported either on two or four sides. The increase in ultimate load is about (1.92 and 1.62) times the value in the similar nonprestressed slabs, and the ultimate moment capacity is about (2.27) times the value in the similar nonprestressed slabs.

2.7.5 Using Shear Reinforcement

Researchers used different types of shear reinforcement in flat plate structures, such as (bent-up bars, stirrups, shear studs, hooked bars and shearheads), each

type has advantages and disadvantages concerning detailing anchorage effectiveness and construction ease.

Above all, these systems are in general expensive and many of them do not only increase the shear capacity of the connection but also flexural capacity.

2.8 Investigation of Reactive Powder Concrete(PRC) and Carbon Fiber Reinforced Polymer (CFRP)

PRC is a developing composite material that will allow the concrete industry to optimize material use, generate economic benefits, and build structures that are strong, durable, and sensitive to environment. A comparison of the physical, mechanical, and durability properties of RPC and HPC (High Performance Concrete) shows that RPC possesses better strength (both compressive and flexural) and lower permeability compared to HPC.

High-Performance Concrete (HPC) is not just a simple mixture of cement, water, and aggregates. It contains mineral components and chemical admixtures having very specific characteristics, which give specific properties to the concrete. The development of HPC results from the materialization of a new science of concrete, a new science of admixtures and the use of advanced scientific equipment's to monitor concrete microstructure.

HPC has achieved the maximum compressive strength in its existing form of microstructure. However, at such a level of strength, the coarse aggregate becomes the weakest link in concrete. In order to increase the compressive strength of concrete even further, the only way is to remove the coarse aggregate. This philosophy has been employed in Reactive Powder Concrete (RPC). Reactive Powder Concrete (RPC) is an

ultra-high-strength and high ductility cementitious composite with advanced mechanical and physical properties. It consists of a special concrete where the microstructure is optimized by precise gradation of all particles in the mix to yield maximum density. It uses extensively the pozzolanic properties of highly refined silica fume and optimization of the Portland cement chemistry to produce the highest strength hydrates [60].

RPC was first produced in the early 1990s by researchers at Bouygues' laboratory in France and developed by P. Richard and M. Cheyrezy. A field application of RPC was done on the Pedestrian/Bikeway Bridge in the city of Sherbrooke, Quebec, Canada. RPC was nominated for the 1999 Nova Awards from the Construction Innovation Forum. RPC has been used successfully for isolation and containment of nuclear wastes in Europe due to its excellent impermeability.

The requirements for HPC used for the nuclear waste containment structures of Indian Nuclear Power Plants are normal compressive strength, moderate E value, uniform density, good workability, and high durability.

RPC should be used in areas where substantial weight savings can be realized and where some of the remarkable characteristics of the material can be fully utilized. Owing to its high durability, RPC can even replace steel in compression members where durability issues are at stake (in marine condition). Since RPC is in its developing stage, the long-term properties are not known[60].

Wasan I. Khalil[61], 2012, produced modified RPC with crushed graded natural aggregate (maximum size 12.5mm). It achieved compressive strength of (150) MPa by using crushed coarse aggregate. It found that a modified RPC

reinforced with different types (crimped and hooked) and volume fractions (0%, 0.5%, and 1%) of steel fibers has a good performance in terms of high strength (Compressive strength, splitting tensile strength, modulus of rupture, impact strength) and static modulus of elasticity.

Nuha H. Al-Jubory [62], 2013, compared plain reactive powder concrete and reactive powder concrete reinforced with 1% and 2% steel fiber. Compressive strength, splitting tensile strength and flexural strength were investigated. It curried out two sets of samples, each set consisted of (54) cubes of (50×50×50mm), (18) cylinder of (100×200mm) and (18) prism of (50×50×300mm). It showed that the maximum compressive strength is 74 MPa with 2% steel fiber and curing in 20°C. The addition of steel fiber by 1% and 2%increased the compressive strength, splitting tensile strength and flexural strength.

Chapter Three

EXPERIMENTAL WORK

3.1 General

The main purpose of the test program is to study the punching shear strength of reactive powder concrete slabs reinforced with CFRP bars.

The slabs were divided into four groups. All slabs were prepared and tested. The main objective of this chapter is to present the properties of materials of reactive powder concrete, the details of the test specimens. The variables of the four groups of slab, the instrumentation and testing setup will be described. Standard specification of the American Society for Testing and Materials (ASTM)-106 and Iraqi specifications No. [5 , 45], 1984 are adopted to determine the properties of materials.

3.2 Reactive Powder Concrete

The term Reactive Powder Concrete (RPC) has been used to describe a fiber-reinforced, superplasticized, silica fume - cement mixture with very low water-cement ratio (w/c) characterized by the presence of very fine quartz sand (0.15-0.60 mm) instead of ordinary aggregate. In fact, it is not a concrete because there is no coarse aggregate in the cement mixture. The absence of coarse aggregate was considered by the inventors to be a key-aspect for the

microstructure and the performance of the RPC in order to reduce the heterogeneity between the cement matrix and the aggregate. However, due to these of very fine sand instead of ordinary aggregate, the cement content of the RPC is as high as 900-1000 kg/m^3. The superplasticizer, used at its optimal dosage, decreases the water to cement ratio (w/c) while improving the workability of the concrete. A very dense matrix is achieved by optimizing the granular packing of the dry fine powders. This compactness gives RPC ultra-high strength and durability.

There are many principles indicated to developing the RPC[60] :

1. Elimination of coarse aggregates for enhancement of homogeneity
2. Utilization of the pozzolanic properties of silica fume
3. Optimization of the granular mixture for the enhancement of compacted density
4. The optimal usage of superplasticizer to reduce w/c and improve workability
5. Application of pressure (before and during setting) to improve compaction
6. Post-set heat-treatment for the enhancement of the microstructure
7. Addition of small-sized steel fibers to improve ductility

So, there are some properties of RPC to enhance the homogeneity and strength shown in Table (3 – 1), and different ingredients of RPC and their selection parameters described in Table (3 – 2).

Table (3-1): Properties of reactive powder concrete[60].

Property of RPC	Description	Recommended Values	Types of failure eliminated
Reduction in aggregate size	Coarse aggregates are replaced by fine sand, with a reduction in the size of the coarsest aggregate by a factor of about 50%.	Maximum size of fine sand is 600 µm	Mechanical, Chemical & Thermo-mechanical
Enhanced mechanical properties	Improved mechanical properties of the paste by the addition of silica fume	Young's modulus values in 50 GPa – 75 GPa range	Disturbance of the mechanical stress field.
Reduction in aggregate to matrix ratio	Limitation of sand content	Volume of the paste is at least 20% greater than the voids index of non-compacted sand.	By any external source (e.g., formwork).

3.2.1 Mixture of RPC

The major parameter that decides the quality of the mixture is its water demand (quantity of water for minimum flow of concrete). In fact, the voids index of the mixture is related to the sum of water demand and entrapped air. After selecting a mixture design according to minimum water demand, optimum water content is analyzed using the parameter relative density (d_0/d_S), where d_0 and d_S represent the density of the concrete and the compacted density of the mixture (no water or air) respectively[63].

Table (3-2) Parameters of reactive powder concrete[60].

Components	**Selection Parameters**	**Function**	**Particle Size**	**Types**
Sand	Good hardness Readily available and low cost.	Give strength, Aggregate	150 µm to 600 µm	Natural, Crushed
Ordinary Portland Cement	C_3S : 60%; C_2S : 22%; C_3A : 3.8%; C_4AF: 7.4%. (optimum)	Binding material, Production of primary hydrates	1 µm to 100 µm	OPC, Medium fineness
Quartz Powder	Fineness	Max. reactivity during heat-treating	5 µm to 25 µm	Crystalline
Silica fume	Very less quantity of impurities	Filling the voids, Enhance rheology, Production of secondary hydrates	0.1 µm to 1 µm	Procured from Ferrosilicon industry (highly refined)
Steel fibers	Good aspect ratio	Improve ductility	--	--
Superplasticizer	Less retarding characteristic	Reduce w/c	--	Polyacrylate based

Relative density indicates the level of packing of the concrete and its maximum value is one. For RPC, the mixture design should be such that the packing density is maximized. The high strength of RPC makes it highly brittle. Steel fibers are generally added to RPC to enhance its ductility.

3.2.2 Limitations of RPC

In a typical RPC mix design, the least costly components of conventional concrete are basically eliminated or replaced by more expensive elements. The fine sand used in RPC becomes equivalent to the coarse aggregate of conventional concrete, the Portland cement plays the role of the fine aggregate and the silica fume that of the cement. The mineral component optimization alone results in a substantial increase in cost over and above that of conventional concrete (5 to 10 times higher than HPC) [64].

3-3: Materials

General description and specification of the materials used in the test program are listed below:

3-3-1: Cement

Ordinary Portland cement (type I) is used. It is stored in dry place to avoid exposure to undesirable atmospheric conditions. The chemical analysis and physical test results of the used cement are given in Tables (3-3), (3-4) and (3-5) respectively. This conforms to the Iraqi Standard Specification No.5/1984[65].

Table (3-3): Chemical analysis of cement*

Compound Composition	Chemical Composition	Percentage By Weight	Limit of IOS: 1984
Lime	CaO	62.22	-
Silica	SiO_2	17.01	-
Alumina	Al_2O_3	3.49	-
Iron Oxide	Fe_2O_3	2.18	-
Magnesia	MgO	2.24	<5
Sulfate	SO_3	1.92	<2.8
Loss on Ignition	L.O.I	1.1	<4
Insoluble residue	I.R	0.5	<1.5

*A chemical tests of cement was a accomplished in the laboratory of Misan Technical Institute

Table (3-4):Main compounds (Bogue's equations) percentage by weight of cement

Tricalcium aluminates (C_3A)	5.58
Tricalcium silicate (C_3S)	38.55
Dicalcium silicate (C_2S)	23.15
Tricalcium alumona ferrite (C_4AF)	8.73

Table (3-5): Physical test of cement*

Physical Properties	Test result	Limit of IOS 5:1984
Fineness using Blaine air permeability apparatus (m^2/kg)	310	> 230
Soundness using autoclave method	0.19 %	< 0.8 %
Setting time using Vicat's instrument Initial (min) Final (hrs:min)	 1:28 4:30	 > 45 min < 10 hr
Compressive strength for cement paste cube (70.7 mm) at 3 days (MPa) 7 days (MPa) 28 days (MPa)	 19.4 29.75 48.33	 >15 > 23 -

*A physical tests of cement was a accomplished in the laboratory of Misan Technical Institute

3.3.2 Fine Aggregate (Sand)

Natural sand brought from AL-Ukhaidher quarry was used as fine aggregate for concrete mixes in this study. The grading of the fine aggregate is (0.15 - 0.6) mm according to the literature studies of reactive powder concrete. The obtained results indicated that the fine aggregate grading and the sulfate content are within the limits of Iraqi specification No. 45/1984 [66].

Table (3-6) shows the specific gravity, sulfate content, absorption and moisture content of the fine aggregate.

Table (3-6) : Properties of Fine Aggregate

Physical properties	***Test results***	***Iraqi specification. 45/1984 for zone No.(1)***
Specific gravity	*2.65*	---
Sulfate content	*0.3 %*	*Not more than 0.5%*
S.S.D.	*1 %*	---

3.3.3: Hooked-End Steel Wire Fiber (HESF)

Throughout this work, hooked-end steel wire fibers were used with volume fraction of (V_f =2%) by volume, Plat (3-1). This type of steel fiber is manufactured by National Standard Company, imported from China. According to ASTM-A820[67], this type of steel fiber is classified as (Type II). The properties of the steel fibers are presented in Table (3-7).The steel fibers come in water-soluble glued bundles, to ensure their good dispersion during the concrete mixing and to make the process of handling more easy.

Plat (3-1): Shape of hooked steel fiber

Table(3-7): Properties of steel fiber*

Property	Specifications
Density	7860 kg/m^3
Ultimate strength	1150 MPa
Modulus of Elasticity	200x10^3 MPa
Strain at proportion limit	5650 x10^{-6}
Poisson's ratio	0.28
Average length	60 mm
Nominal diameter	1.0 mm
Aspect ratio (L_f/D_f)	60

*Data sheet of hooked-steel fiber

3.3.4 Mixing Water

Ordinary tap water was used for concrete mixing and curing.

3.3.5 Superplasticizer

Sika ViscoCrete - 5930 used in the work, it's the third generation of high-range water reducing (superplasticizer) for concrete and mortar. It meets the requirements for super plasticizer according to ASTM – C – 494[68]. Types G and F. It facilitates extreme water reduction, excellent flowability at the same time optimal cohesion and highest self- compacting behavior.

3.3.6 Silica Fume

Silica fume is an ultrafine material with spherical particles less than (1 μm) in diameter, the average being about (0.15 μm), this makes it approximately 100 times smaller than the average cement particle. The bulk

density of silica fume depends on the degree of densification in the silo and varies from 130 (undensified) to 600 kg/m3. The specific gravity of silica fume is generally in the range of 2.2 to 2.3. The specific surface area of silica fume can be measured with the BET method or nitrogen adsorption method. It typically ranges from 15,000 to 30,000 m2/kg[69]. Because of its extreme fineness and high silica content, silica fume is a very effective pozzolanic material. Standard specifications for silica fume used in cementitious mixtures are ASTM C1240[70]. Silica fume is added to Portland cement concrete to improve its properties, in particular its compressive strength, bond strength, and abrasion resistance. These improvements stem from both the mechanical improvements resulting from addition of a very fine powder to the cement paste mix as well as from the pozzolanic reactions between the silica fume and free calcium hydroxide in the paste. Addition of silica fume also reduces the permeability of concrete to chloride ions, which protects the reinforcing steel of concrete from corrosion

Densified micro silica is used, it is a special high quality micro- silica, approved as a concrete additive according to the ASTM-C-1240[70]. In this work it used a MEYCO MS610. It is a concrete additive for high quality concretes, it changes the porous structure of the concrete in a definitive manner and makes it denser and more resistant to any type of external influence, and must be used in combination with a plasticizer or a superplasticizer.

3.3.6.1 Benefits and properties of MEYCO- MS610

There are many features and benefits of using MEYCO MS610 as fallow:

1. Increased strengths
2. Substantially improved resistance to chemical and mechanical attack
3. Prevents bleeding and segregation in fresh concrete
4. Reduced dosages of activators/accelerators
5. Larger layer thicknesses sprayable

3.4 Carbon Fiber Reinforced Polymer (CFRP) Bars

Smooth CFRP imported from china with (ϕ = 6mm), it allows designers to utilize the greater modulus and tensile strengths of carbon fiber in a non-metallic reinforcing bar. It used for both new construction and as a strengthening material for the new technique known as "Near Surface Mount" or NSM strengthening. All bars treated after making the reinforcement mesh by making nodes on each bar of mesh shown in Plate (3-2), with steel wire and to ensure rough surface and the activity of steel nodes on bars, they coated by epoxy resin "sikadur – 330". This treatment made to ensure the slipping is not happened and to get the perfect bond between the bars and concrete.

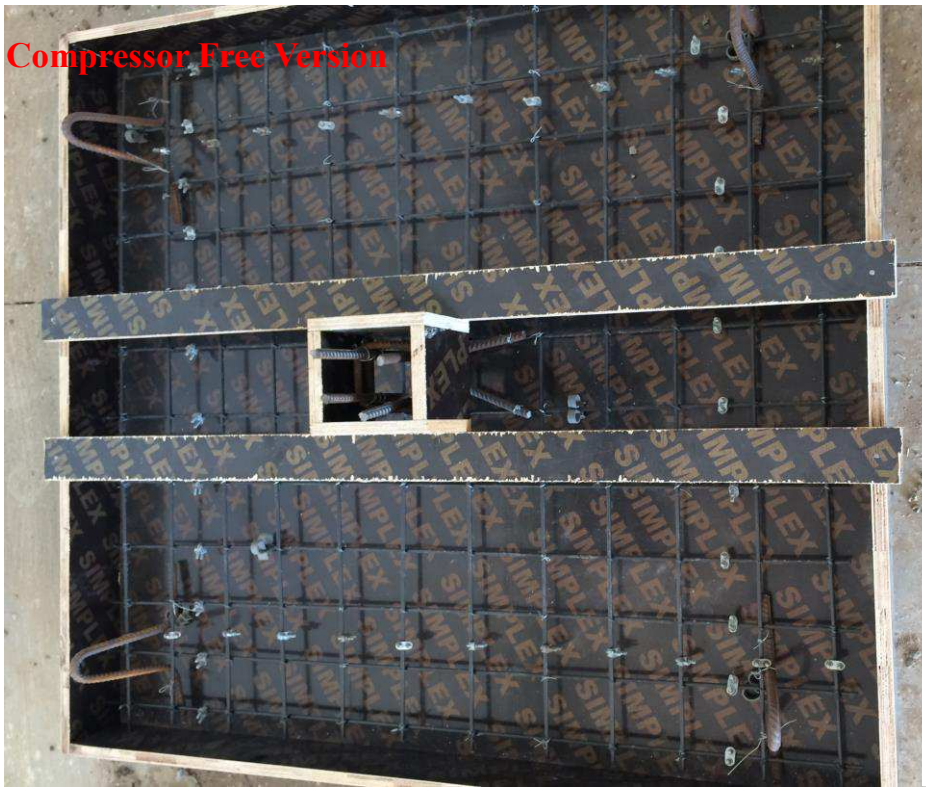

plate (3-2): CFRP mesh used this research work

3.4.1 Epoxy Resin

Impregnating resin of type Sikadur-330, comprising of two parts (Resin part A + Hardener part B) was used in this study to get steel nodes on mesh of reinforcement and rough surface of bars , Table (3-8) shows the properties of the bonding epoxy taken from manufacturer's specification (Technical Data Sheet of Sika 2005) **.**

Table (3-8): Properties of the Epoxy Resin

Appearance	***Mixing ratio***	***Open time min.***	***Tensile strength MPa***	***Tensile E-modulus MPa***	***Elongation***
Part A: white *Part B: gray*	*A:B* *4:1*	*30 (at +35°C)*	*30*	*4500*	*0.9%*

3.4.2 Tensile Stress and Modulus of Elasticity

Tensile stress values shown are determined as the average failure load divided by the nominal bar diameter minus three standard deviations. Per ACI440-1R definition, this is the "Guaranteed Tensile Strength, f_{fu} ". This modulus of elasticity is the mean modulus of a sample of test specimens. Unlike steel materials, the stress-strain curve of FRP is linear elastic to failure(date sheet of smooth CFRP) ; see Figure (3-1).

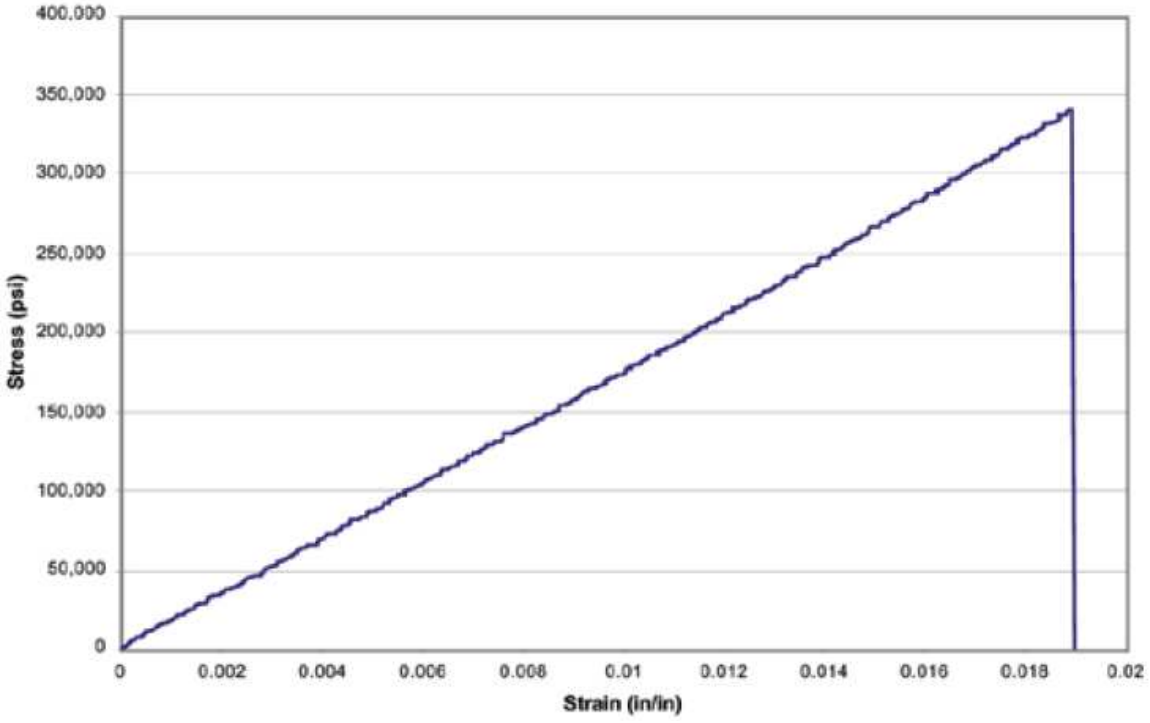

Figure (3-1): Typical stress-strain curve of CFRP

3.5 Reactive Powder Concrete Mix Design

There are three trial mixes of reactive powder concrete made, according to literature studies of reactive powder concrete. It was considered three cylinder (100 x 200) mm as shown in Plate (3-5), for each one and tested at 28 day, and the same number of cubes (150 x 150) tested at 7 day, to the

average of compressive strength for each trial mix, then the higher one be considered. Table (3-9) shown the details of these trial mix.

Table (3-9): Amounts of materials used for the trial mixes

Materials	**Trials mix 1**	**Trials mix 2**	**Trials mix 3**
Cement (kg/m^3)	740	768	800
Silica fume (kg/m^3)	180	192	200
Fine sand (kg/m^3)	1012	1140	1100
Superplasticizer (kg/m^3)	30	40	48
Water (kg/m^3)	220	144	210
Steel fiber (kg/m^3)	118	157	157

The trial mix 2 was considered which, it gave the maximum average compressive strength of cylinders (108 MPa) as shown in Table (3-10).

Table (3-10): The compressive strength of each trial mix at 28 days

Tested at 28 days	**Trial mix 1**			**Trial mix 2**			**Trial mix 3**		
Compressive strength (MPa)	100.23	104.25	103.63	107.67	109.34	107.05	109.88	107.45	104.2
Average	102.7			108.02			107.17		

Plate (3-3): Casting and testing of RPC cylinders and cubes

3.5.1 Compressive Stress-Strain Curve

Three of the cylindrical specimens that were tested in compression were previously instrumented with strain gauges, (two strain gauges for each cylindrical specimen); see Fig.(3-2-a). This configuration allowed to record the ascending branch of the stress-strain curve, as well as the concrete strain corresponding to the compressive strength. The stress-strain curves for the average of three cylinders are shown in Fig.(3-2-b).

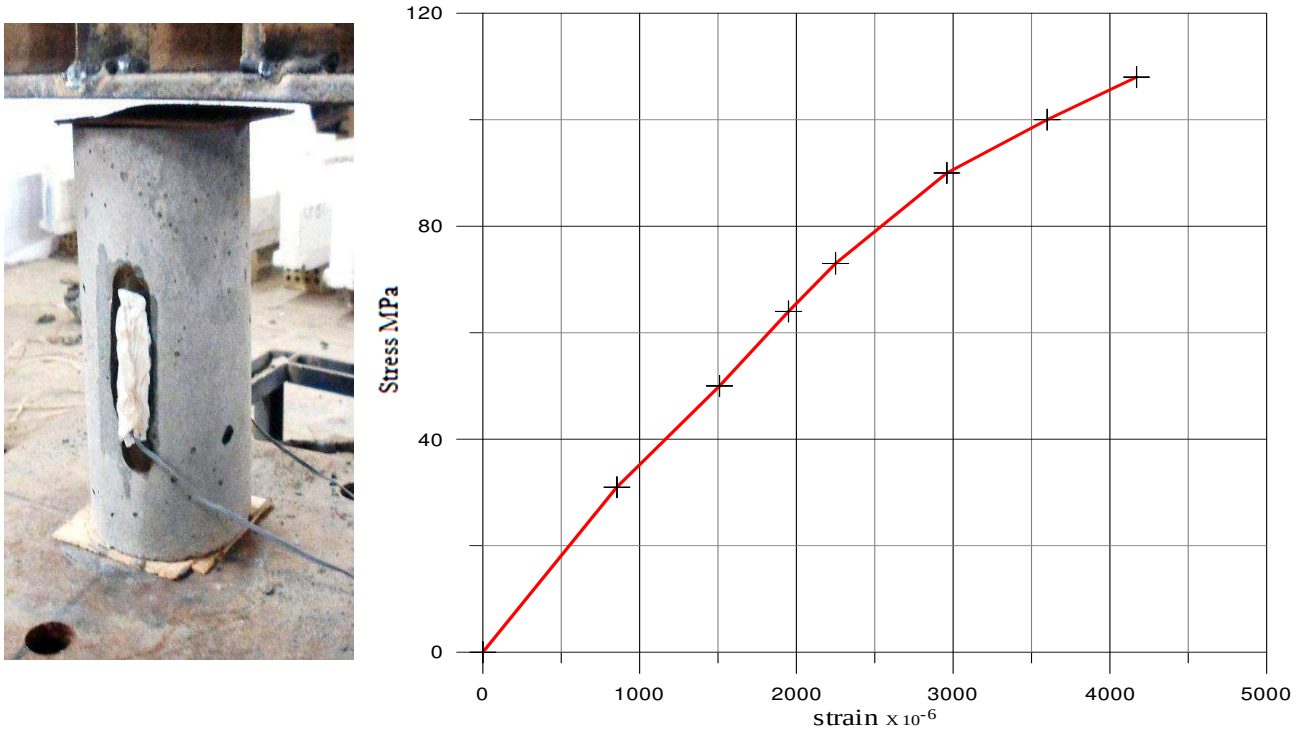

a) 2 strain gauges for tested cylinder

b) Experimental Stress-Strain curve of RPC

Figure (3-2): Compressive stress-strain curve

3.5.2 Tensile Strength

In this work, the concrete tensile strength was determined using splitting tensile tests on cylindrical specimens and by the flexural tensile strength of prismatic specimens. The equipment used to perform these tests was a

universal ELE Machine model with a capacity of 2000 kN; see plate (3-4). The average results of three specimens was adopted for each test and reaching 14 MPa in this work. The modulus of rupture of the average three tested specimens reached 18.4 MPa

Plate (3-4): Test of mechanical properties of RPC

3.6 Specimens Description and Casting

Fourteen RPC square two-way slabs were casted and cured under laboratory conditions, the specimens were designed to study the punching shear response of RPC two-way slabs reinforced by CFRP bars. All of the tested slabs were of the same lateral dimensions (1150×1150) mm as shown in Figure (3-8). the specimens are divided into four groups according to the parameters which are as variables

1. CFRP reinforcement ratio (ρ_f).

2. Thickness of slab (t).
3. The dimension of square column(c).
4. Arrangement of CFRP reinforcement, as shown in Figures (3-4) to (3-7).

All fourteen slabs were tested to study the effect of these variables and the details of specimens are shown in Table (3-11)

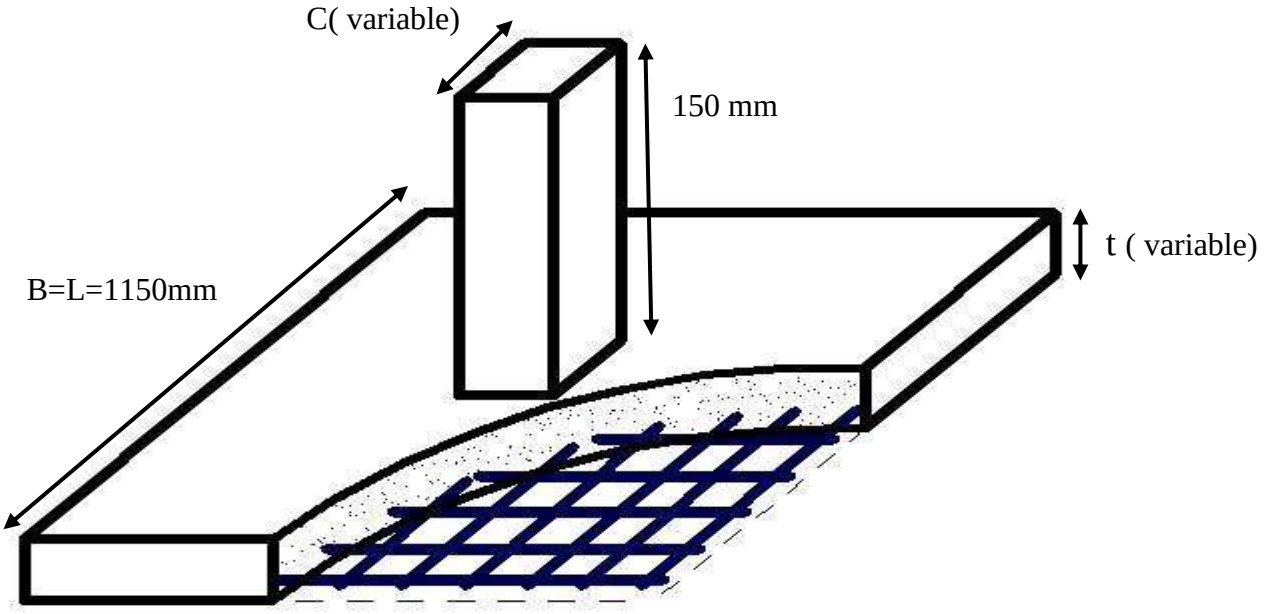

Figure (3-3): Details of section of slab specimen

Table (3-11): Details of slab specimens

Slab Designation	***Thickness of slab h (mm)***	***Column* side length C(mm)**	***CFRP ratio*** %	***No. of bars in each direction***	***Arrangement of reinforcement***
S – 1	100	150	0.3686	12	One mesh
S – 2	100	150	0.3993	13	One mesh
S – 3	100	150	0.43	14	One mesh
S – 4	100	150	0.4607	15	One mesh
S – 5	80	150	0.368	12	One mesh
S – 6	100	150	0.4607	15	One mesh
S – 7	120	150	0.44217	18	One mesh
S – 8	150	150	0.453	22	One mesh
S – 9	100	100	0.3686	12	One mesh
S – 10	100	125	0.3686	12	One mesh
S – 11	100	150	0.3686	12	One mesh
S – 12	100	175	0.3686	12	One mesh
S – 13	100	150	0.276	9	One mesh
S – 14	100	150	0.3378	11	One mesh
S – 15	100	150	0.3378	11	One mesh
S – 16	100	150	0.3378	11	One mesh

9 bars ϕ 6mm @ 143mm, in each direction

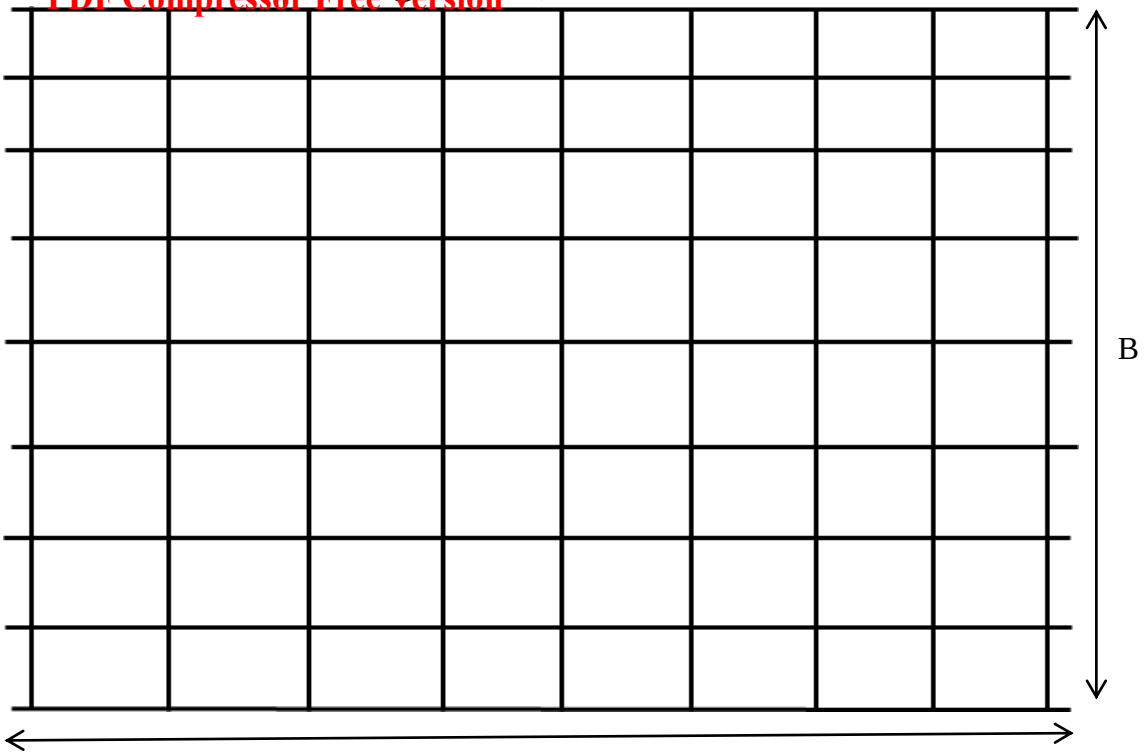

B =L = 1150 mm

Figure (3-4): Arrangement of CFRP bars of S - 13

11 ϕ 6mm with fixing the CFRP bars out of the parameter of punching shear

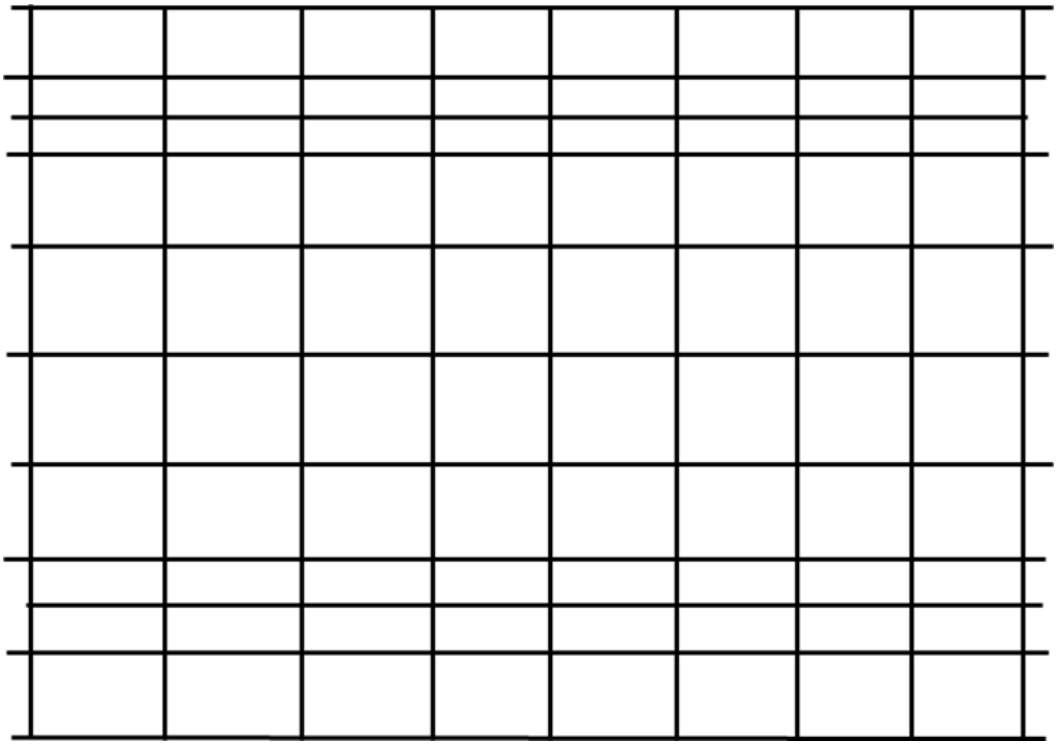

Figure (3-5): Arrangement of CFRP bars of S - 14

11 ϕ 6mm with fixing the CFRP bars in the parameter of punching shear

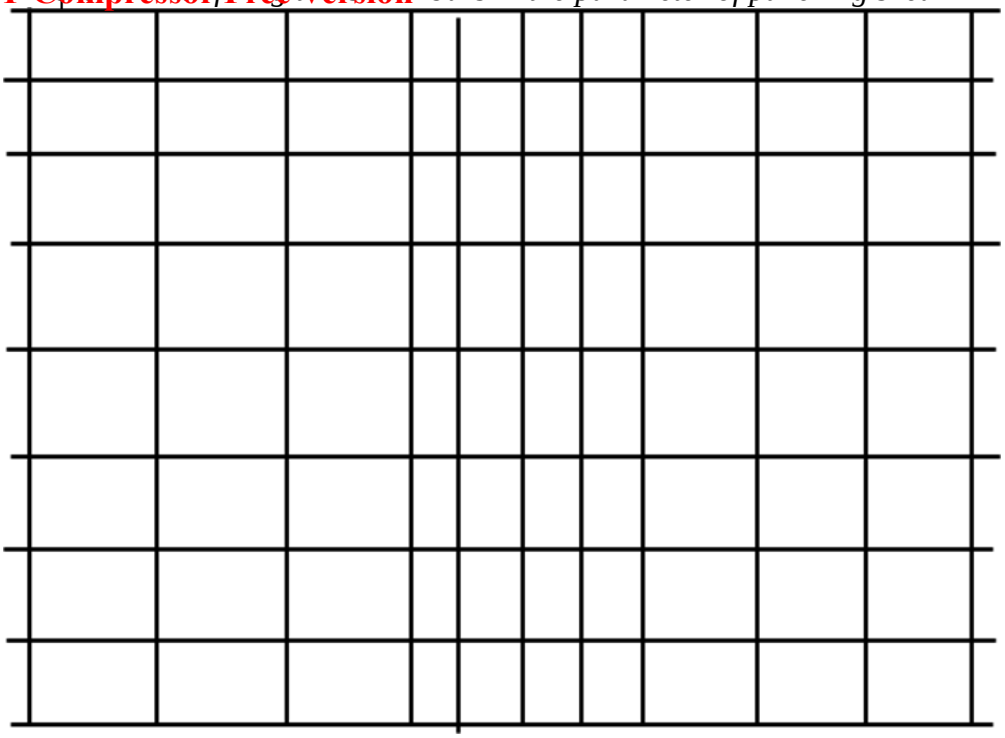

Figure (3-6): Arrangement of CFRP bars of S - 15

11 ϕ 6mm with make a mesh in the parameter of punching shear

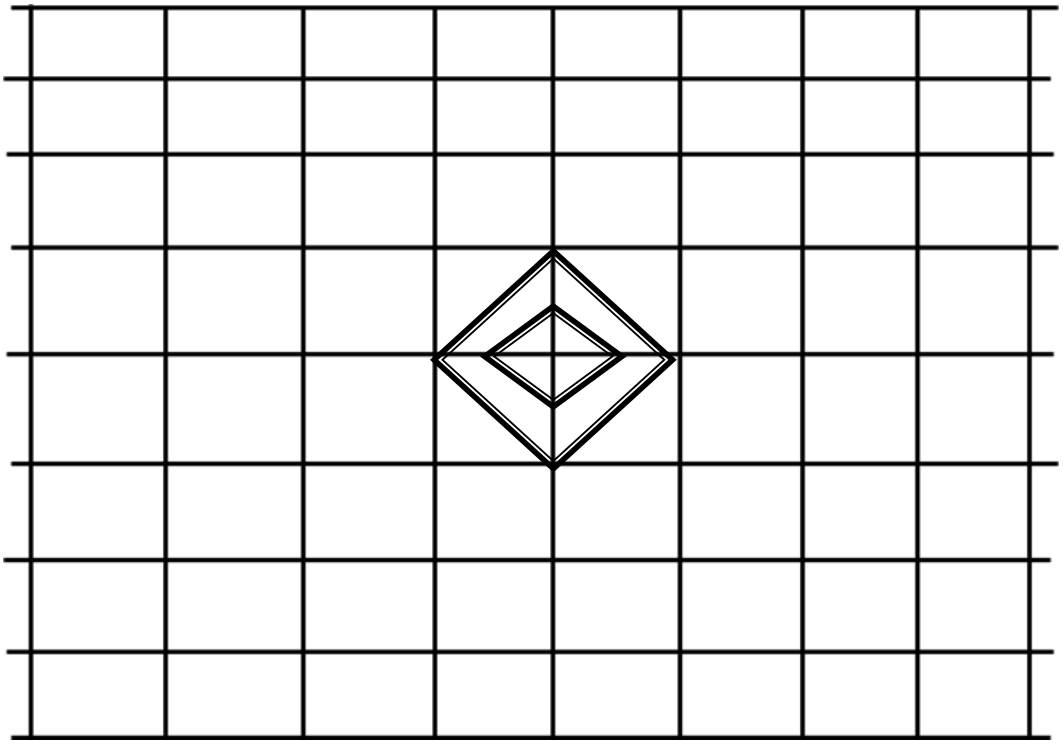

Figure (3-7): Arrangement of CFRP bars of S - 16

The fourteen slab specimens are casted and cured as in plate (3-5) and (3-6) in the materials laboratory of the Civil Engineering department of the University of Misan. The concrete casting and curing procedure is described below:

1. The molds of specimens, cubes and cylinders are treated with oil before putting the CFRP reinforcement grid or casting the concrete.

2. CFRP grid for each specimen is placed in their correct position and the specified protection cover is checked, plate (3-6).

3. Before mixing, all the quantities are weighted and packed in a clean containers.

4. Sand is added with part of the mixing water. After starting the mixer, the cement and silica fume are added with part of superplasticeser, the mix is kept for 3 min. then add all te remaining water and superplasticeser, rest another 3 min. final mixing.

5. After the mixing process is completed, Concrete is poured in the molds in two layers, and each layer is compacted by rod vibrator. The upper surface of concrete is smoothly finished after casting is completed using hand trowel.

6. After casting, the molds are left in the laboratory for about 24 hours, and then the specimens are removed from their molds. The sacks are placed over the slabs and wetted down. The sacks are monitored and kept wet for successive seven days.

7. Once the slabs are cured, they are placed off to the side until they could be tested. The same procedures are performed on the concrete test cubes and cylinders.

The slabs were placed on four straight edges of 1000 mm length simply supported on all four sides and subjected to a central concentrated load over column area. All the support lines were 75 mm distance from the slab edges, so the effective span of the slab in both directions was 1000 mm.

Plate(3-5): Molds used to cast the specimens

Plate(3-6): Casting of RPC slabs

3.7 Testing Setup:

3.7.1 Support and Loading Conditions

All slab specimens are tested using steel frame with hydraulic jack shown in Plate (3-7), with a maximum capacity of 600 kN. The slabs are simply supported on four sides each 1150mm long (knife edge) resting on rigid steel frame subjected to a central concentrated load over the area of column . All four support lines are 75 mm from the slab edges, so the effective span of the slab in both directions is 1000mm . The slabs are tested under static loads, loaded in successive increments, up to failure. For each increment, the load is kept constant until the required readings are recorded.

Plate (3-7): Steel frames and testing specimens

3.7.2 Instrumentation

Dial gauges 50 mm and 30mm max. reading of 0.01 mm accuracy were used to detect the deflection of the slabs at every loading stage. During each load step the corresponding central deflection and concrete strains at central slabs of top face slab at (**d/2** in two direction, **d**, **2d**) of the face of column are recorded. The first crack load and the failure load are recorded. The tests were continued up to failure and the ultimate load was recorded.

Deflection of the slab specimens is measured at mid-slab using a dial gauge graduated to 0.01 mm divisions and (30mm) capacity.

3.7.3 Electrical Strain Gauges

TML Strain gauge Type PFL-30-11-3L Plate(3-8) is used in all tests. All gauges had a nominal resistance of 120.4 $\pm$ 0.5 ohms and a nominal gauge factor of 2.11 $\pm$ 1%. The Gauge Factor is an expression for the change in resistance given and it is dependent on Poisson's ratio of the material on which the gauge was tested.

Plate(3-8): Electrical strain gauges used for measuring concrete strain

3.8 Testing Procedure

All the slab specimens are tested under monotonically increasing load up to failure. The load is applied vertically at the centre of the top face of column over reinforced concrete slabs. Then the initial deflection is recorded and the specimens are loaded with constant rate of loading, and the load is increased gradually up to failure of the slab. Readings of strains and

central deflection are recorded at each load intervals. Also the crack formation and propagation are examined at each load step, as well as recording the first crack load and the failure load of the slab. Testing mechanism and treatment of slab specimens are shown in Plate (3-9).

Plate (3-9): Testing mechanism and treatment of slab specimens before testing

Chapter Four

RESULTS OF EXPERIMENTAL WORK

4.1 General

Test results and discussion of 14 slabs designed to fail in punching shear are presented in this chapter, the clear span of all slabs are (1000×1000)mm .

The effect of following variables on the punching shear behavior and strength are investigated:

1. CFRP reinforcement ratio.
2. Slab thickness.
3. Column dimensions.
4. The shape of distribution of CFRP in the slabs.

Four slabs have be tested to study the effect of each variable, so the slabs divided into four groups as shown in Table (4-1), then the ultimate experimental punching shear capacity is compared with the ACI-440-1R(Eq. 2-18) and EL-Gamal equation (Eq. 2- 19) for punching shear of slab reinforced with FRP or steel.

4.2 General Behavior of Slabs Under Loading

The general behavior (crack pattern and failure mechanism) of (14) slabs are all nearly identical, When the load is applied to the slab specimen, the first visible crack (bending cracks) is observed at the tension face of the tested slab at load level equal to (21.54 – 55.56)% of ultimate load as shown in Table (4-1). In all slabs, cracking on the tension

failure began near the center and radiated towards the edges (semi- random phenomena). At higher loads, the already formed cracks get widened while new cracks started to form. The new formed cracks are roughly circular or elliptical in shape and occurred in the tension surface of the slab. Failure of the slab occurred when the cone of failure radiating outward from the point of load application pushed up through the slab body (brittle failure with limited warning). At failure, the slab is no longer capable of taking additional load.

No cracks are observed in the compression face of any slab, except those which are initiated around the loaded area at failure, which are almost the same as that of the loading column dimensions.

Table (4.1): Crack load and ultimate experimental load

Slabs Designation		Column Dimensions C (mm)	Thickness Of Slabs (mm)h	CFRP Ratio %	Ultimate Experimental load ($P_{u.}$) kN	First Crack load ($P_{cr.}$) kN	$P_{cr.}/P_u$ %
S – 1	**Group 1**	150	100	0.3686	140	45	32.21
S – 2		150	100	0.3993	165	55	33.34
S – 3		150	100	0.43	170	58	34.12
S – 4		150	100	0.4607	175	60	34.28
S – 5	**Group 2**	150	80	0.368	90	30	33.334
S – 6		150	100	0.4607	175	60	34.28
S – 7		150	120	0.44217	155	55	35.48
S – 8		150	150	0.453	270	150	55.56
S – 9	**Group 3**	100	100	0.3686	130	40	30.77
S – 10		125	100	0.3686	135	42	31.112
S – 11		150	100	0.3686	140	45	32.21
S – 12		175	100	0.3686	170	60	35.3
S – 13	**Group 4**	150	100	0.276	130	28	21.54
S – 14		150	100	0.3378	130	30	23.07
S – 15		150	100	0.3378	150	35	23.34
S – 16		150	100	0.3378	160	55	34.37

4.3 The Ultimate Punching Strength.

4.3.1 Effect of CFRP Reinforcement Ratio

Table (4-2) shows the effect of CFRP reinforcement ratio on the ultimate resistance of the slabs when all the other variables remain constant. It is clear that increasing the reinforcement ratio leads to increases the ultimate punching resistance of the slabs about 18% , 21.5% , 25% for (S-2, S-3, S-4) respectively, with respect to S-1. This is mainly due to the effect of reinforcement in resisting cracking propagation.

From comparison the ultimate experimental load with the ultimate load of ACI- 440-1R equation, it was found that the ratios were ranging from (1.3 - 1.48).

The ratio of the ultimate experimental load to ultimate load of El-Gamal equation is ranging from (1.54 – 1.8).

Table (4-2): Details of group 1 (slabs ultimate load)

Slab	*Thickness of slab t (mm)*	*Column* C(mm)	*CFRP ratio %*	*No. of bars in each direction*	$\rho_f/\rho_{b.}$	*Experimental load* P_u*(KN)*	$\frac{P_{u(S-n)}-P_{U(S-1)}}{P_{u(S-1)}}$ %	$P_{ACI-440}$ *(KN)*	P_{Gamel} *(KN)*	$P_{exp.}/p_{aci}$	$P_{exp.}/p_{Gam.}$
S – 1	100	150	0.3686	12	1.14	140	0	107.15	90.781	1.3	1.54
S – 2	100	150	0.3993	13	1.236	165	18	111.08	92.63	1.48	1.78
S – 3	100	150	0.43	14	1.33	170	21.5	114.93	95.718	1.48	1.78
S – 4	100	150	0.4607	15	1.426	175	25	118.65	97.78	1.48	1.8

where:

$$\rho_{fb} = \alpha_1\beta_1 \frac{f'c}{f_{fu}} \frac{E_f \varepsilon_{cu}}{E_f\varepsilon_{cu}+f_{fu}} \qquad \text{.....Eq. (4-1)}$$

$$\alpha_1 = 0.85 - 0.0015(f'c) \geq 0.67\,, \qquad \beta_1 = 0.97 - 0.0025(f'c) \geq 0.67$$

4.3.1.1 Effect of Reinforcement Ratio on Behavior of Slabs

Load-deflection curve for group 1 is shown in Figure (4-2). In general, all load deflection curves of all tested slabs have almost the similar behavior, and there are three stages can be seen in load-deflection curve. First, linear relationship between load and deflection this zone of load-deflection curve is called elastic zone and the first crack occurs at the end of this zone. Second, also linear relationship between load and deflection which is the load continue with deflection (loading stage), the third stage will start and the deflection continues to increase without any increasing in load (brittle failure). The deflection of all slabs is measured at two points, at center of slab . It is appeared that with increasing reinforcement ratio the deflection is decreased during loading stage. The strain of concrete is decreased by increasing the reinforcement ratio as shown from Figures (4-3) to (4-5) which is studied at four position of the compression zone of slab at (d/2 right of column, d/2 left of column, d of column, and 2d of the column as shown in Figure (4-1).

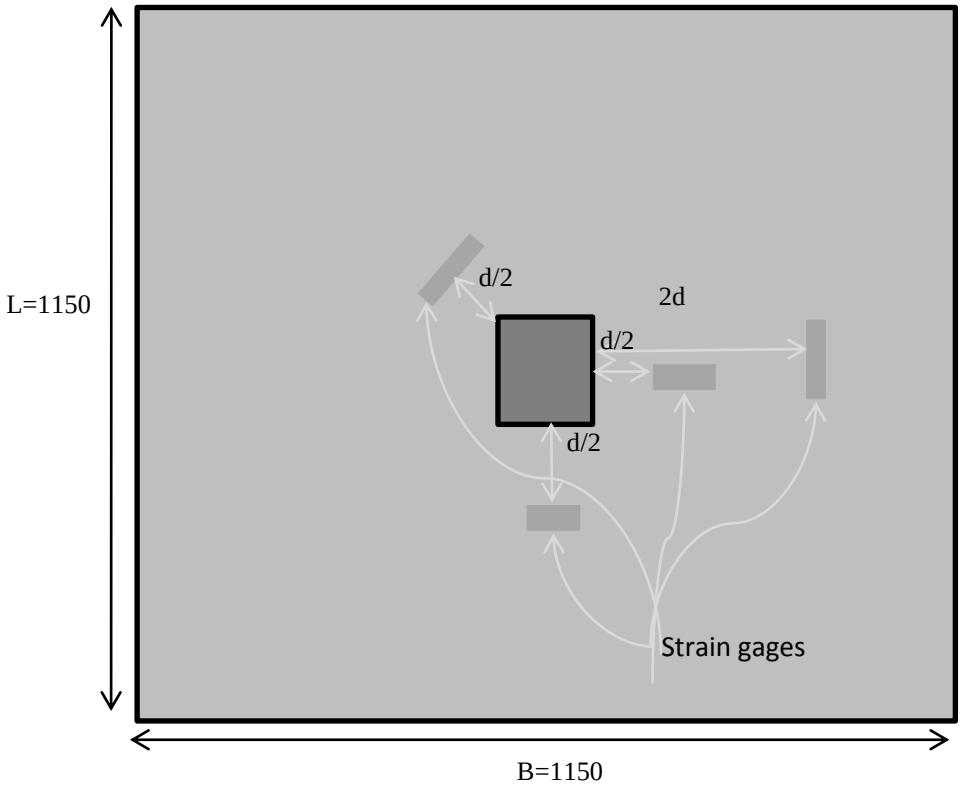

Fig (4-1): The position of strain gauges for all tested slabs

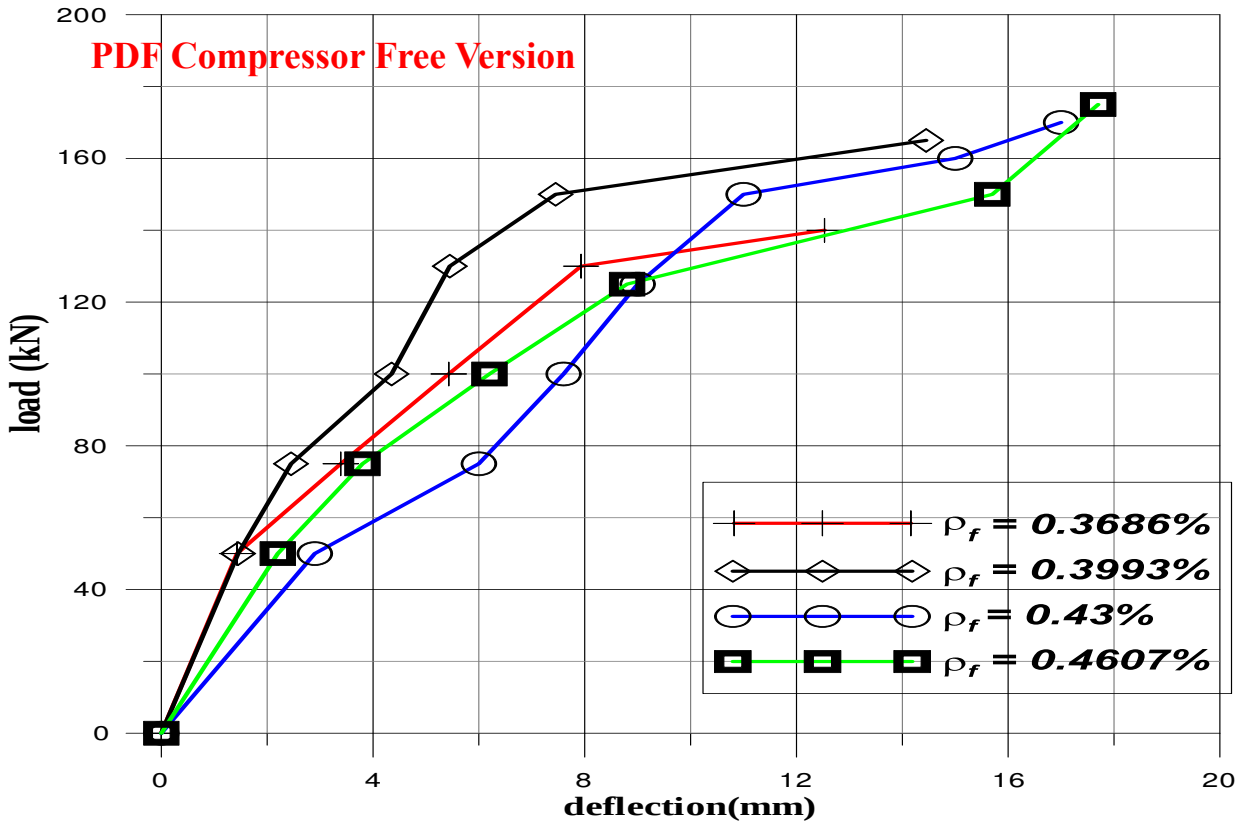

Fig (4-2): Load – deflection curve of group 1

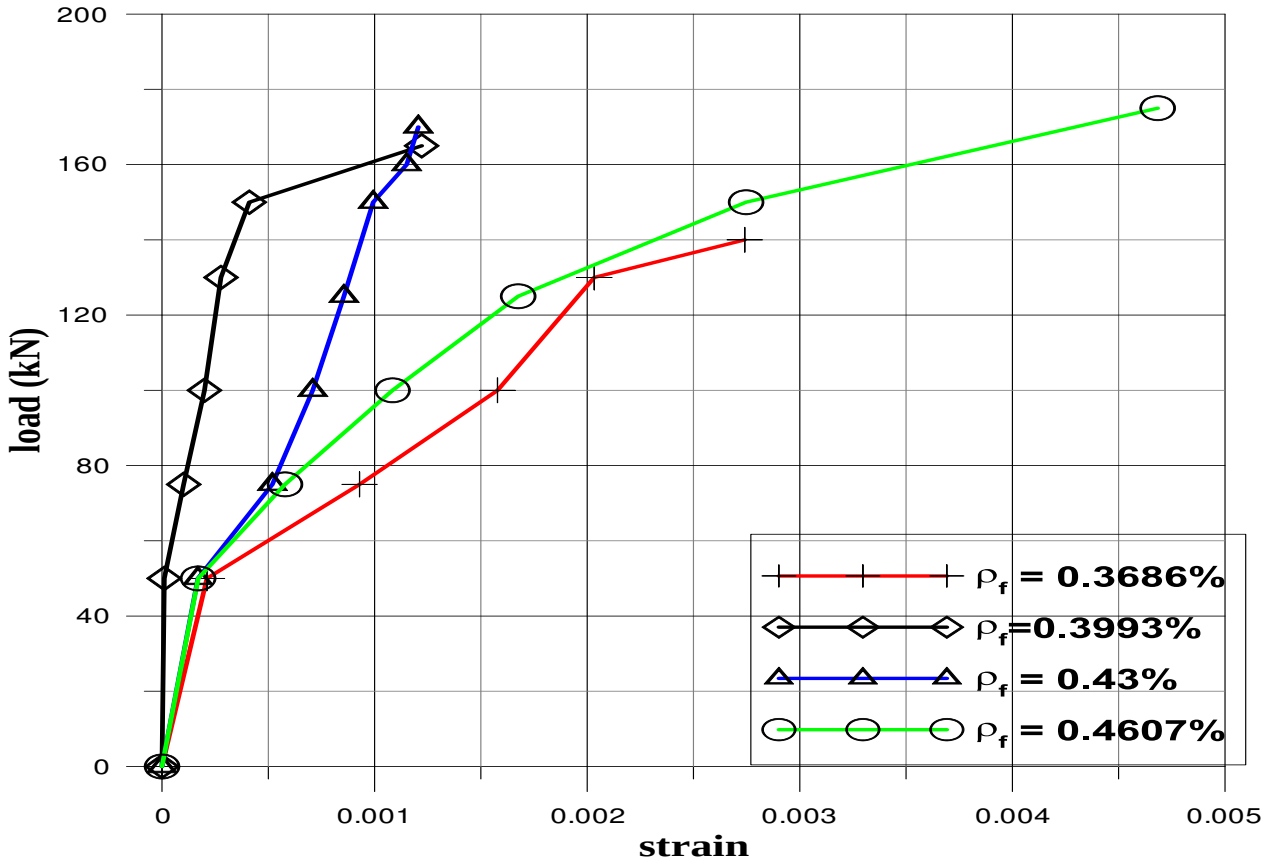

Fig (4-3): Load –Strain curve of group 1, at (d/2) right of face of column

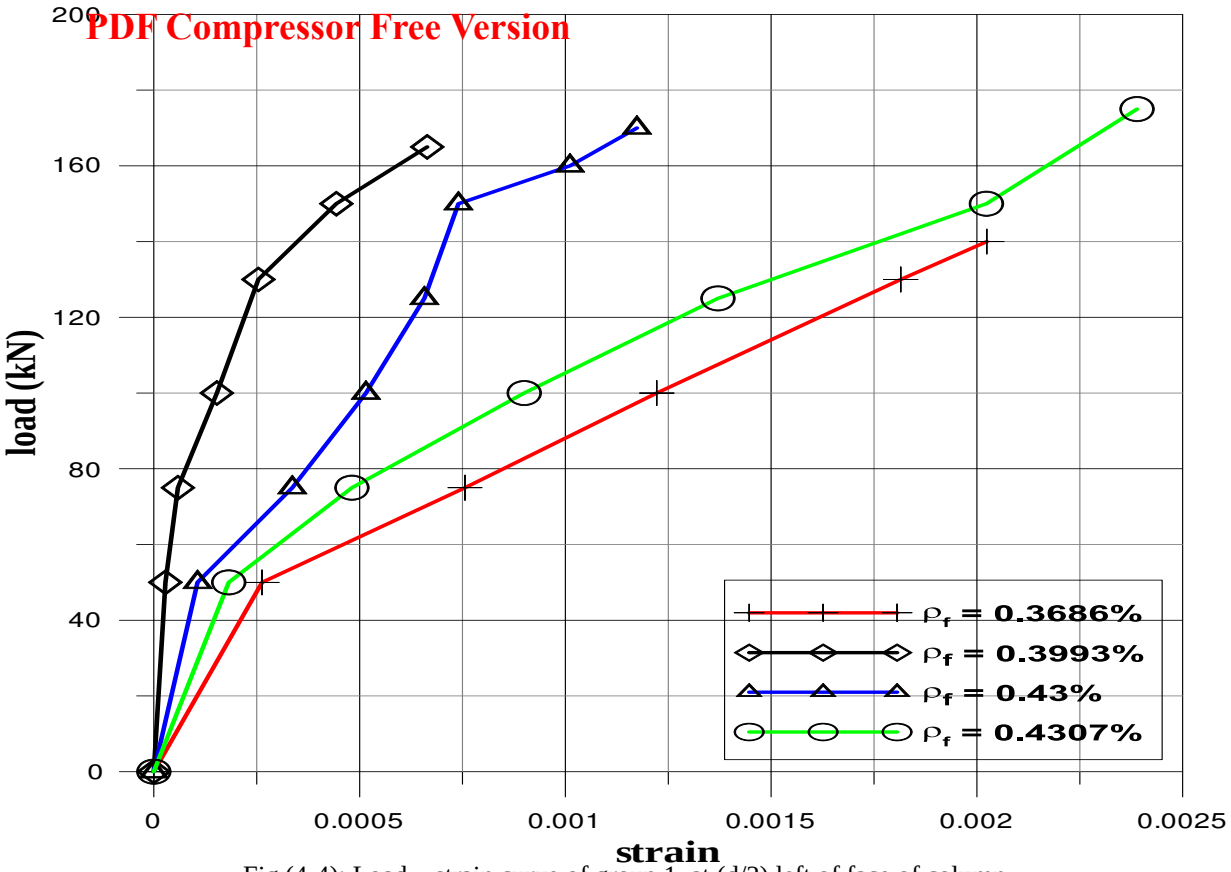

Fig (4-4): Load – strain curve of group 1, at (d/2) left of face of column

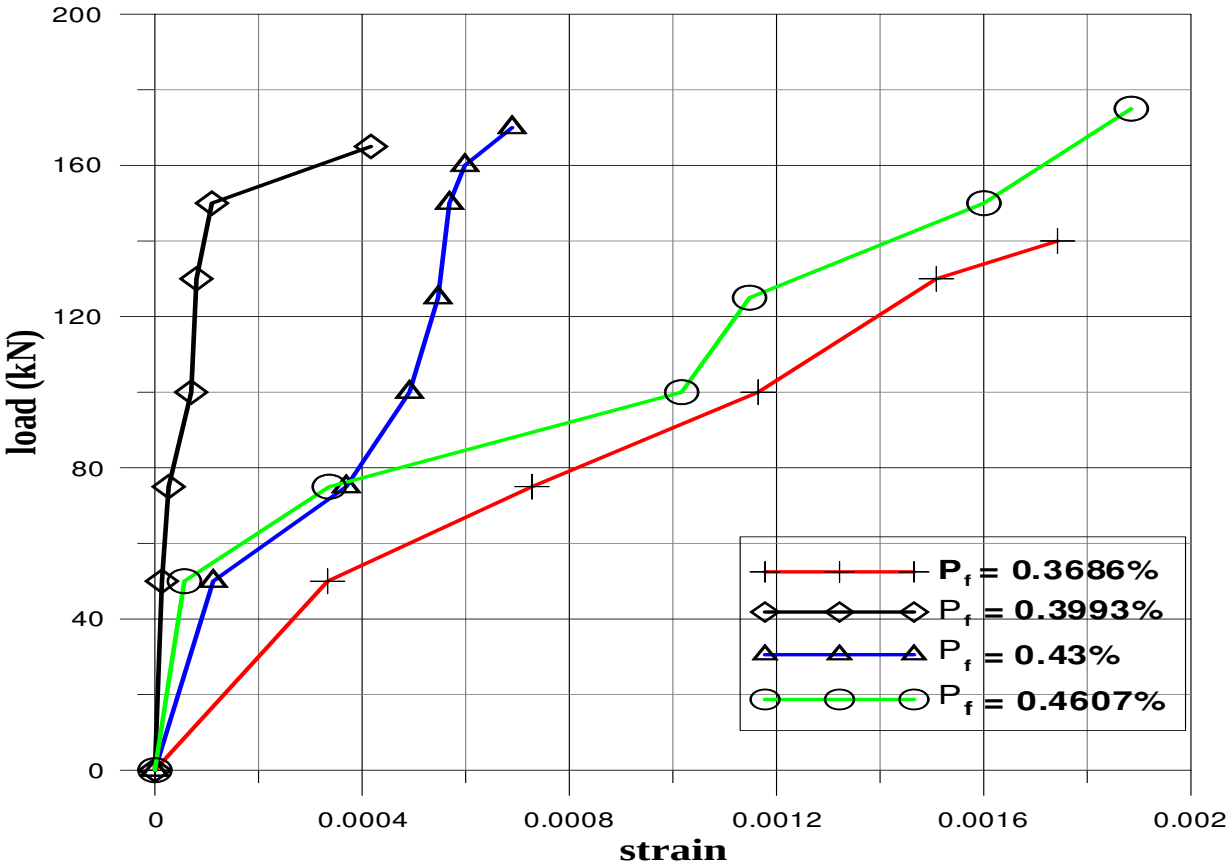

Fig (4-5): Load – Strain curve of group 1, at (2d) of face of column

4.3.2 Effect of Slab Thickness

Table (4-3) shows the effect of the slab thickness on the ultimate punching resistance of the slab. It was noted that by increasing the thickness of slab the ultimate punching shear capacity was increased, and its noted that by increasing the thickness of slab approximately 55% that's lead to increasing in punching resistance about 70%.

From comparison the ultimate experimental load with the ultimate load of ACI- 440-1R equation it was found that the ratio of their ranging approximately from (1 - 1.475).

The ratio of the ultimate experimental load to ultimate load of El-Gamal equation is ranging from (1.03 – 1.78).

From Figure (4-6), it was noted that the deflection is decreased because of the increasing in thickness of slabs and that is causing increasing in moment of inertia of section (Ig).

The strain of concrete was decreased by increased the thickness of slab and approximately linear relationship at loading stage at all position of strain gages as shown from Figure (4-7) to (4-10)

Table (4-3): Details of group 2 (slabs ultimate load)

Slab	*CFRP ratio %*	*Thickness of slab h (mm)*	*Column* C(mm)	*No. of bars in each direction*	$\rho_f / \rho_{b.}$	*experimen load* P_u*(KN)*	$P_{ACI-440}$ *(KN)*	P_{Gamel} *(KN)*	$P_{exp.}/P_{aci}$	$P_{exp.}/P_{Gam}$
S – 5	0.368	80	150	12	1.14	90	73.36	51	1.23	1.76
S – 6	0.4607	100	150	15	1.426	175	118.65	97.78	1.475	1.78
S – 7	0.4421	120	150	18	1.37	155	155.22	151.028	1	1.03
S – 8	0.453	150	150	22	1.4	270	205.4	218.66	1.32	1.23

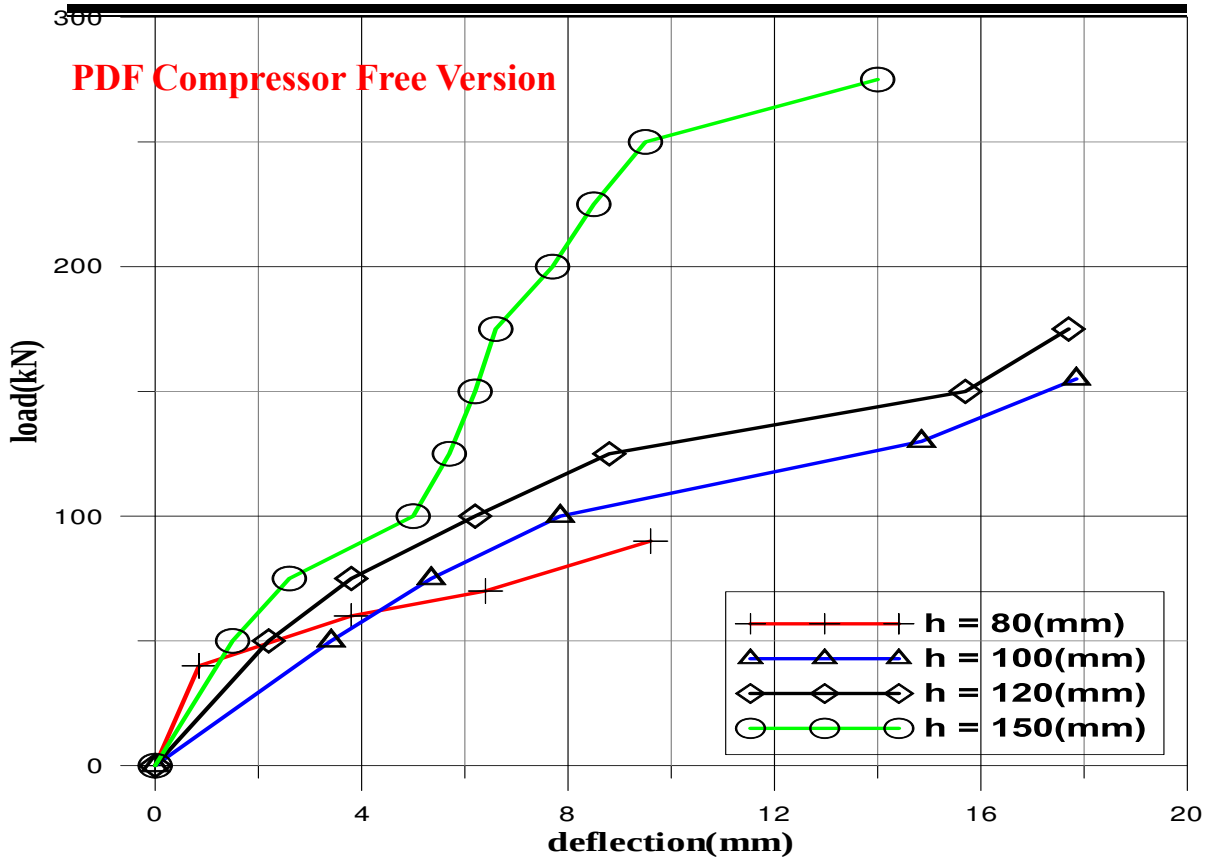

Fig (4-6):Load – deflection curve group 2,

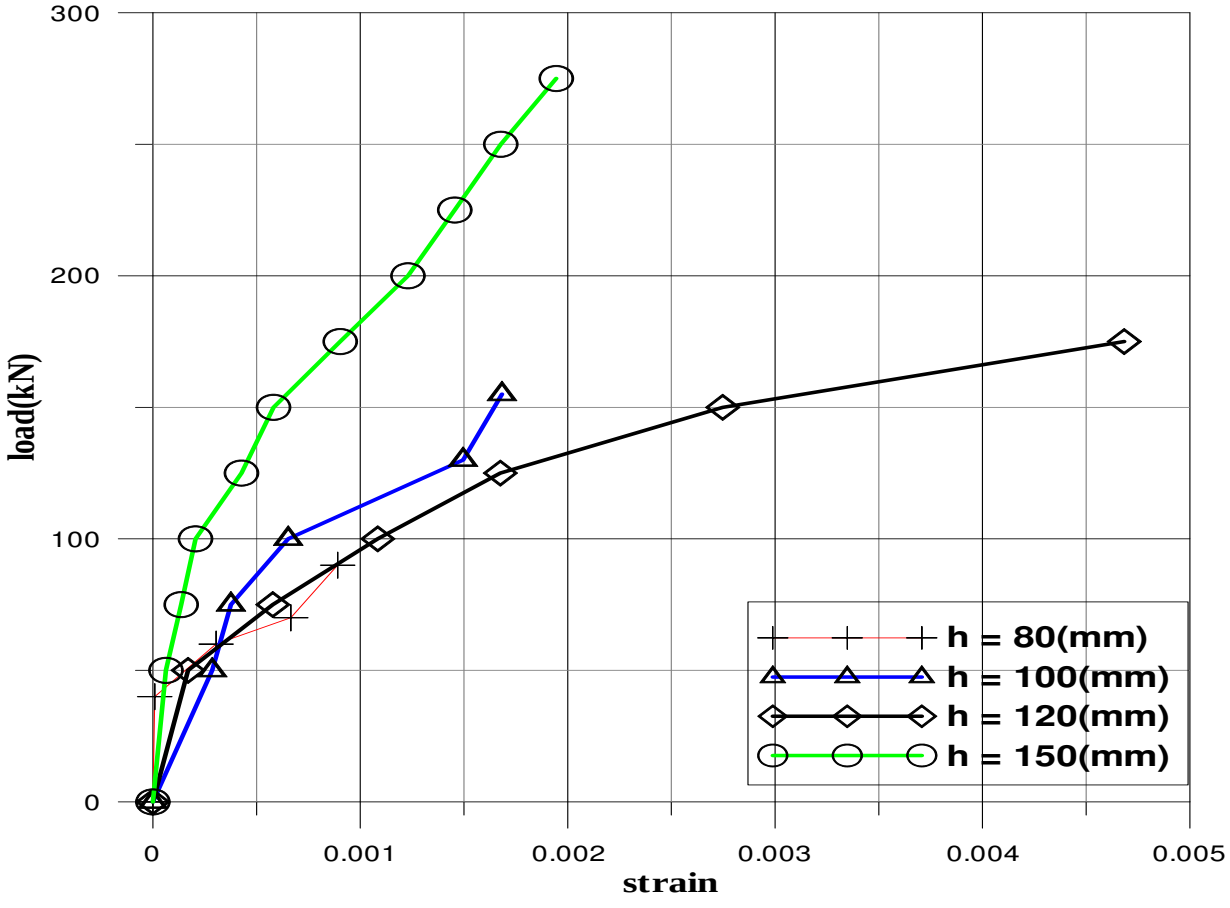

Fig (4-7):Load – strain curve of group 2, at (d/2) of face of column

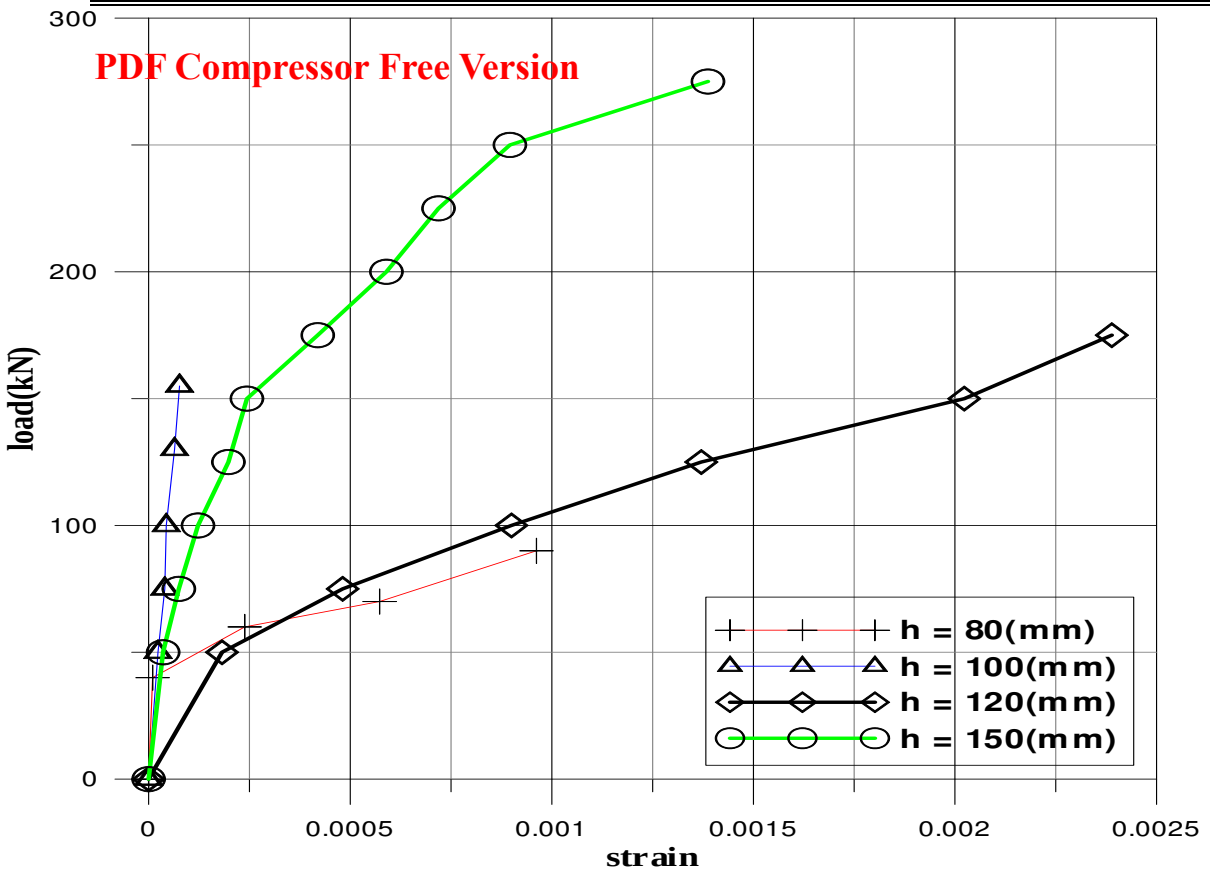

Fig (4-8):Load – strain curve of group 2, at (d.2) left of face of column

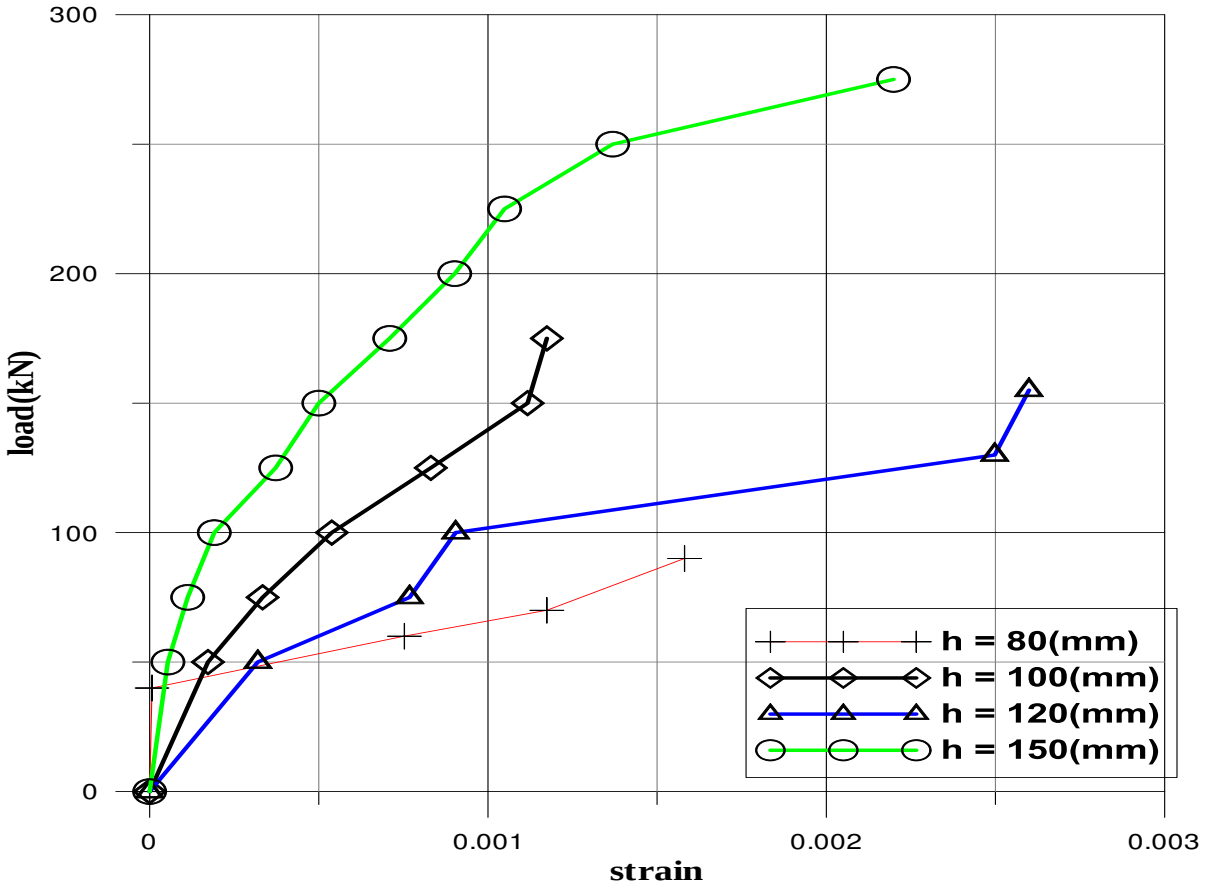

Fig (4-9):Load – strain curve of group 2, at diagonal (d/2) of face of column

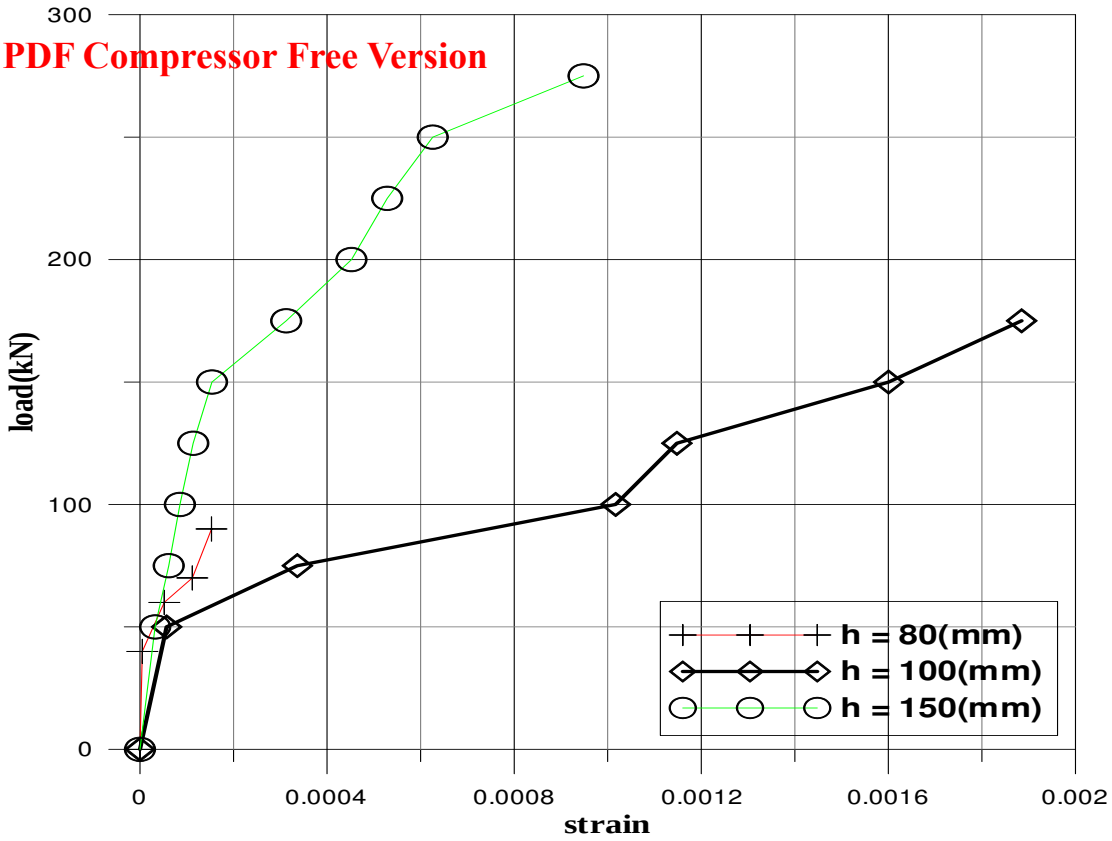

Fig (4-10):Load – strain curve of group 2, at (2d) of face of column

4.3.3 Effect of Column Dimension

Table (4-4) shows the effect of column dimension (parameter of column) on the ultimate punching shear capacity of the slab. Its noted that by increasing the perimeter of column the ultimate punching shear capacity is increased because of the influence of distribution of stress in the slab – column connection area. The ultimate punching resistance of the slabs about 4% , 8% , 31% for (S-10, S-11, S-12) respectively, by increasing the parameter 25%, 50%,and 75% with respect to S-9.

From comparison the ultimate experimental load with the ultimate load of ACI- 440 equation it was found that the ratio of their ranging from (1.36 - 1.54).

The ratio of the ultimate experimental load to ultimate load of El-Gamal equation is ranging from (1.5 – 1.87).

The strain of concrete is decreased by increasing the column area and approximately linear relationship at loading stage for all position of strain gauges as shown from Figure (4-12) to(4-15).

Table (4-4): Details of group 3 (slabs with ultimate load)

Slab	*CFRP ratio %*	*Thickness of slab h (mm)*	*Column* C(mm)	*No. of bars in each direction*	$\rho_f/\rho_{b.}$	*experimen load* P_u*(KN)*	$\frac{P_{u(S-n)} - P_{U(S-9)}}{P_{u(S-9)}}$ %	$P_{ACI-440}$ *(KN)*	P_{Gamel} *(KN)*	P_{exp}/P_{aci}	P_{exp}/P_{Gam}
S – 9	0.368	100	100	12	1.14	130	0	84	90.781	1.54	1.43
S – 10	0.368	100	125	12	1.14	135	4	95.5	90.6	1.41	1.5
S – 11	0.368	100	150	12	1.14	140	8	107	90.781	1.36	1.54
S – 12	0.368	100	175	12	1.14	170	31	119	90.781	1.42	1.87

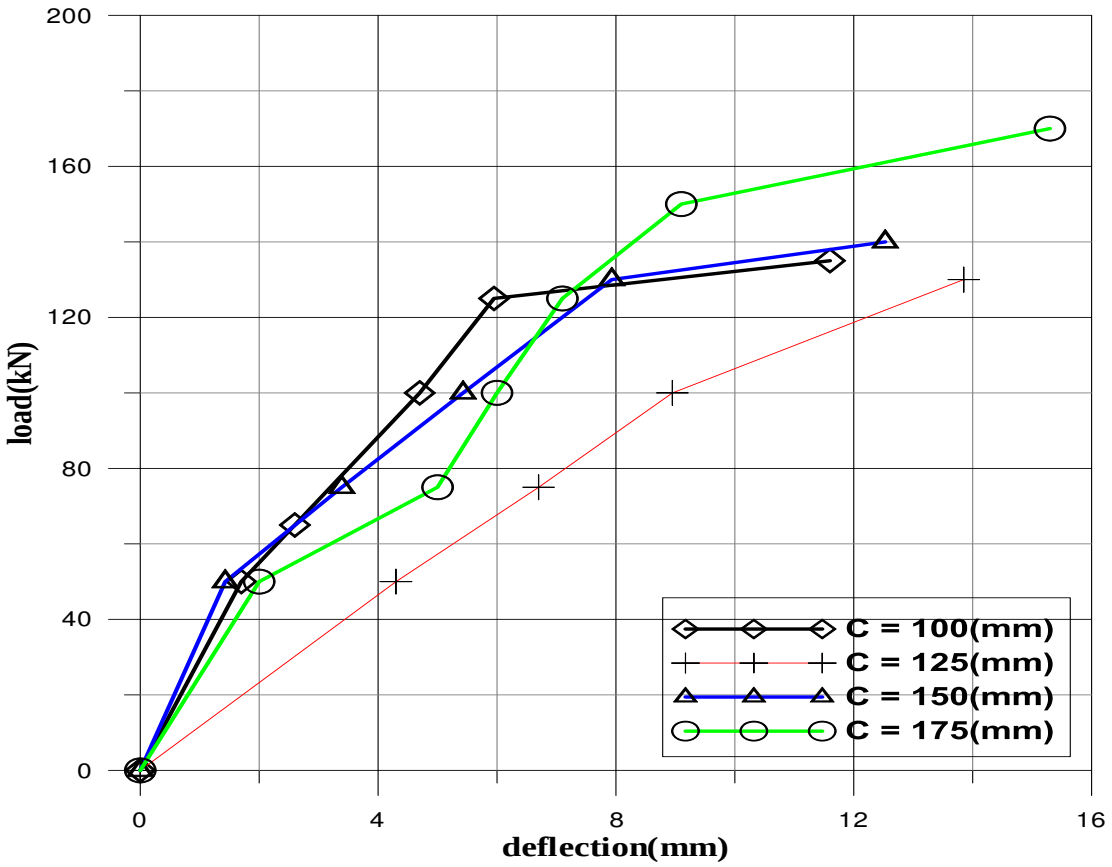

Fig (4-11):Load – deflection curve of group 3

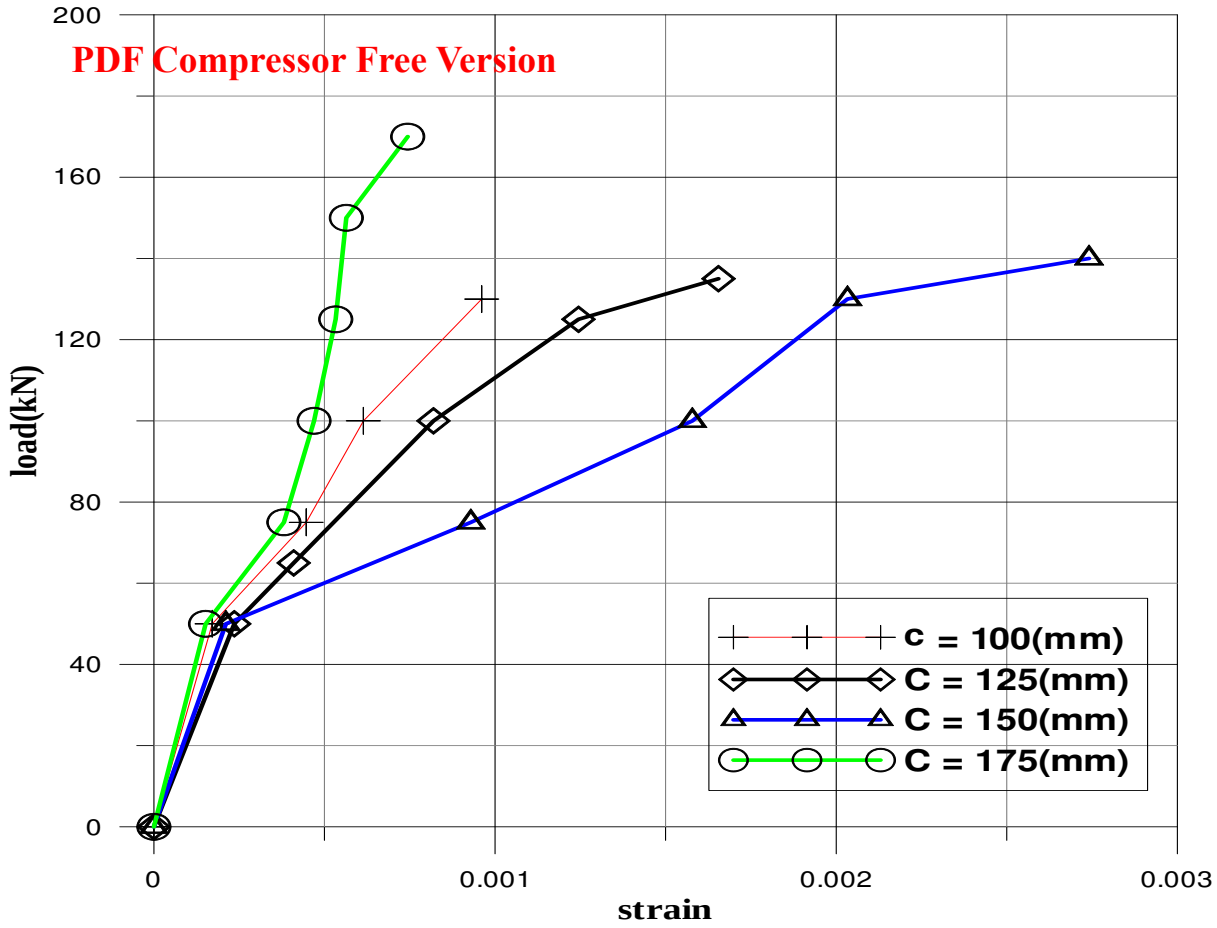

Fig (4-12):Load – strain curve of group 3, at (d/2) right of face of column

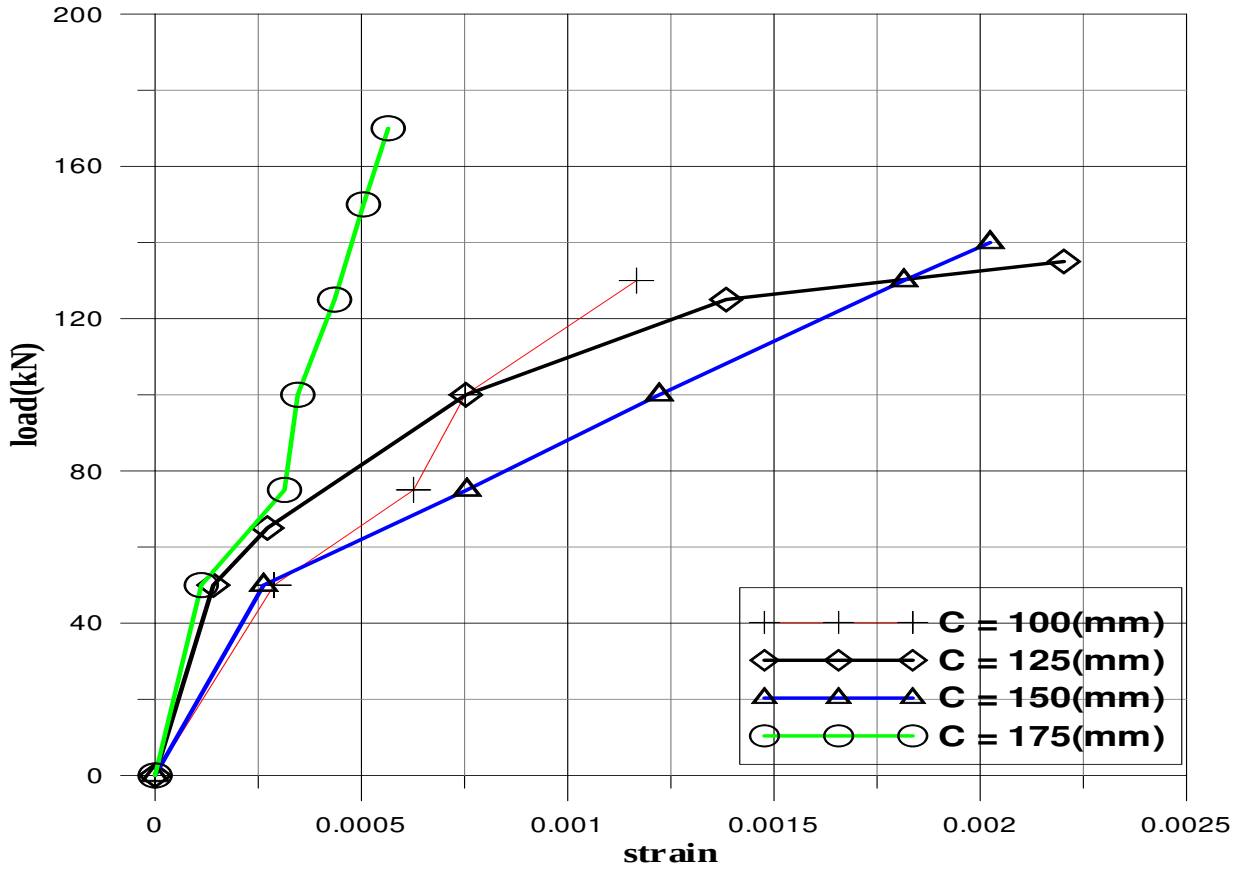

Fig (4-13):Load – strain curve of group 3, at (d/2) left of face of column

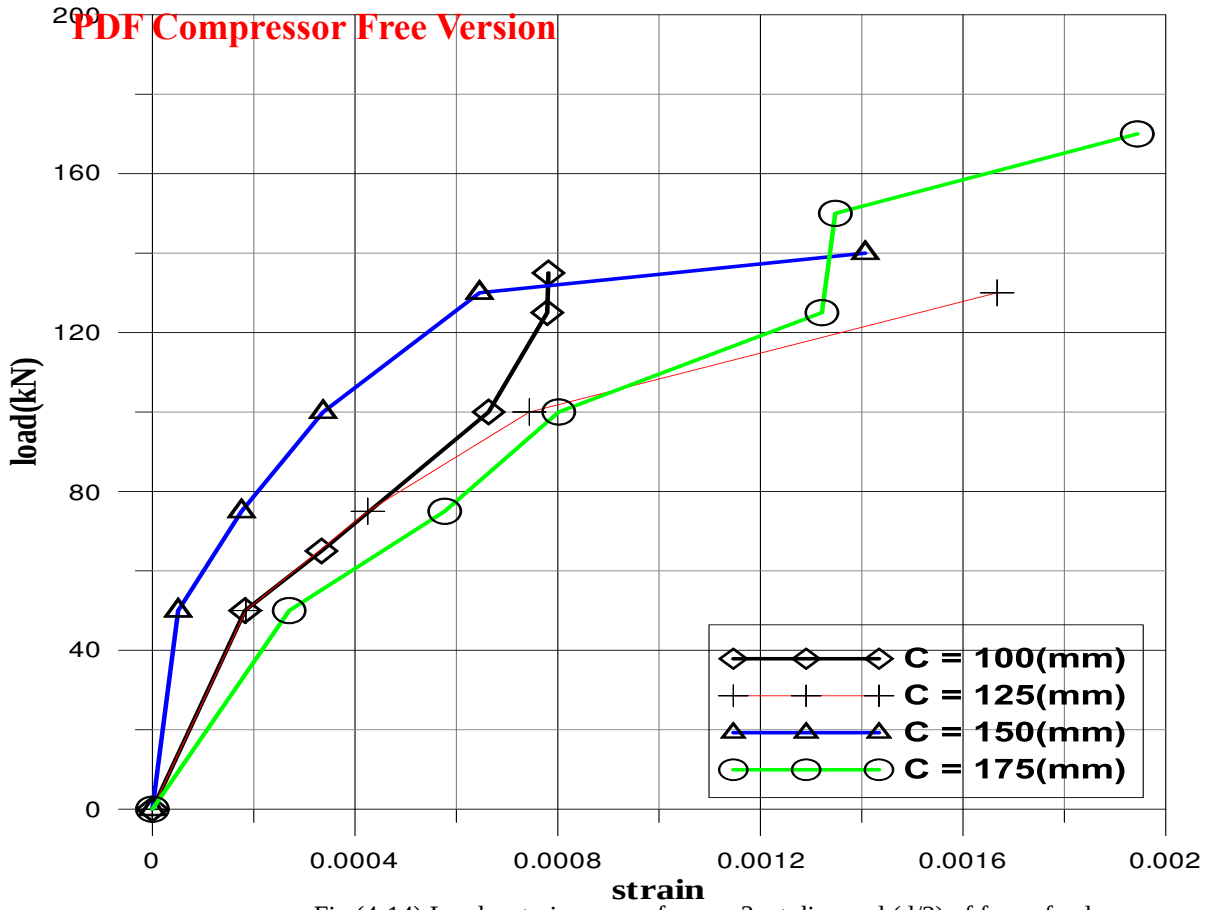

Fig (4-14):Load – strain curve of group 3, at diagonal (d/2) of face of column

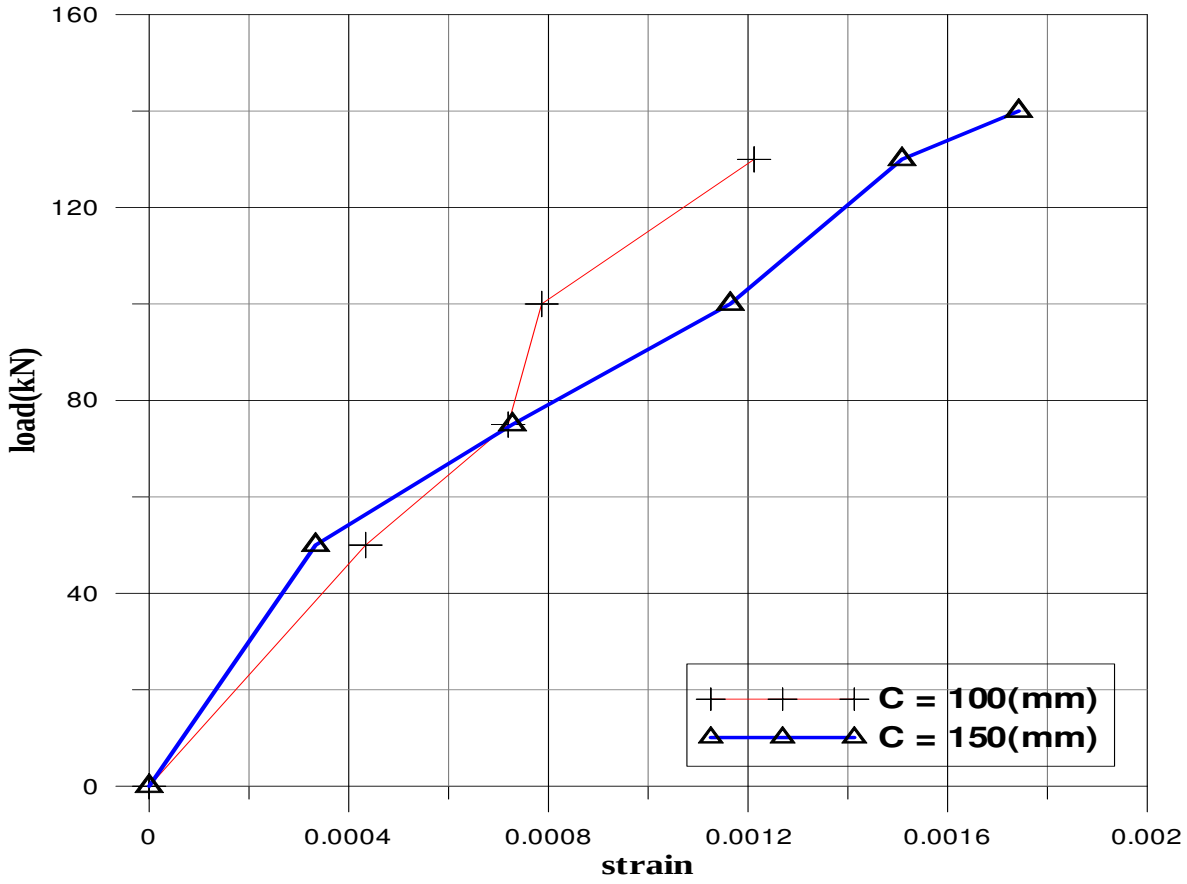

Fig (4-15):Load – strain curve of group 3, at (2d) of face of column

4.3.4 Effect of Arrangement of CFRP Reinforcement

Table (4-5) shows the effect of arrangement of CFRP reinforcement on the ultimate punching shear capacity and from comparison the ultimate experimental load with the ultimate load of ACI-440 equation it's found that the ratio of their ranging from (1.26 - 1.55).

The ratio of the ultimate experimental load to ultimate load of El-Gamal equation is ranging from (1.474 – 1.8).

All slabs design with the same variable except s-13 it is design with reinforcement ratio less than balance reinforcement ratio (ρ_b), to study the effect of increasing steel bar and notes the effect of absence of steel fiber at the perimeter of punching shear 4(C + d) on punching shear capacity and then its compared with the ACI-440-1R and El-gamal equation. Its noted that s-13 and s-14 have the same ultimate punching capacity from this it can be said that the increasing of steel bars in the perimeter of punching shear contribute, and the ratios of ultimate punching resistance are (1, 1.15, 1.23) for S-14, S-15, S-16 with respect of S-13. It is clear that the increasing of CFRP bars in critical zone contribute of increasing the punching shear capacity and decreasing the deflection as shown in Figure (4-16), that is because the reinforcement and steel fiber resist the cracks specially in the pperimeter of punching shear 4(c + d). All details of strain results show were shown in Figure (4-17) to (4-20).

Table (4-5): Details of group 4 (slabs with ultimate load)

Slab	*CFRP ratio %*	*Thickness of slab h (mm)*	*Column* C(mm)	*No. of bars in each direction*	$\rho_f / \rho_{b.}$	*experimen load* P_u(KN)	$P_{ACI-440}$ (KN)	P_{Gamel} (KN)	P_{exp}/P_{aci}	P_{exp}/P_{Gam}
S – 13	0.276	100	100	9	0.855	130	93.77	81.6	1.38	1.6
S – 14	0.3378	100	100	11	1.05	130	103	88.2	1.26	1.474
S – 15	0.3378	100	100	11	1.05	150	103	88.2	1.45	1.7
S – 16	0.3378	100	100	11	1.05	160	103	88.2	1.55	1.8

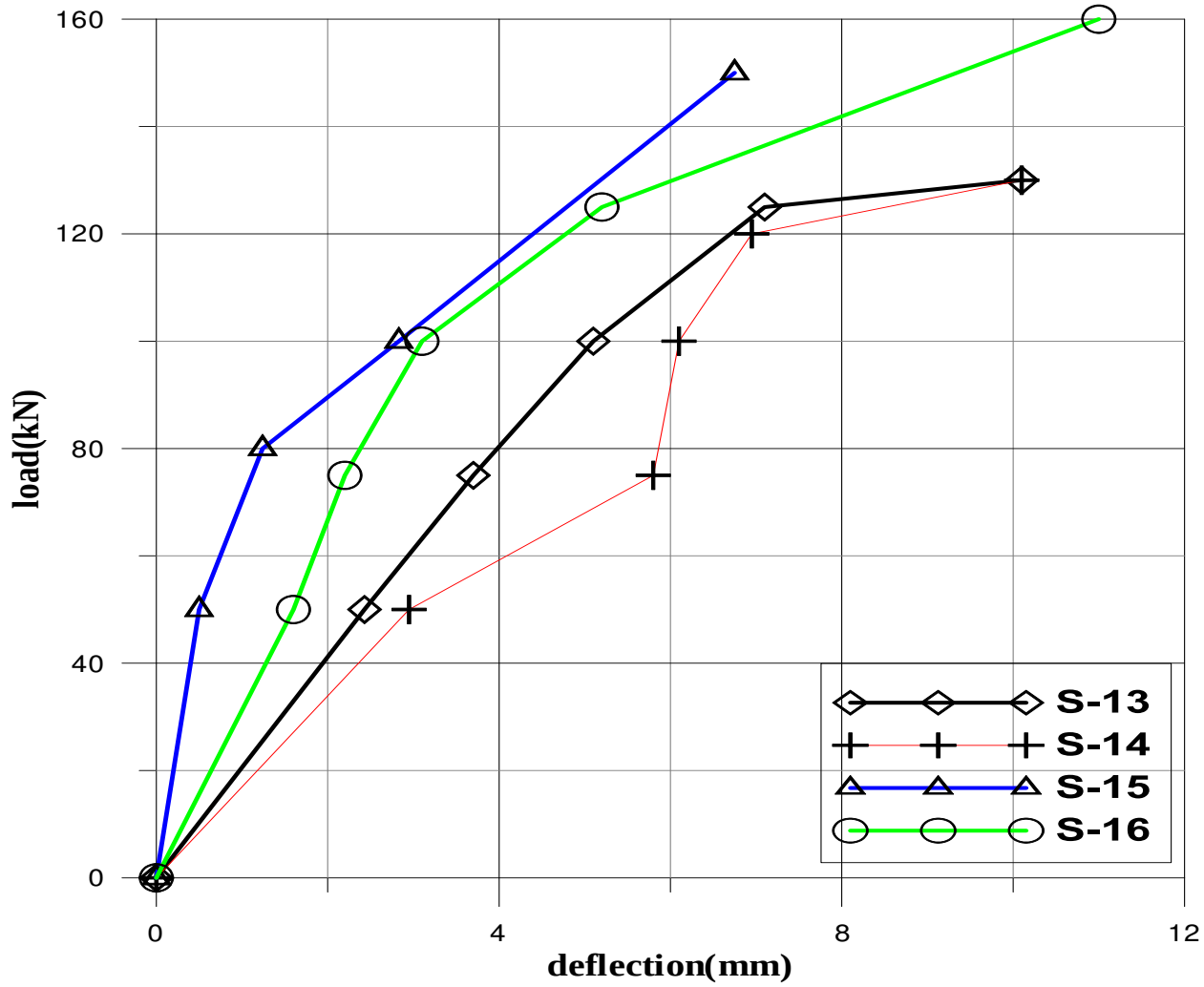

Fig (4-16):Load – deflection curve of group 4

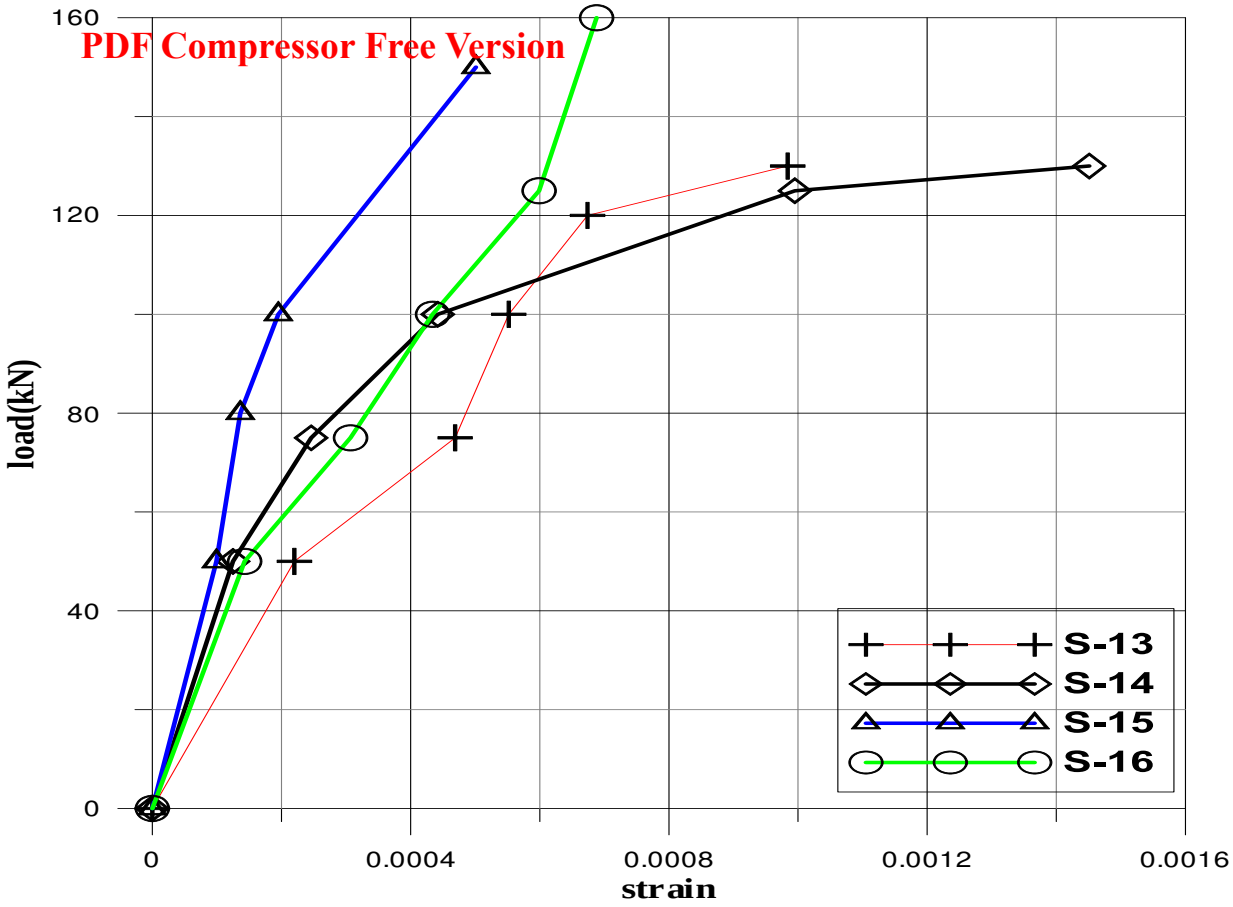

Fig (4-17):Load – strain curve of group 4, at (d/2) right of face of column

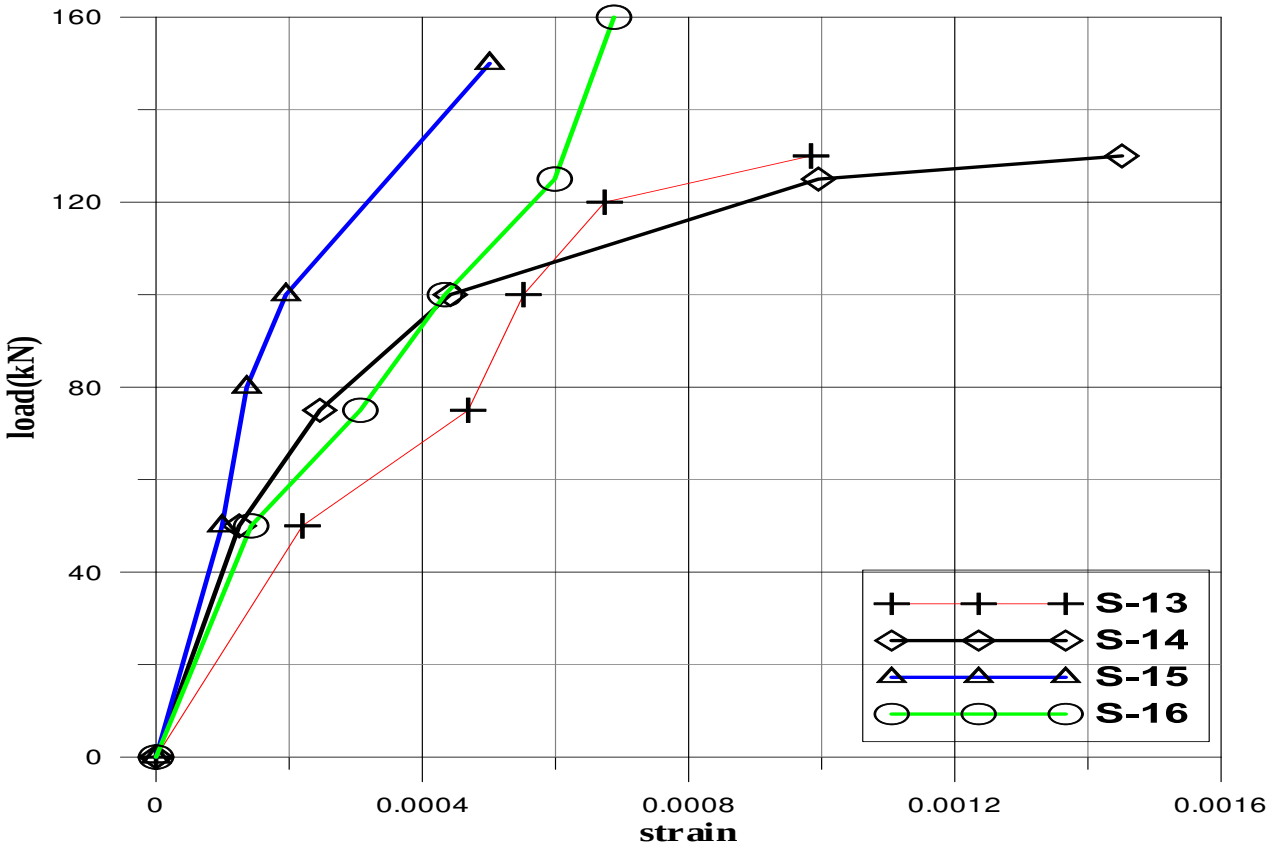

Fig (4-18):Load – deflection curve of group 4, at (d/2) left of face of column

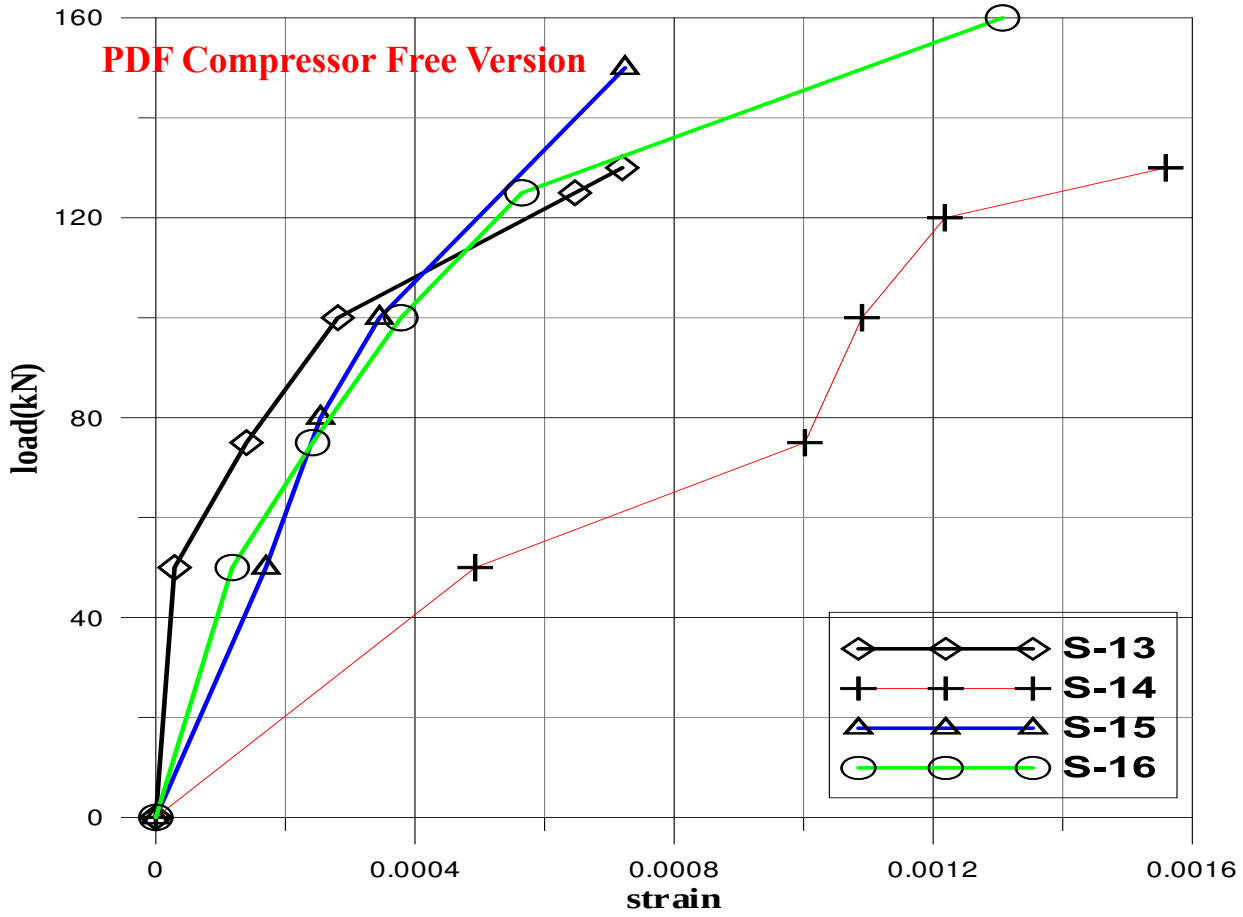

Fig (4-19):Load – strain curve of group 4, at diagonal (d.2) of face of column

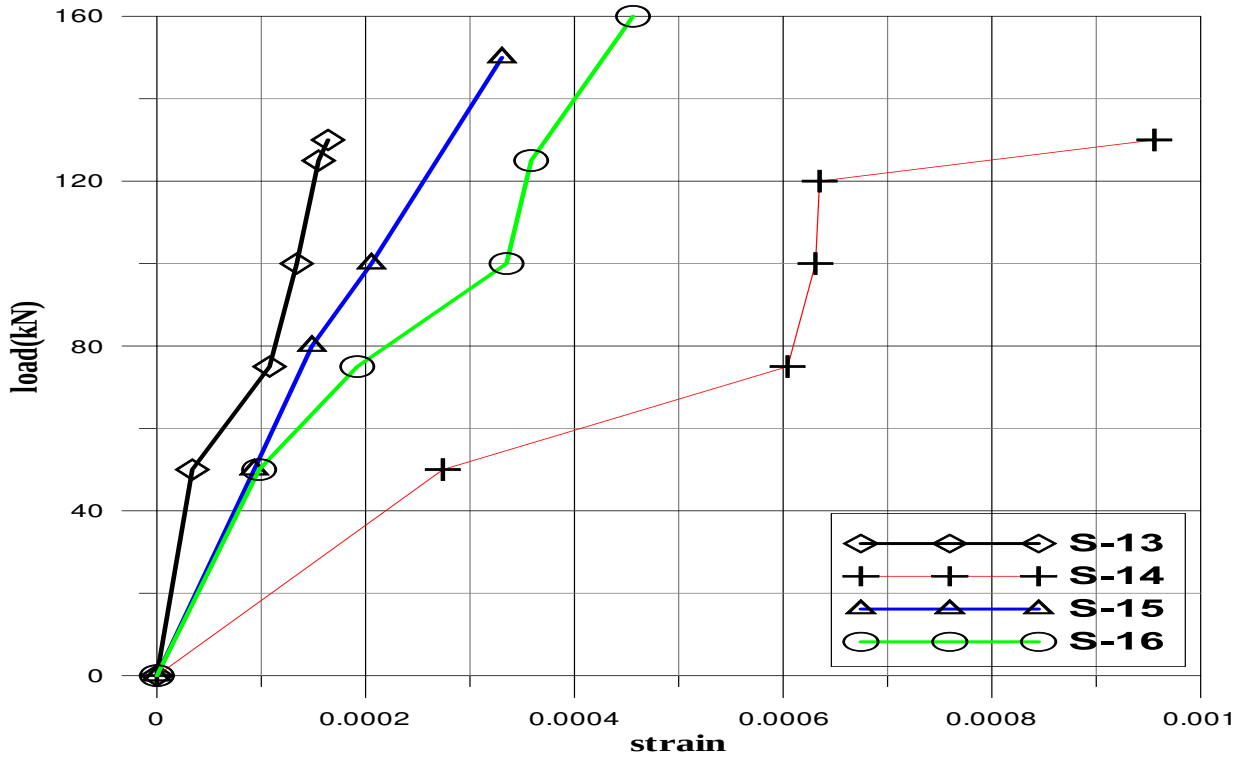

Fig (4-20):Load – strain curve of group 4, at(2d) of face of column

4-4: Failure Angles and Proposed Equation

The angles of failure, Figure (4-21), of the punching pyramid are measured by indicating the dimensions of crushed zone at the center line passing through the loaded area . It was observed that the angles of failure zone are about (19.71 -24.45) for the first group of tested slabs this indicated that the angle failure is decreased by increasing the reinforcement ratio because that the reinforcement ratio is restraint the path of cracks. The angle of failure rated from 18.12 to 24.01 for the second group of tested slabs its noted that by increasing the thickness of slab that leads to decrease the failure angle. It was (15.8-29.66) for the third group of tested slabs and (22.76-35.1) for the fourth group. It's clear that by increasing the area of loading the angle of failure is decreased.

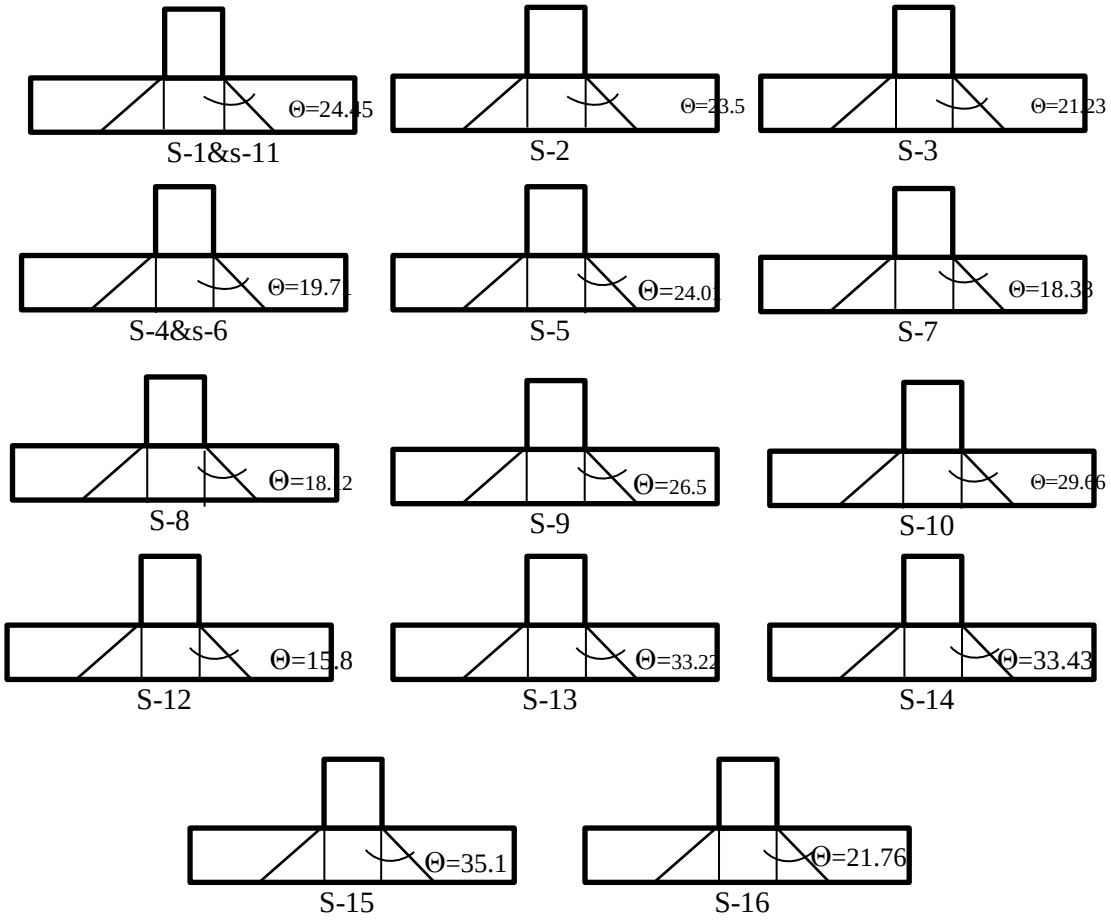

Fig. (4-82): Angles of failure for the tested slabs

From the angle of failure of the tested slabs, it can be noted that the critical distance of punching shear is approximately about (d/4) from the face of column therefor the critical parameter become [4(c + d/2)]. From the experimental results, a new equation of punching shear capacity is proposed as follow:

$$v_c = \frac{1}{K}\ \sqrt{f'c}\ \times\ 4\left(c + \frac{d}{2}\right)\ d\left(\frac{\rho_f}{100}\right)$$ .....Eq. (4-2)

where:

K= parameter that founded experimentally*

f'_c= compressive strength

c = column dimension

d = effective depth of slab

ρ_f = CFRP reinforcement ratio

From experimental result it was found that (*K*) = 1.6 , approximately, a comparison of the proposed equation with experimental results (P_u) and ACI-440-1R equation is shown in Figure (4-21).

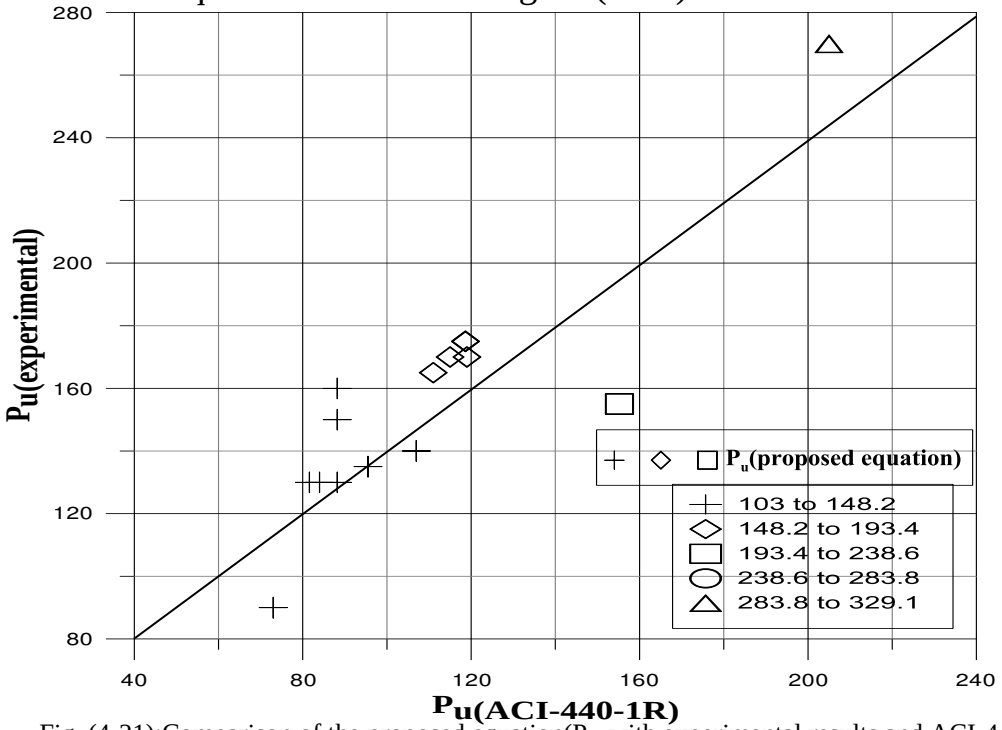

Fig. (4-21):Comparison of the proposed equation(P_u) with experimental results and ACI-440-1R

Chapter Five

FINITE ELEMENT ANALYSIS AND NUMERICAL MODELING

5.1 General

The nonlinear response of RC structures can be computed using the finite element method (FEM). This analytical method, gives the interaction of different nonlinear effects on RC structures. The success of analytical simulation is in selecting suitable elements, proper material models and in selecting proper solution method. The FEM is well suited for modeling composite materials with material models. The various finite element software packages are available. ANSYS (Analysis System), is an efficient finite element package available for the nonlinear analysis. This software becomes the most popular software in mechanical engineering, civil construction and science of materials namely with composite material and hybrid-materials structures. This chapter discusses the procedure for developing analysis model and materials simulations of RPC slab reinforced by CFRP bars in ANSYS Ver.11. The necessary steps to create the calibrated model are explained in detail and the steps taken to generate the analytical load-deformation response of the member are discussed.

5.2 ANSYS Computer Program

ANSYS is a comprehensive general-purpose finite element computer program that contains over 100,000 lines of code and more than (180) different elements. It is capable of performing static, dynamic, heat transfer,

fluid flow, and electromagnetism analysis. It can be used in many engineering

fields, including structures, aerospace, electronic and nuclear problems [71].

One of the main advantages of ANSYS is the integration of the three phases of finite element analysis: preprocessing, solution and post processing.

Preprocessing routines in ANSYS define the model, boundary conditions, and loadings. Displays may be created interactively on a graphics terminal as the data are input to assist the model verification. Post processing routines may be used to retrieve analysis results in a variety of ways. Plots of the structure's deformed shape and stress or strain contours can be obtained in the post processing stage.

5.3 Equilibrium Conditions

To form the element equations, the principle of virtual work is used in the equilibrium equation for a nonlinear structure in a static equilibrium. The principle states that " if a general structure in equilibrium is subjected to a system of small virtual displacements within a compatible state of deformation, the virtual work due to the external action is equal to the virtual strain energy due to the internal stress [71].; Thus:

$$W_{int.} = W_{ext.} \quad \text{……………………………………………..} \quad (5\text{-}1)$$

Where:

$W_{int.}$ = internal work (strain energy)

$W_{ext.}$ = external work (work done by the applied force)

The virtual internal work is:

$$W_{\text{int.}} = \int_{v} \{\partial\varepsilon\}^{T} \{\sigma\}.dV \quad \text{…………………………………………} \quad (5\text{-}2)$$

where:

$\{\varepsilon\}$ = elements of virtual strain vector

$\{\sigma\}$ = elements of real stress vector

dV = infinitesimal volume of the element

By using the general stress-strain relationship, stresses, $\{\sigma\}$ can be determined from the corresponding strains $\{\varepsilon\}$ as:

$$\{\sigma\} = [C]\cdot \{\varepsilon\} \quad \text{..... (5-3)}$$

Where:

$[C]$= constitutive matrix

After substituting equation (5-3) into (5-2), the virtual internal work can be written as:

$$W_{\text{int.}} = \int_v \{\partial\varepsilon\}^T [C] \{\varepsilon\}\, dV \quad \text{..... (5-4)}$$

The displacements $\{U\}$ within the element are related by interpolation to nodal displacements $\{a\}$ by:

$$\{U\} = [N]\cdot\{a\} \quad \text{..... (5-5)}$$

Where:

$[N]$ = shape function matrix

$\{a\}$ =unknown nodal displacements vector (local displacements)

$\{U\}$= body displacements vector (global displacements).

By differentiating equation (5-5), the strains for an element can be related to its nodal displacements by:

$$\{\varepsilon\} = [B]\ \{a\} \quad \text{..... (5-6)}$$

Where:

$[B]$= strain-nodal displacement relation matrix, based on the element shape functions.

Assuming that all effects are in the global Cartesian system, and then combining equation (5-6) with equation (5-4) yields:

$$W_{int.} = \{\partial a\}^T . \int_v [B]^T [C] [B] \, dV . \{a\} \quad \text{..... (5-7)}$$

The external work, which is caused by the nodal forces applied to the element, can be accounted for by:

$$W_{ext.} = \{a\}^T \cdot \{F\} \quad \text{..... (5-8)}$$

Where:

$\{F\}$= nodal forces applied to the element

Finally, equations (5-1), (5-7) and (5-8) may be combined to give:

$$\{\partial a\}^T \int_v [B]^T [C] [B] \, dV \, \{a\} = \{\partial a\}^T \{F\} \quad \text{..... (5-9)}$$

Noting that $\{\partial a\}^T$ vector is a set of arbitrary virtual displacements, the condition required to satisfy equation (5-9) can be reduced to:

$$[K^e] . \{a\} = \{F\} \quad \text{.....(5-10)}$$

Where:

$$[K^e] = \int_v [B]^T [C] [B] \, dV \quad \text{..... (5-11)}$$

$[K^e]$ = Element stiffness matrix

$dV = dx . dy . dz$

Equation (5-10) represents the equilibrium equation on a one-element basis. For all elements, the overall stiffness matrix of the structure $[K]$ is built up by adding the element stiffness matrices (adding one element at a time), after transforming from the local to the (overall) global coordinates, this equation can be written as:

$$[K] \{a\} = \{F^a\} \quad \text{..... (5-12)}$$

Where:

$[K] = \sum_{n} [K^e]$ = overall structural stiffness matrix.

$\{F^a\} = \{F\}$ = vector of applied loads (total external force vector).

n = total number of elements.

5.4 Finite Element Representation

In structural analysis, the finite element method has been used as a general method of stress and deformation analysis. A three dimensional solid element is an alternative way to finite element representation of the structures. These elements that are used in ANSYS program are shown in Table (5-1) [71].

Table (5-1): Finite element representation of structural components

Structural component	**Finite element representation**	**Element designation in ANSYS**
Concrete (RPC)	8-node brick element (3 translation DOF per node)	SOLID 65
CFRP reinforcement bars	2-node discrete element (3 translation DOF per node)	LINK 180

5.4.1Finite Element Representation of Reinforced Concrete

The finite element idealization of reactive powder concrete RPC slab should be able to represent the concrete cracking, crushing, the interaction between concrete and reinforcement, the interaction between concrete and steel fibers to reduce crack growth and the capability of concrete to transfer shear after cracking by aggregate interlock. However, In order to investigate failures where shear plays a major role, the three dimensional elements are to be used [72].

In the current study, a three-dimensional brick element with 8 nodes (SOLID-65) was used to model the RPC concrete. The element has eight corner nodes, and each node has three degrees of freedom (u, v and w in x, y and z direction, respectively). The steel fiber reinforcement modeling is done by assuming steel fiber embedded in solid 65 element. The element is capable of plastic deformation, cracking in three orthogonal directions, and then crushing. The geometry and node locations for this element type are shown in Figure (5-1) [71].

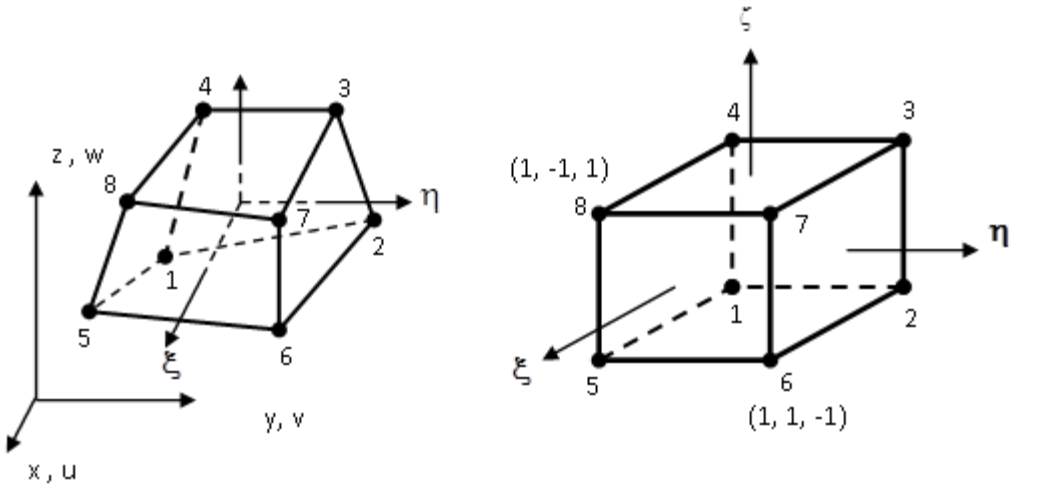

a) General 8-node Brick Element in Global Coor.

b) 8-node Brick Element in Local Coordinates

Fig. (5-1) : Three-dimensional 8-node brick (SOLID 65) element [71]

5.4.2 Finite Element Model of Reinforcement

Three techniques exist to model steel reinforcement in finite element models for reinforced concrete [73], these are:-

5.5.2.1 Discrete Representation

In the discrete representation which has been widely used the reinforcement is modeled as one dimensional bar or beam elements that are connected to concrete mesh nodes as shown in Figure (5-2a). Therefore, the concrete and the reinforcement mesh share the same nodes and the same

occupied regions. Full displacement compatibility between the reinforcement

and concrete is a significant advantage of the discrete representation. The disadvantages are the restriction of the mesh and the increase in the total number of elements.

5.4.2.2 Embedded Representation

The embedded representation is often used with high order isoparametric elements. The bar element is built in a way that keeps reinforcing steel displacements compatible with the surrounding concrete elements as shown in Figure (5-2b). When reinforcement is complex, this model is very advantageous.

5.5.2.3 Smeared (Distributed) Representation

The stiffness matrix of the reinforcing steel is evaluated separately and then added to that of the concrete to obtain the global stiffness matrix.

The smeared model assumes that reinforcement is uniformly spread in a layer throughout the concrete element in a defined region of the finite element mesh as shown in Figure (5-2c). This approach is used for large scale models where the reinforcement does not significantly contribute to the overall response of the structure.

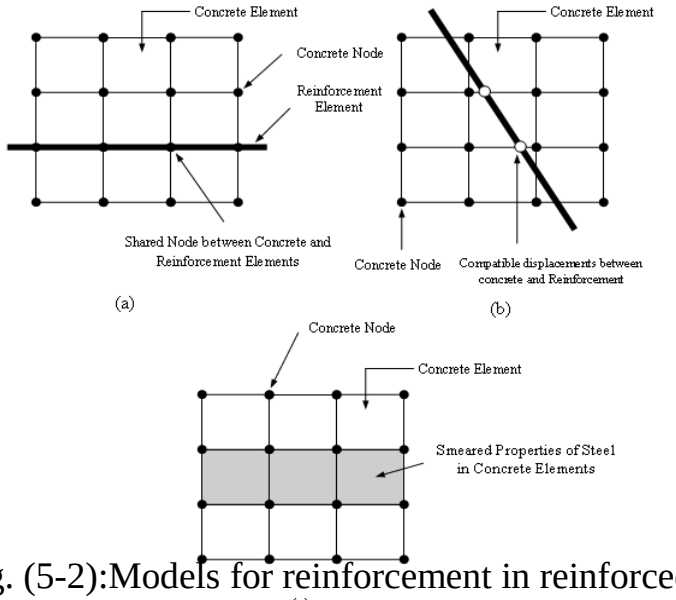

Fig. (5-2):Models for reinforcement in reinforced concrete:
(a) discrete;(b) embedded; and (c) smeared [73]

In the present study, the main CFRP reinforcement is represented by using 2-node discrete representation (LINK180 element in ANSYS V.11) as shown in fig (5-3). The CFRP reinforcement is assumed to be capable of transmitting axial forces only, and perfect bond is assumed to exist between the concrete and the reinforcing bars. To provide the perfect bond, the link element for the steel reinforcing bar was connected between nodes of each adjacent concrete solid element, so the two materials share the same nodes.

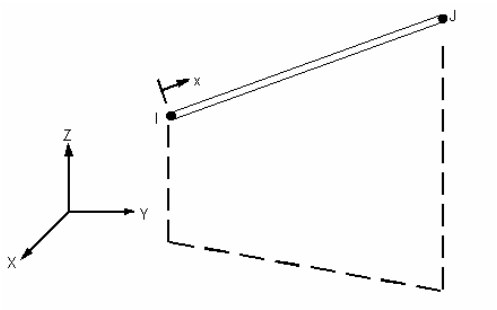

Fig. (5-3) LINK180 Element [71]

5.5 Nonlinear Solution Techniques

Most phenomena in solid mechanics are nonlinear. However in many applications, it is convenient and practical to use linear formulation for problems to obtain engineering solutions. On the other hand, some problems definitely require nonlinear analysis if realistic results are to be obtained such as postyielding and large deflection behavior of structures.

For reinforced concrete members, the nonlinear finite element analysis yields a wide range of useful information about displacements, strains, distribution of normal and shear stresses in concrete, crack pattern at different stages of loading and forces in the flexural steel reinforcements.

Nonlinear structural behavior arises from a number of cases, which can be grouped into these principal categories [74]:

1. Changing Status: Many common structural features exhibit nonlinear behavior that is status-dependent. For example, a tension-only cable is either slack or taut .

2. Geometric Nonlinearities: These arise when a structure experiences large deformations in geometric configuration that are sufficient to change the way by which the load is applied .

3. Material Nonlinearities: These arise when the properties of the material suffer from nonlinearity changes during the load history .

In the analysis of reinforced concrete and reactive powder concrete, the behavior of a nonlinear material is due to the continual and sudden change in the element stiffness which arises from cracking, crushing of concrete, fiber debonding, yielding of steel reinforcement and the plastic deformation of concrete and reinforcement. These represent the main sources of the nonlinearity. In the present study, the material nonlinearity is considered.

In the finite element analysis, the structural response to loading can be followed relatively easily in linear problems. While, in nonlinear problems, more sophisticated solution techniques should be employed. Usually, a nonlinear solution is obtained by making successive linear approximations until the constitutive laws and equilibrium conditions are satisfied within an acceptable error [75].

The solution of equation (5-12) for a linear elastic structural problem can be obtained directly. In nonlinear problems, a direct solution is no longer possible since the stiffness matrix [K] depends on the displacement level ([K] = [K (a)], and therefore, it cannot be exactly calculated before the determination of the unknown nodal displacements {a}. For a nonlinear solution, the state of equilibrium of a structural system corresponding to the applied load must be found. These equilibrium equations can be derived by

applying equilibrium conditions to the structural system. The equilibrium

equations can be expressed as:

$$\{r\} = \{p\} - \{F^a\} \quad \text{..... (5-13)}$$

where

$\{r\}$=out of balance force vector.

$\{p\}$=vector of the nodal forces equivalent to the internal stress level,

which is given by:

$$\{p\} = \int_v [B]^T \{\sigma\}\, dV \quad \text{..... (5-14)}$$

The equivalent internal forces also depend on the displacement level, $\{P\} = \{p\ (a)\}$, and have to be approximated in successive steps until equation (5-12) is satisfied.

The solution of nonlinear problems by the finite element method is usually attempted by one of the following three basic techniques:

1-Iterative techniques

2-Incremental techniques

3- Incremental- Iterative techniques

In the present work Incremental-Iterative techniques were utilized.

5.5.1 Incremental-Iterative Techniques

This technique, Fig.(5-4), is usually carried out by applying the external loads as a sequence of sufficiently small increments, and within each increment of loading, iterations are performed until equilibrium is satisfied according to some selected convergence criterion. This mixed method is widely used in the analysis of reinforced concrete structures because of its accuracy and capability to provide information throughout the loading history.

The incremental-iterative solution procedures, which have been used in the present study, use the following procedures [76]:

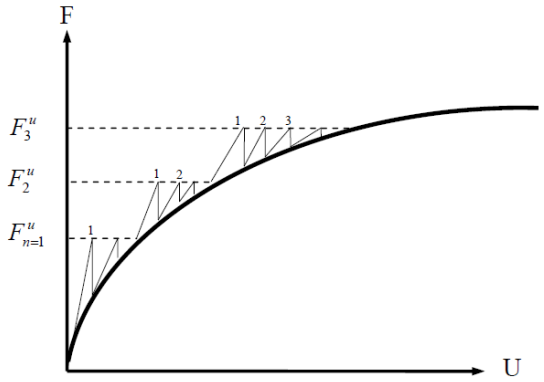

Fig.(5-4): Incremental-iterative techniques [76]

5.5.1.1 Full Newton-Raphson Procedure

In this procedure, the stiffness matrix is updated at every equilibrium iteration, thus a large amount of computation may be required to form and solve the stiffness matrix, Fig.(5-5) [76].

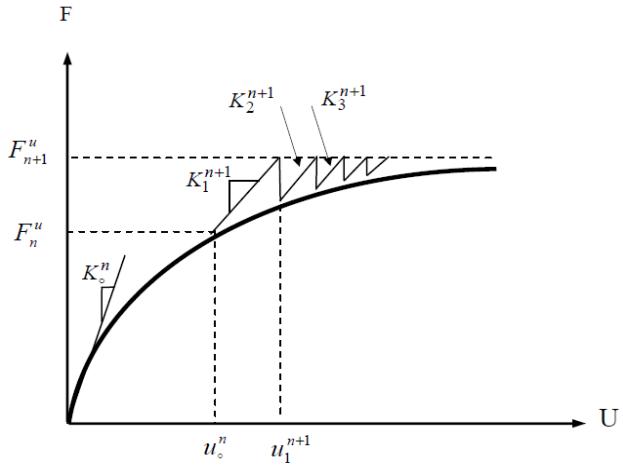

Fig. (5-5): Full Newton-Raphson method [76]

5.5.1.2 Modified Newton-Raphson Procedure

The modified forms of the Newton-Raphson method are most common. In one the stiffness matrix is updated at the beginning of the first iteration of every load increment (KT1 method). In case of two modifications, the stiffness matrix is calculated at the beginning of the second iteration (KT2

method), so that the nonlinear effects are more accurately represented in the stiffness matrix.

These methods are more economical than the full Newton-Raphson method because they involve fewer stiffness matrix reformulations, but the convergence is slower and a large number of iterations is required to achieve a converged solution, Fig.(5-6) [76].

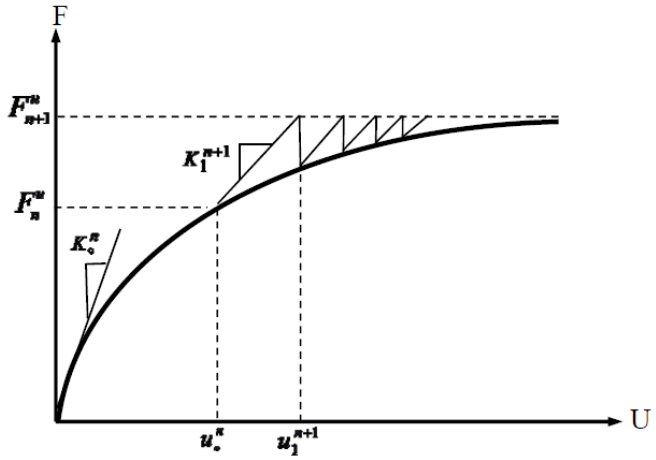

Figure (5-6): Modified Newton-Raphson [76]

5.5.1.3 Initial-Stiffness Procedure

In this procedure, the stiffness matrix is formed and solved only once at the beginning of the analysis, and the program uses this initial stiffness matrix at every equilibrium iteration. For this procedure, the computation cost per iteration is significantly reduced, but in case of strong nonlinearities (such as large deformation analyses), the method often fails to converge**,** Fig.(5-7).

In the present study, ANSYS Ver.11 uses the full Newton-Raphson method with the finite element method in analyzing the tested specimens [76].

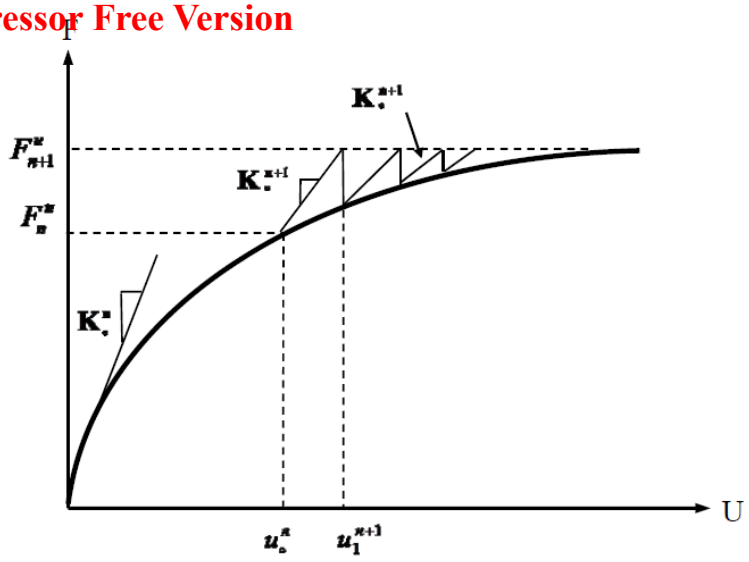

Fig.(5-7): Initial stiffness method [76]

5.5.2 Convergence Criterion

For the incremental-iterative solution method, the progress of the iterative procedure is monitored with reference to a specified convergence criterion. Convergence is assumed to occur when the difference between the external and internal forces becomes negligibly small, and the iterative process is then terminated. Selecting a suitable convergence tolerance usually specifies accuracy of the approximate solution. If the convergence tolerance is too loose, inaccurate results may be obtained, and if the tolerance is too tight, additional computational effort is spent to obtain needless accuracy.

However, nonlinear structural analysis with several convergence criteria can be used to monitor equilibrium. These criteria are usually based on out of balance forces, displacement or internal energy. The convergence criterion, adopted in the present study, uses the out of displacement convergence. The incremental displacements at iteration (i) relative to the total displacement are considered in the criterion. When the incremental displacements are within a given tolerance of the total displacements the solution is considered to have converged. The criterion can generally be written in the form [76]:

$$\left\|\{\Delta D_i\}\right\| = \left(\sum \Delta D_i^2\right)^{0.5} \le T_n \left(\sum D_i^2\right)^{0.5} \qquad \text{..... (5-15)}$$

Where: T_n = tolerance [varied between (0.0005-0.01) in this study].

$\{\Delta D_i\}$ = incremental displacement vector at (i) iteration.

n = total number of degrees of freedom.

5.5.3 Equilibrium Iteration (Analysis Termination Criterion)

The nonlinear finite element analysis used in simulating the response of reinforced concrete structures must include as well a criterion to terminate the analysis when failure of the structure is reached. In a physical test under load control, collapse of a structure takes place when no further loading can be sustained; this is usually indicated in the numerical tests by successively increasing iterative displacements and a continuous growth in the dissipated energy. Hence, when the convergence of the iterative process cannot be achieved and then it is necessary to specify a suitable criterion to terminate the analysis.

In the present study, a maximum number of iterations for each increment of load is specified to stop the nonlinear solution if the convergence tolerance has not been achieved. A maximum number of iterations in the range of (100) is used, because it is observed and found that this range is generally sufficient to predict the solution's divergence or failure [76].

5.6 Modeling of Materials Properties

Behavior of concrete extensively depends on the properties of each of its components; cement mortar, aggregates and air voids. In case of RPC, additional variables also influence its properties, such as the steel fiber volume fraction, silica fume and superplasticezar .

In many cases, the analysis and design of reinforced concrete structures encounters practical difficulties due to the complex material behavior involving phenomena such as inelasticity, cracking and interaction between

concrete and reinforcement. These complexities have led to the development

of many models for the analysis of plain and reinforced concrete.

The reinforcing steel can be considered as a homogeneous material and its properties are generally well defined.

On the other hand, plain concrete and fibrous concrete are heterogeneous materials having completely different properties in compression and in tension. Because of this heterogeneity, it is difficult to define their properties accurately.

Linear elastic orthotropic properties of the CFRP composite are assumed throughout this study. In addition, full bond between the concrete and CFRP is assumed to model the strength of reinforced slab.

5.6.1 Modulus of Elasticity

Modulus of elasticity is strongly influenced by the concrete materials and their proportions. It is a function of modulus of elasticity of each component and its content ratio in the composite. An increase in the modulus of elasticity of concrete is expected with an increase in the compressive strength since the slope of the ascending branch of the stress-strain diagram becomes steeper [77].

5.6.1.1 Static Modulus of Elasticity

Many researchers studied and carried out an experimental investigations to evaluate the modulus of elasticity for the RPC slab specimens tested at age of 28 days, depending on the specifications illustrated in ASTM C469 which states that, the static modulus of elasticity is calculated by the following equation:

$$E_c = (S_2 - S_1)/(e_2 - 0.00005) \quad \text{.....(5-15)}$$

where:

E_c : static modulus of elasticity, (MPa).

S_2 : stress corresponding to 40% of ultimate load, (MPa).

S_1 : stress corresponding to a longitudinal strain (0.00005), (MPa).

e_2 : longitudinal strain produced by stress S_2.

5.6.2 Poisson's Ratio (υ)

Experimental data on values of Poisson's ratio (υ) (i.e., the ratio of lateral to longitudinal strain) for RPC under uniaxial compressive stress are very limited. Poisson's ratio of UHPC may not differ too much from other concretes, but it may have a smaller range [78] as shown in Fig.(5-8). Within the elastic range the Poisson ratio for all investigated is always about 0.2 [78]. Others [79] found a similar value in the elastic strain region, and Poisson's ratio starts to increase only when the load exceeds 90 % of the peak strain. This ratio of 0.2 is also adopted in the present finite element analysis.

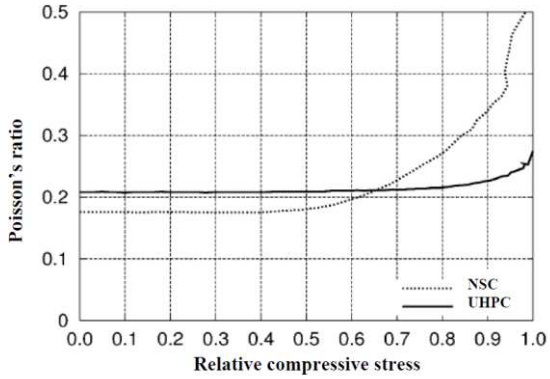

Fig.(5-8): Poisson's ratio vs relative compressive strength [78]

In this study, the concrete is assumed to be homogeneous and initially isotropic. The following paragraph deals with the material properties modeled in ANSYS Ver.11 .

5.7 Modeling of Cracked Concrete

The main feature of concrete behavior is its low tensile strength, which results in tensile cracking at very low stress, as compared with the failure stress in compression. When a principal stress exceeds its limiting value, a crack is assumed to occur in a plane normal to the direction of the offending

principal stress. Once a crack has formed it is generally assumed that tensile

stress cannot be sustained across the crack and the stiffness of the material is reduced to a negligible value in this direction.

With increased loading, additional cracks can form between the initial cracks, if the tensile stress exceeds the concrete tensile strength between previously formed cracks. Since cracking is the major source of material nonlinearity in the serviceability range of reinforced concrete structures, realistic cracking models need to be developed in order to accurately predict the load-deformation behavior of reinforced concrete members. Since the overall load-deflection is of primary interest in the present study, the cracking of concrete is modeled as "smeared-cracking model" as shown in Fig.(5-9) [76].

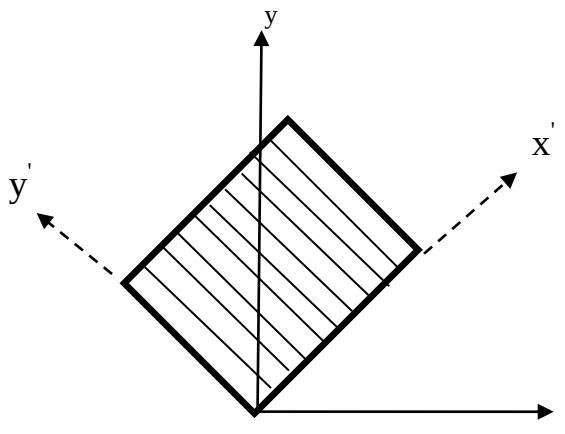

Fig. (5-9): Smeared Crack Modeling [76]

In this model, it is assumed that the cracked concrete becomes as an elastic orthotropic material after the first crack with reduced elastic modulus in the direction normal to the crack plane. A crack is represented by an infinite number of parallel fissures across that part of the finite element.

When cracking occurs at an integration point, it is modeled through an adjustment of materials properties, which effectively treats the cracking as a smeared band of cracks with fixed crack orientation. The cracking is permitted in three orthogonal directions at each integration point, when the failure criteria are to be satisfied in that direction [80].

5.8 Shear Retention Coefficients (Shear transfer across the cracks)

In tension, the stress-strain curve for concrete is assumed to be linearly elastic up to the ultimate tensile strength. After this point, the concrete cracks and the shear stiffness is reduced. Furthermore, once cracking has developed, the opposite faces of opened crack will be interlocked when they are subjected to parallel differential movement. This interlock depends on the texture of the cracked surface as well as the constrained (clamping) force that can keep the cracked surfaces from moving apart. The rough surfaces of the cracked concrete can partially transmit shear across the crack due to aggregate interlock and dowel action of the crossing reinforcement as the reinforcing bars provide some constraint somewhere along the cracked surface.

The ability of concrete to transfer shear forces across the crack interface is accounted for by introducing a reduction factor (β) to the shear modulus of originally uncracked concrete. Two coefficients of shear strength reduction were used, thus (β_o) is introduced for the case of opened crack and (β_c) is introduced for the case of closed crack. The values of (β_o) and (β_c) are always in the range of ($1 > \beta_c > \beta_o > 0$) [81].

In present study, (β_o) is assumed to be in the range (0. 4-0.7) and (β_c) is assumed to be (0.3-0.7). These values were selected to avoid convergence problems during iteration.

5.9 Crushing Modeling

When the material at an integration point fails in uniaxial, biaxial or triaxial compression, the material is assumed to crush at that point. Based on the concrete brick element adopted in ANSYS, crushing is defined as the complete deterioration of the structural integrity of the materials (material spalling). Under conditions when crushing has occurred, material strength is

assumed to have degraded to an extent such that the contribution to the stiffness of an element at the integration point can be ignored [81].

The uniaxial crushing stress in this model (ANSYS model) was based on the uniaxial unconfined compressive strength ($f`_c$). It was entered as the value of compressive (108 Mpa) .

5.10 Modeling of Reinforcing Bars

Since the reinforcing bars are normally long and relatively slender, they can generally be assumed to be capable of transmitting axial forces only. For the finite element models, the constant values for the modules of elasticity and yield stress of CFRP is used.

The real constants for the model studied in this research are shown in Table (5-2).

Table (5-2): Real Constants representation for materials used in present study

Real constant set	**Element type**	**Constants**			
1 (concrete)	**Solid 65**		Real constant for Rebar1	Real constant for Rebar2	Real constant for Rebar3
		Material number	3	3	3
		Volume Ratio (Steel Fiber)	0.00667	0.00667	0.00667
2 (main reinforcement CFRP)	**Link 180**	Cross-sectional area(mm^2)	28.26		
		Initial strain(mm/mm)	0		

Real Constant Set 1 is used for the Solid65 element. It requires real constants for rebars assuming a smeared model for steel fibers reinforcement

layers embedded in solid 65 elements. Values can be entered for Material Number, Volume Ratio, and Orientation Angles. The material number refers to the type of material for the reinforcement. The volume ratio refers to the ratio of steel to concrete in the element. The orientation angles refer to the orientation of the reinforcement in the smeared model. ANSYS allows the user to enter three rebar materials in the concrete. Each material corresponds to x, y, and z directions in the element [Fig.(5-1)]. The reinforcement has uniaxial stiffness and the directional orientation is defined by the user. In the present study the beam is modeled using discrete reinforcement. Therefore, a value of zero was entered for all real constants which turned the smeared reinforcement capability of the (Solid 65) element off, except in case of representation of steel fiber as a smeared layer. In this work Material Number, was entered 3 (which refers steel fiber material number), and Volume Ratio as it is assumed (its value and orientation). The summation of the distribution ratios in x, y and z direction is equal to the main volume fraction of steel fiber in the matrix V_f =2% .

Real constant sets 2 is defined for the Link 180 element. Values for cross-sectional area and initial strain were entered. Cross-sectional areas in set 2 refer to the main reinforcing bars section area. A value of zero was entered for the initial strain because there is no initial stress in the reinforcement.

Chapter six

MODELING AND ANALYSIS METHODOLOGY AND DISCUSSION OF RESULTS

6.1 General

To study more thoroughly the structural behavior of RPC specimens slab reinforced by CFRP bars, a nonlinear finite element analysis has been carried out to analyze some experimentally tested specimens. The analysis was performed by using the finite element models presented in chapter five in the finite element package ANSYS Ver.11.

Verification is done in this chapter, in order to check the interest and accuracy of the model of finite element. The exactness of the finite element models was determined by ensuring that the types of failure are correct, the ultimate load is reasonably prophesy the experimental results, and the maximum deflection is nigh to the experimental behavior.

The case study which the column dimensions are variable were analyzed. Load - Deflection curves, shape of failure and the ultimate load, compared with experimental results are discussed.

6.2 Modeling of Specimen

For the tested specimens and the modeling of specimen the actual dimensions are shown in Fig.(6-1). By taking the whole specimen's geometry and loading, the entire model specimen was used for finite element analysis, using the benefit of high performance processor of PC.

The origin of coordinates coincides with the left down corner of the specimen.

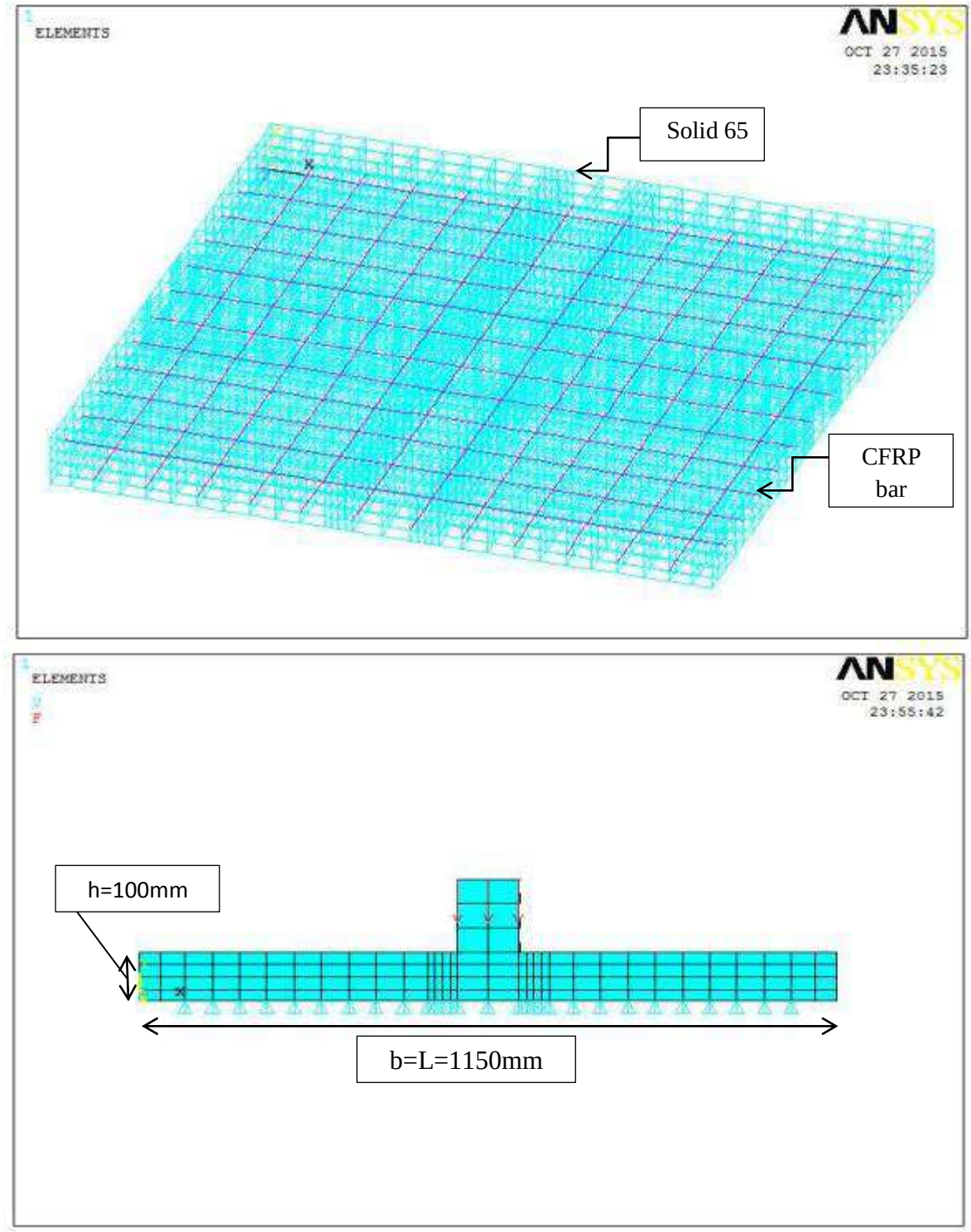

Figure(6-1): Modeling presented specimens by ANSYS V.11.

The bond strength between the concrete and CFRP bars must be considered. However, perfect bond between concrete and CFRP bars is assumed, in this study.

6.3 Meshing

For the Solid 65 element to obtain good results, "the use of a square mesh is recommended. Therefore, the mesh was set up such that square elements with varied dimension were created [71]. The same square element was used to mesh the column up to the slab, Fig.(6-1). This properly set the length of elements in the plates to be consistent with the elements and nodes in the concrete portions of the model. The overall mesh of the concrete is shown in Fig.(6-1). The necessary element divisions are noted. The meshing of the reinforcement is a special case compared to the volumes. No mesh of the reinforcement is needed because individual elements were created in the modeling through the nodes created by the mesh of the concrete volume. However, the necessary mesh attributes need to be set before each section of the reinforcement is created.

6.4 Loads and Boundary Conditions

Displacement boundary conditions are needed to constrain the model to get a unique solution. To ensure that the model acts the same way as the experimental slab boundary conditions need to be applied at points of the column. The boundary conditions for the analyzed specimens are shown in Fig.(6-2). The supports were modeled in such a way that pin supports were created. A single line of nodes on the slab for the four direction were given constraint in the, UY direction for the pin support. By doing this, the slab will be allowed to rotate in X and Z directions". The load, P, applied at the column. The applied load, P, was distributed at the nodes of column.

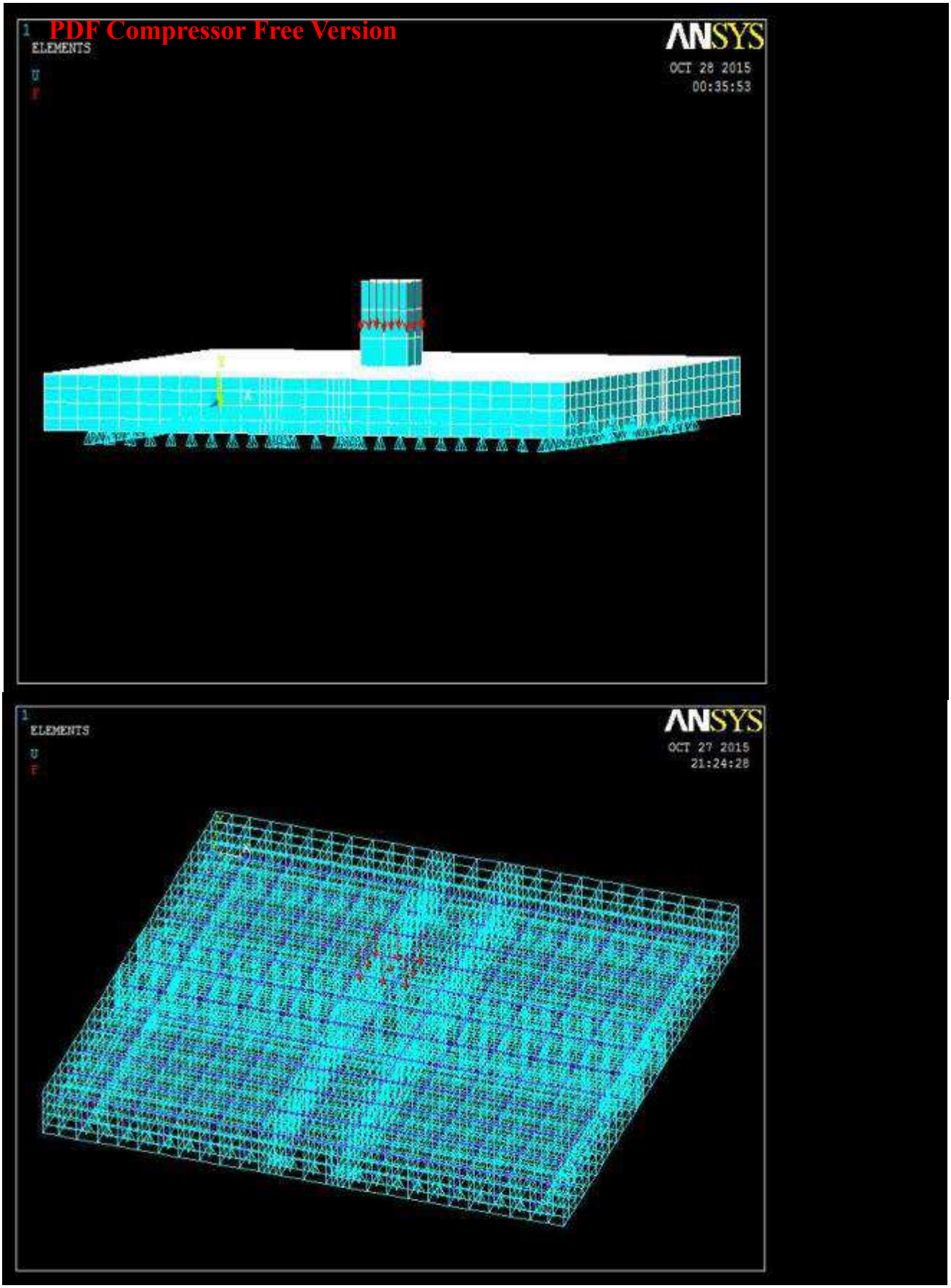

Figure (6-2): Loading and boundary conditions of modeled specimens

6.5 Results and Discussion

Four RPC slabs reinforced by CFRP bars were analyzed by ANSYS program and compared with experimental result. The case study that the properties and the dimension of slabs are constant while the column dimensions are varied were analyzed. After check the numerical and experimental results were adequate, another case was studded, four slabs with the same dimensions and the same dimension of column but with varied compressive strength of slabs were tested shown in table (6-3). Load deflection curves were obtained by ANSYS program. Number of iterations was made by changing Number of sub-steps and maximum number of sub-steps of solution phase to obtain full load deflection curve. It was noted that solutions diverge at load less than failure load if no adequate number of sub-steps were chosen. However, figures show that the finite element solutions substantially converge to experimental results, and the computed loads at the failure stage for all slabs are the same or very nigh to the corresponding experimental failure loads. These load deflection curves were shown in Fig. (6-3) to (6-6), and load deflection curves for anew numerical case study shown in fig. (6-11) to (6-14). The numerical load deflection curves show very good agreement with experimental results especially for approximately the initial 75% of the failure load. It is very important to mention that the warp points appeared at some numerical curves gained from ANSYS are attributed to making the restart solution at the load steps in the level of that points after stopping the program due to the non-convergence case.

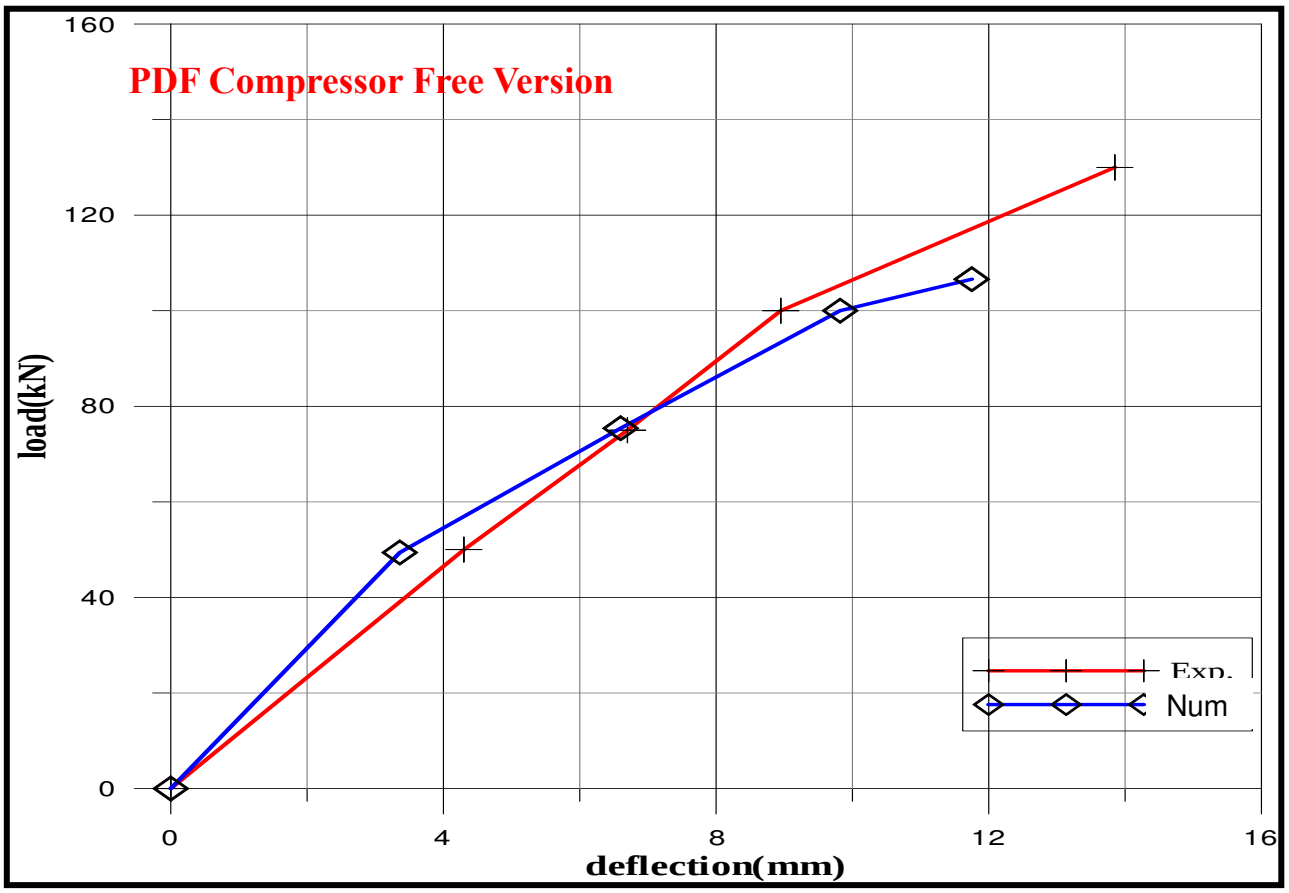

Fig. (6-3):Experimental and numerical Load Deflection Curves at center of **S - 9**

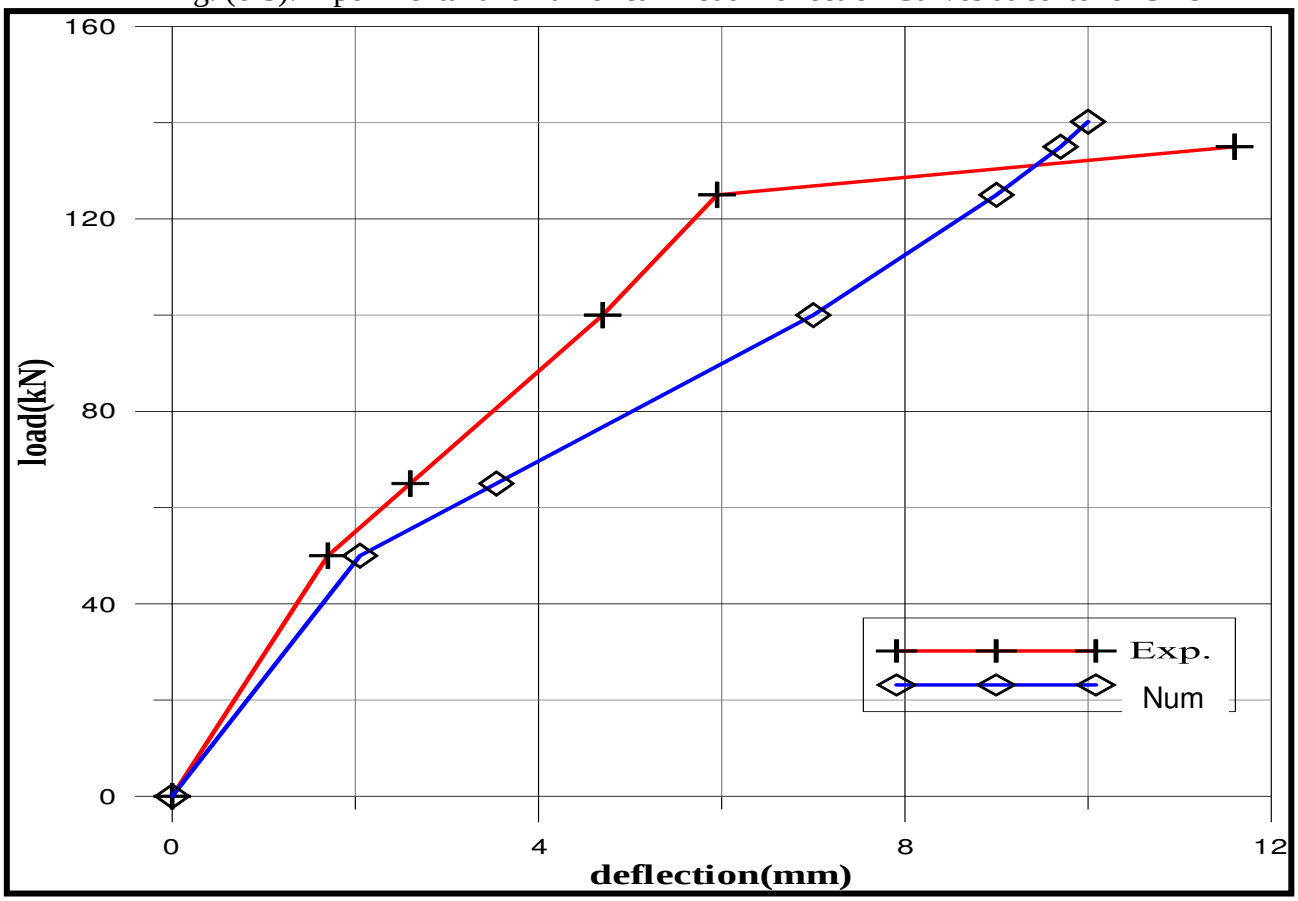

Fig. (6-4):Experimental and numerical Load Deflection Curves at center of **S - 10**

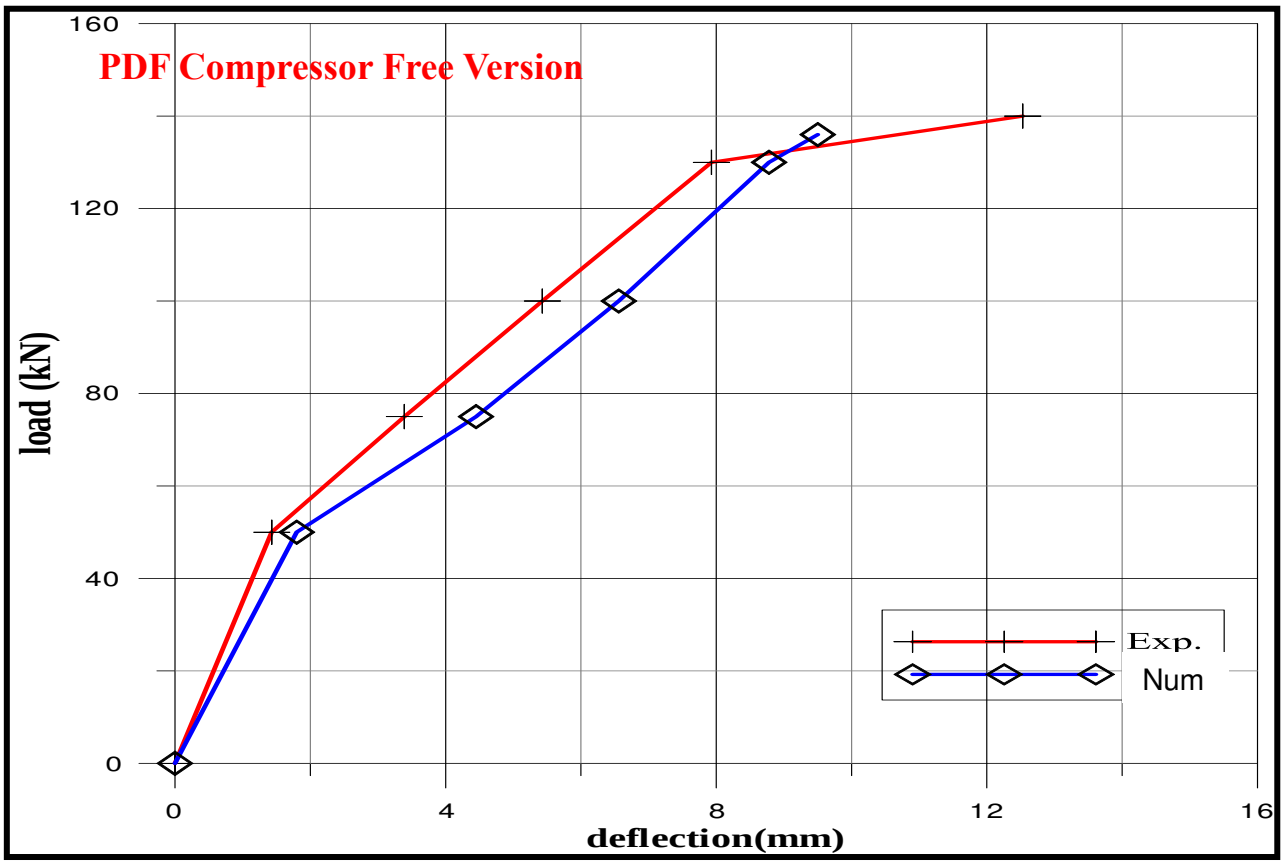

Fig. (6-5):Experimental and numerical Load Deflection Curves at center of **S - 11**

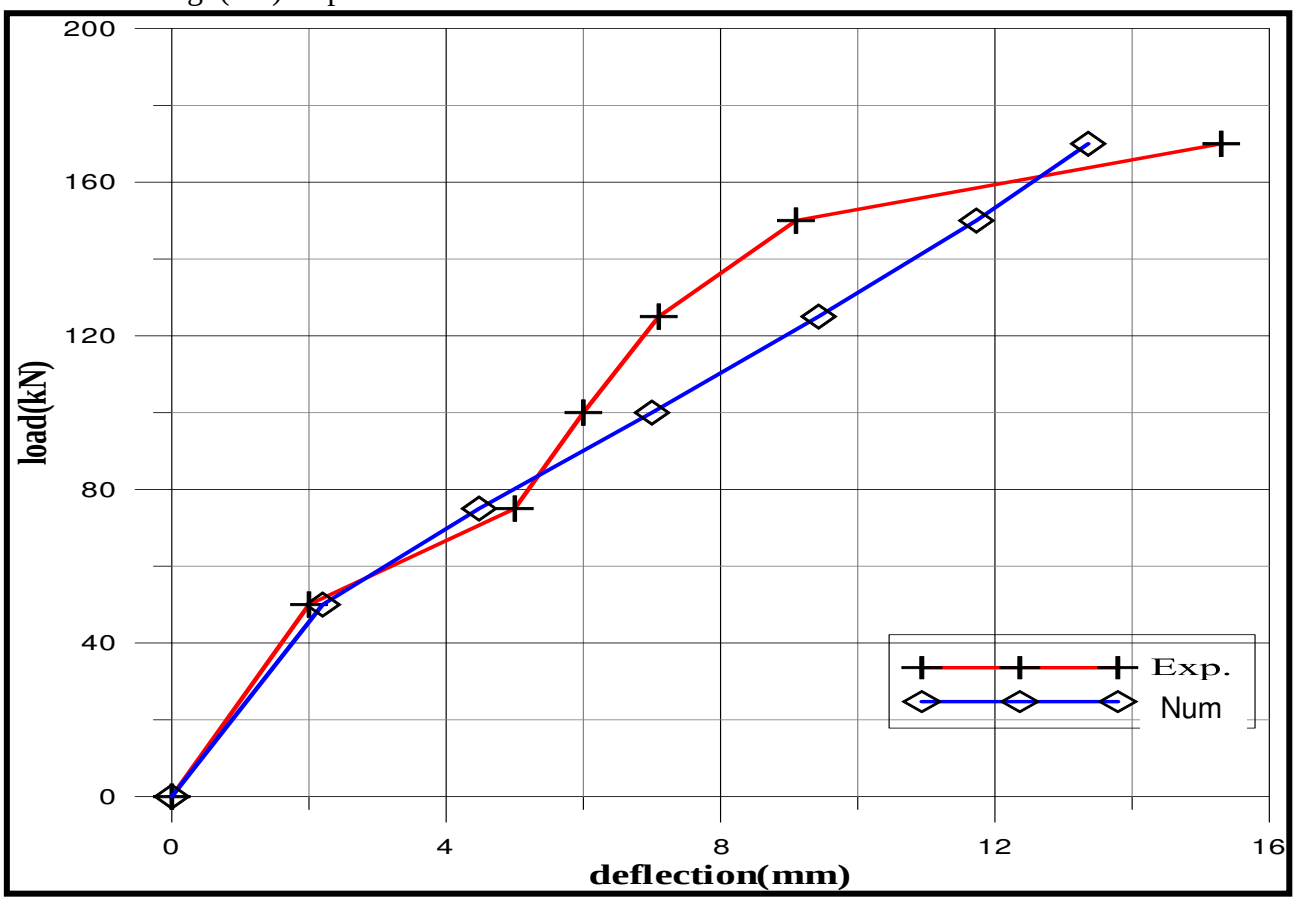

Fig. (6-6):Experimental and numerical Load Deflection Curves at center of **S - 12**

6.6 Cracking Patterns

The cracking behavior of same slab specimen is discussed in the following to compare between ANSYS-11 and experimental results:

Fig.(6-7) to (6-10) show the crack patterns for tested slabs. The circular crack was appearing clearly in slabs, and they have the same shape of cracks if compared with the specimen tested experimentally.

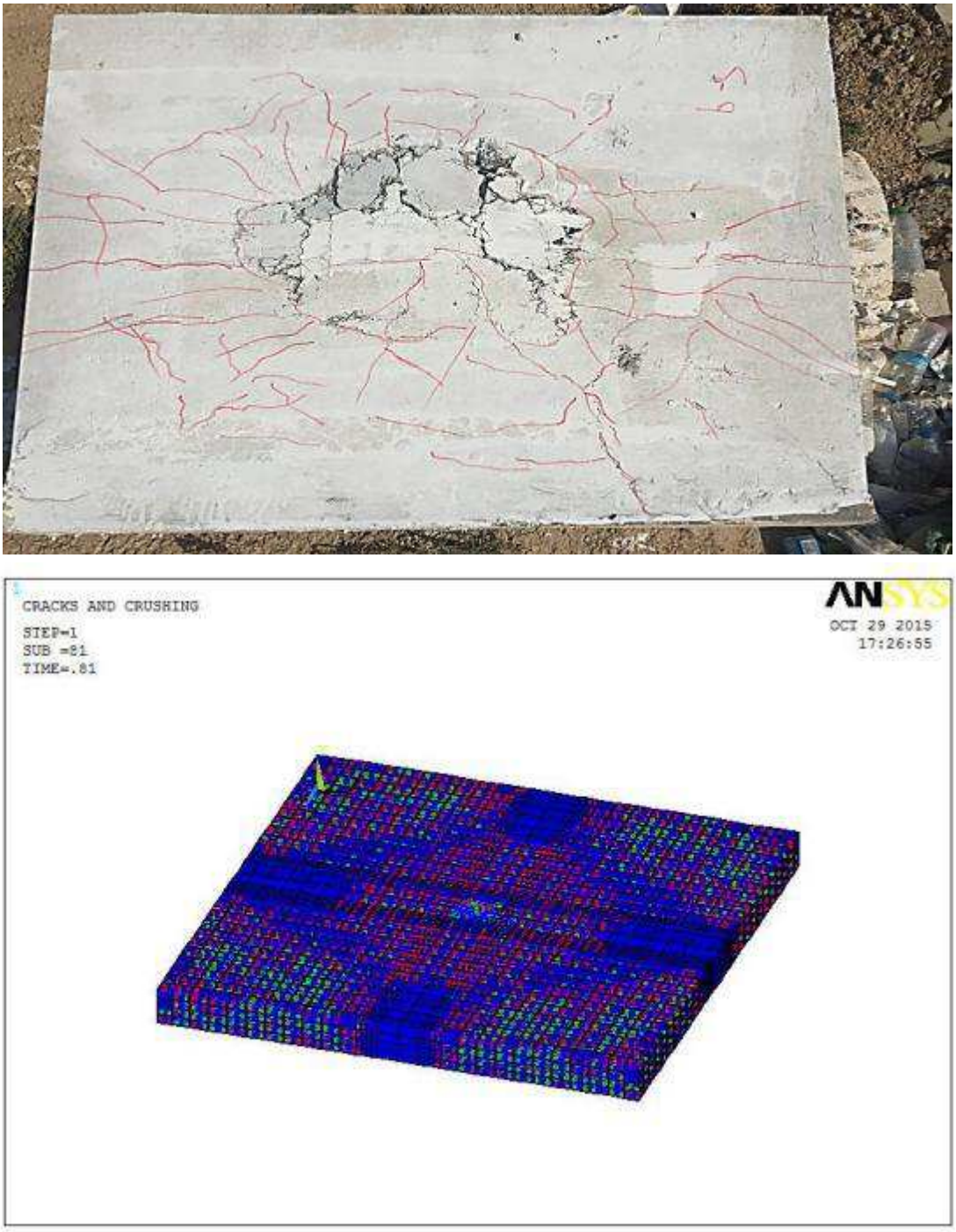

Fig. (6-7): Experimental and numerical crack pattern of **S - 9**

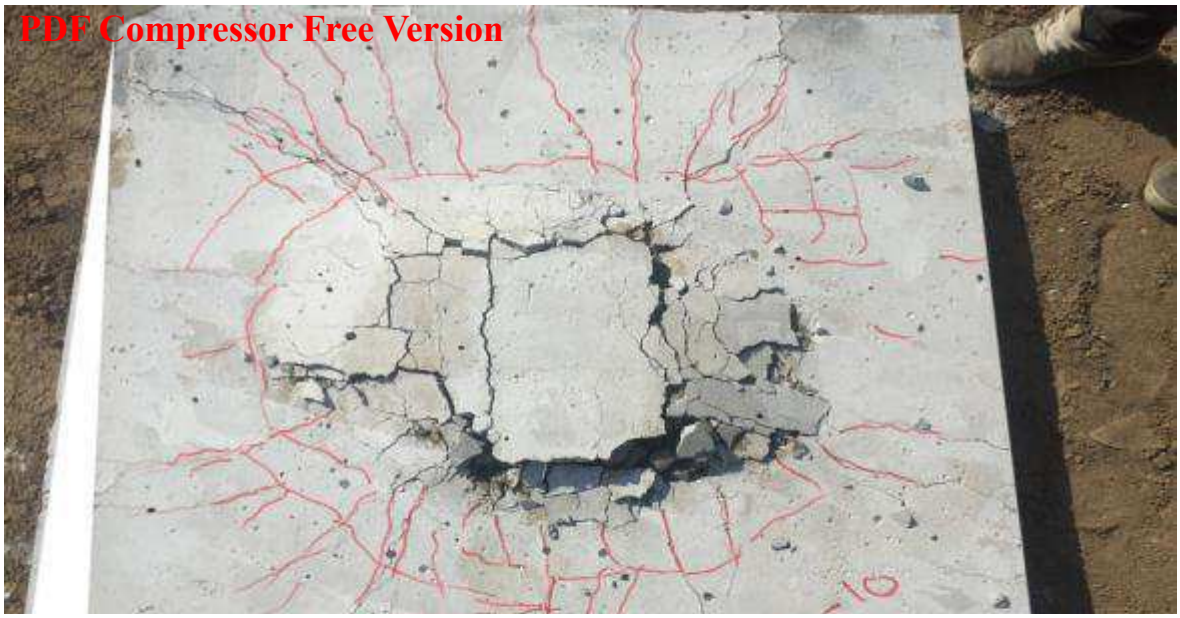

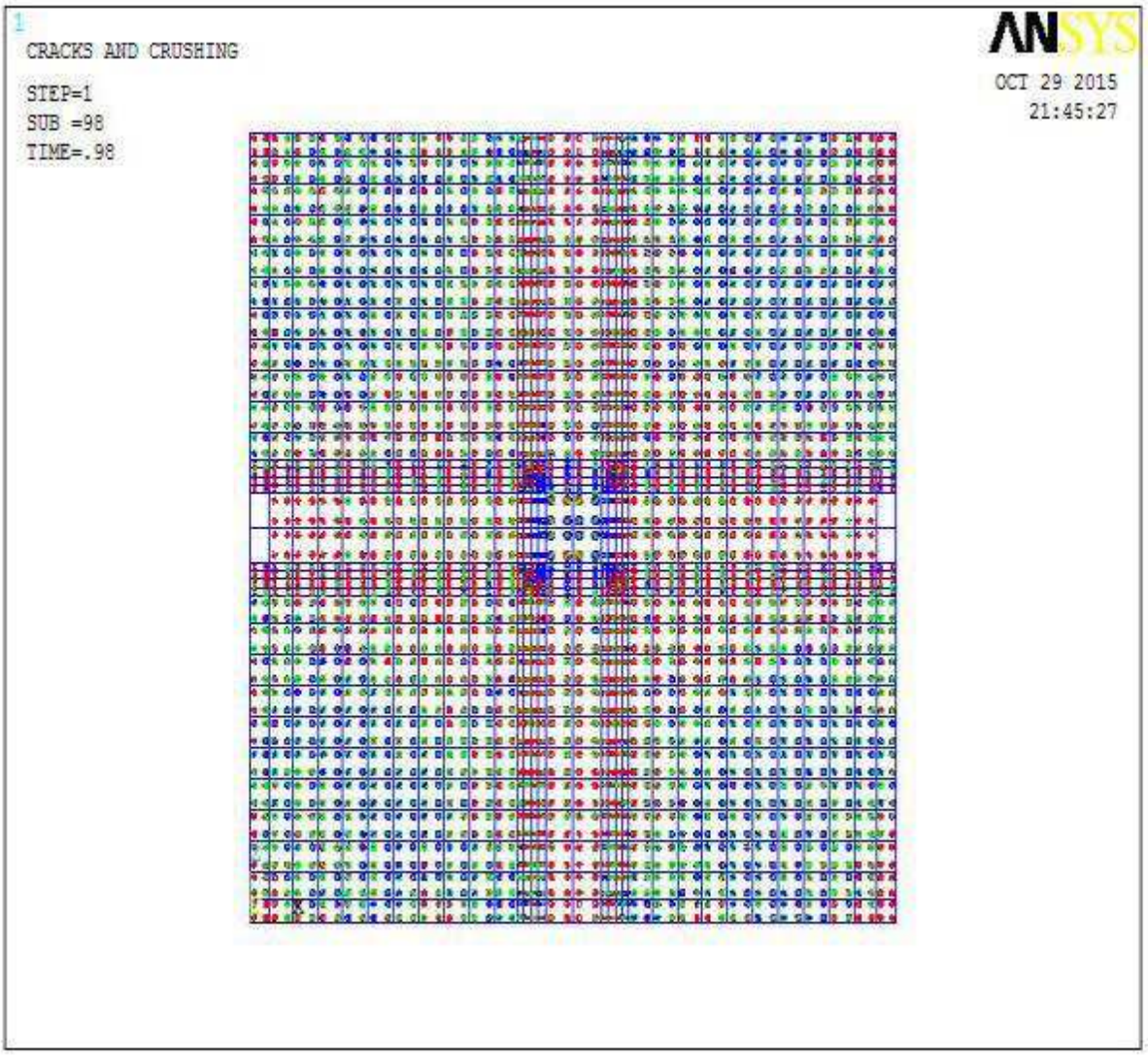

Fig. (6-8): Experimental and numerical crack pattern of **S - 10**

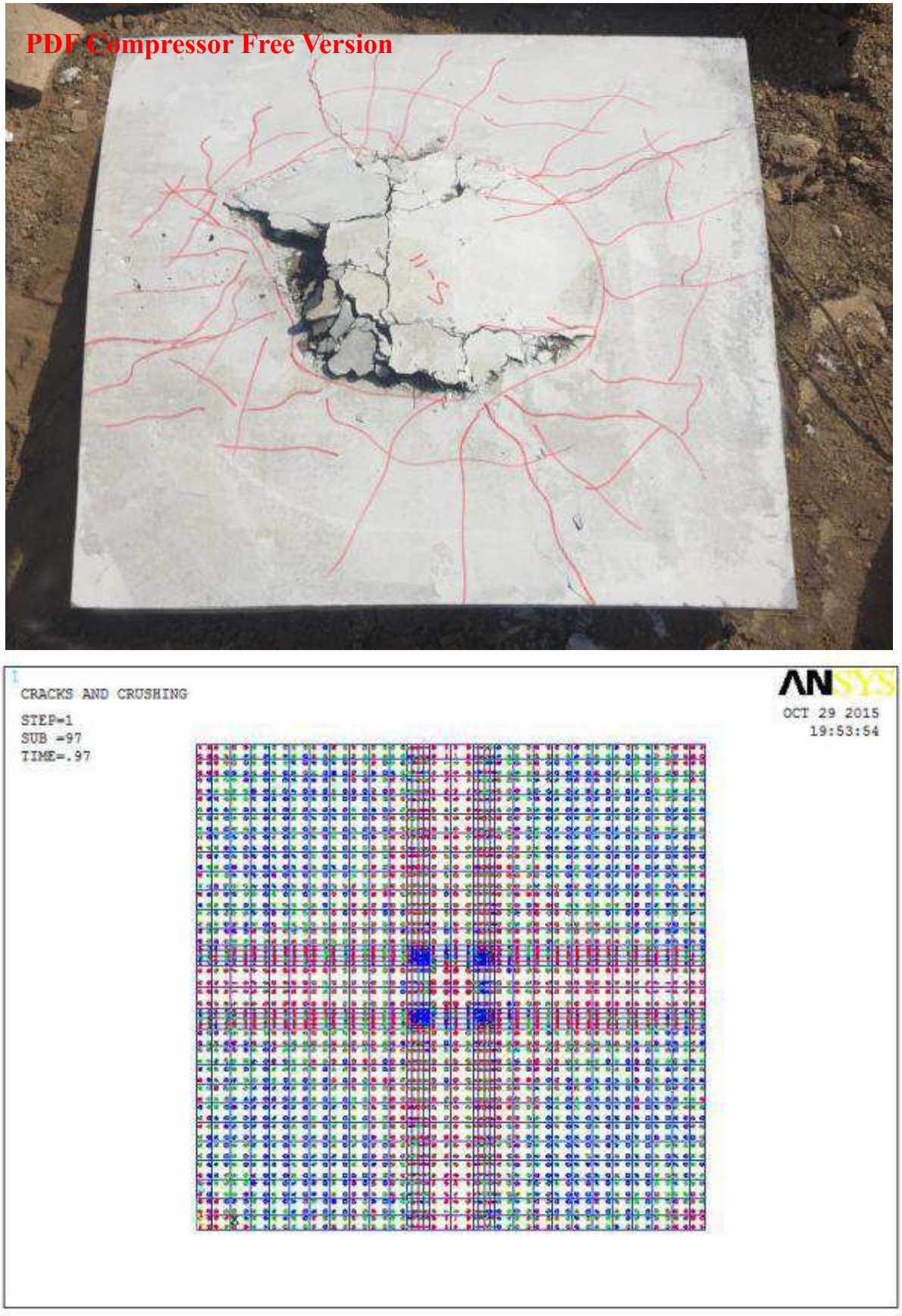

Fig. (6-9): Experimental and numerical crack pattern of **S - 11**

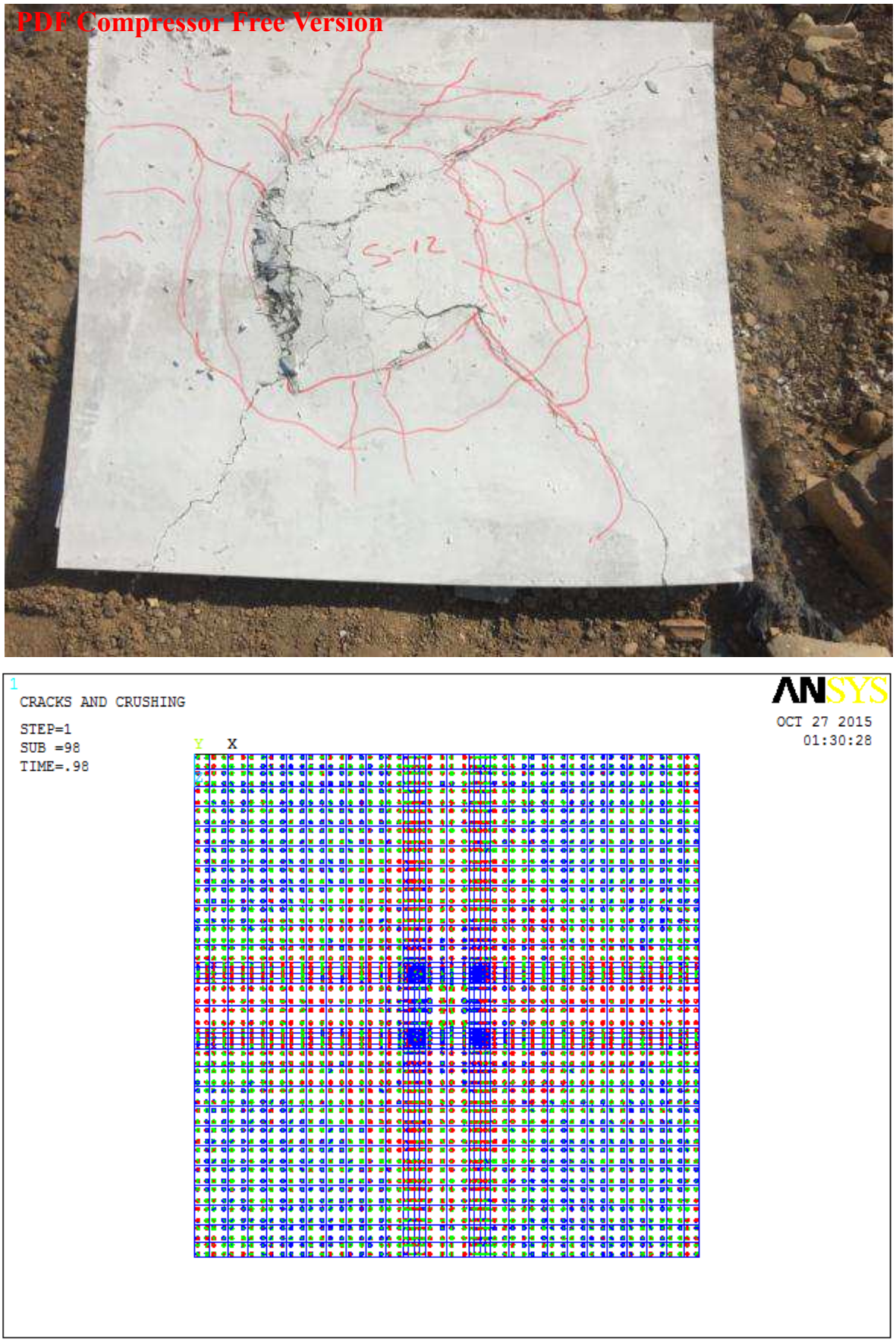

Fig. (6-10): Experimental and numerical crack pattern of **S - 12**

6.7 Ultimate Loads

Table (6-1),shows that the ratio of numerical to experimental of the ultimate load for two way slabs is ranged from (0.82 to 1.04),the difference in this ratio may be attributed to the difficulty of choosing the open shears and closed shear coefficients.

Table (6-1): Experimental and numerical ultimate load

Slab	Experimental Ultimate Load (kN)	Numerical Ultimate Load (kN)	$\frac{p_{Num.}}{p_{Exp.}}$
S – 9	130	106.6	0.82
S – 10	135	140.4	1.04
S – 11	140	135.8	0.97
S – 12	170	166.6	0.98

6.8 Maximum Deflection Comparison

Table (6-2) shows the comparison between the maximum midspan (center of slabs) deflection of the experimental specimens, $(\Delta y)_{EXP.}$, and the maximum midspan deflection from the finite element models (numerical), $(\Delta y)_{NUM.}$ at the failure load. The resulting mean was 1.1782 for the ratio of $(\Delta y)_{EXP.} / (\Delta y)_{NUM.}$. As shown in Table (6-1), the maximum midspan deflection obtained from the numerical model agree well with the corresponding values of the experimental specimens in the tested slabs. Results from the tests and ANSYS were compared at the same load level of the tested specimens were failed; While the numerical specimens may have failed with a different load value. The difference in failure load for some cases may be due to the reasons mentioned earlier.

Table (6-2): Comparison Between Experimental and numerical (ANSYS V.11) Maximum Midspan Deflection

SLAB	Maximum midspan deflection (mm)		$\frac{(\Delta y)_{EXP.}}{(\Delta y)_{NUM.}}$
	$(\Delta y)_{EXP.}$	$(\Delta y)_{NUM.}$	
S – 9	13.85	11.75	1. 178
S – 10	11.6	10.1	1.14
S – 11	12.53	10	1.25
S - 12	15.3	13.355	1.145
			$\bar{m}$ 1.1782

6.9 Numerical Parametric Study

The good agreement obtained of the numerical analysis with comparison to some experimental one encouraged the use of the numerical analysis to study more varying parameters, further what were performed experimentally in this work. A numerical parametric study was carried out on the RPC slab to investigate the effect of some important parameters on the punching shear capacity of these slabs. The parameters included in this study was the compressive strength of slabs,(125, 150, 175, 200) MPa. Table (6-3) shown the details of tested slabs and the ultimate numerical load. Fig.(6-11) to (6-14) shown the load deflection curves for the four slabs which they tested numerically by ANSYS V. 11. Its noted that by increasing the compressive strength of RPC slab about 20% the ultimate punching shear capacity increased about 18.5% by average. Fig. (6-15) to (6-18) shown the cracks pattern for slabs, it's clear from the shape of cracks that's all the tested slab failed in punching shear and approximately in the same parameter as of the specimens which they tested experimentally.

Table (6-3): Details and ultimate load for numerical case study

Slab	CFRP ratio %	Thickness of slab h (mm)	Column C(mm)	No. of bars in each direction	Numerical Ultimate load P_u(KN)	Compressive strength $F'c$ (MPa)
S – A	0.3686	100	100	12	149	125
S – B	0.3686	100	100	12	175.77	150
S – C	0.3686	100	100	12	207.36	175
S – D	0.3686	100	100	12	238.14	200

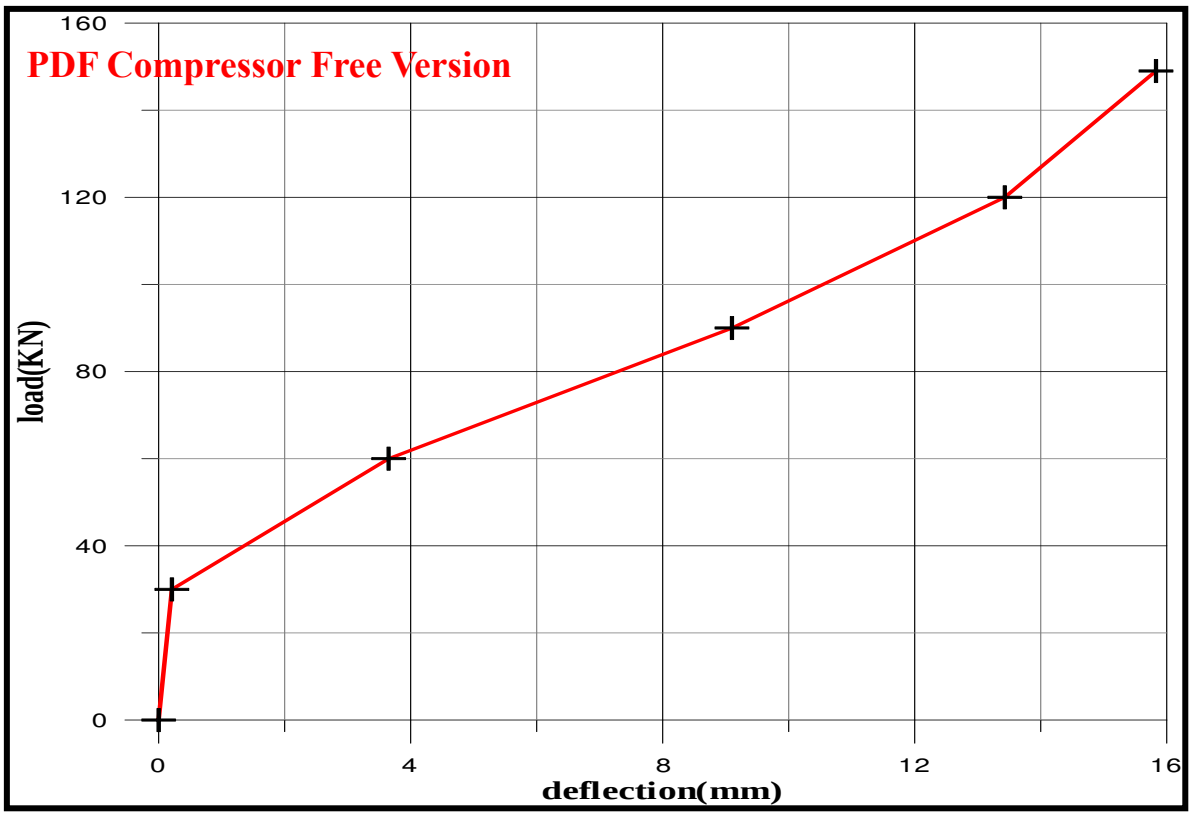

Fig.(6-11): load deflection curve for **S - A**

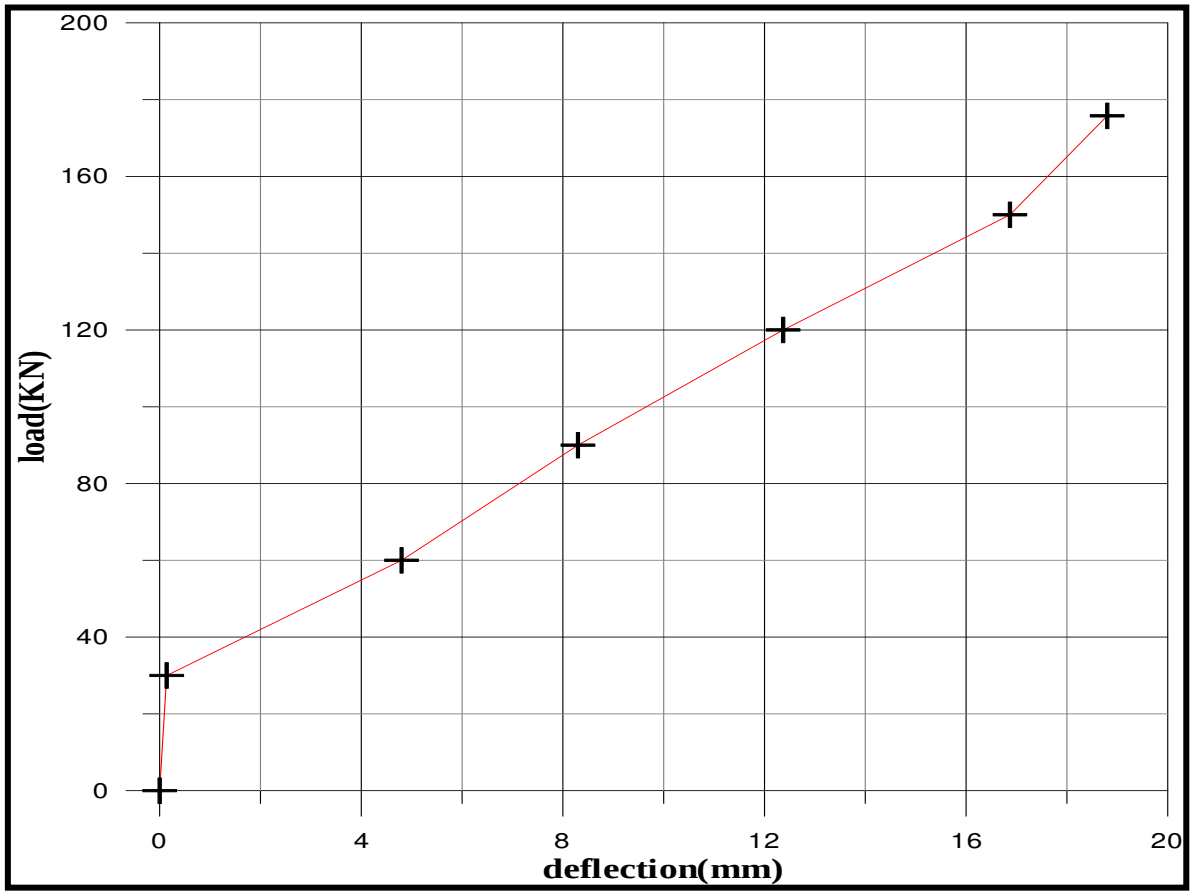

Fig.(6-12): load deflection curve for **S - B**

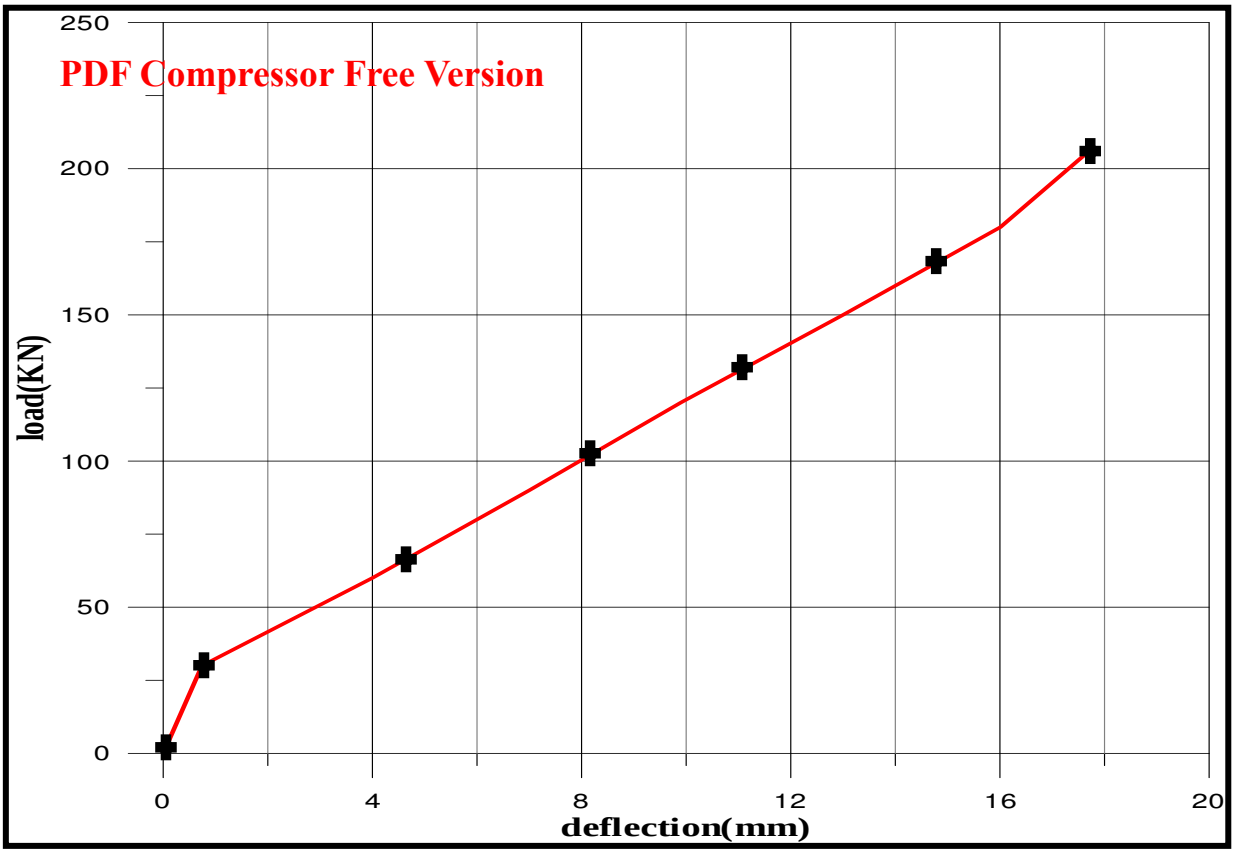

Fig.(6-13): load deflection curve for **S - C**

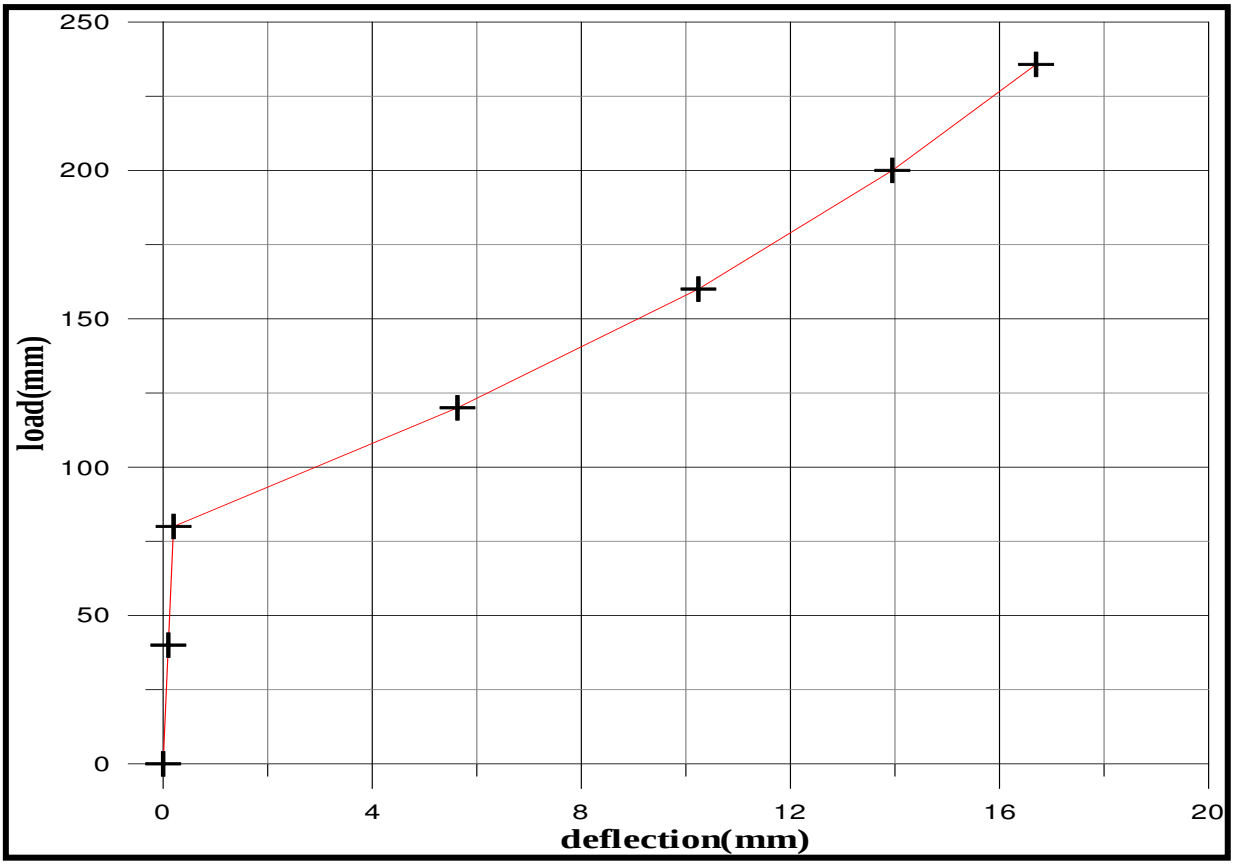

Fig.(6-14): load deflection curve for **S - D**

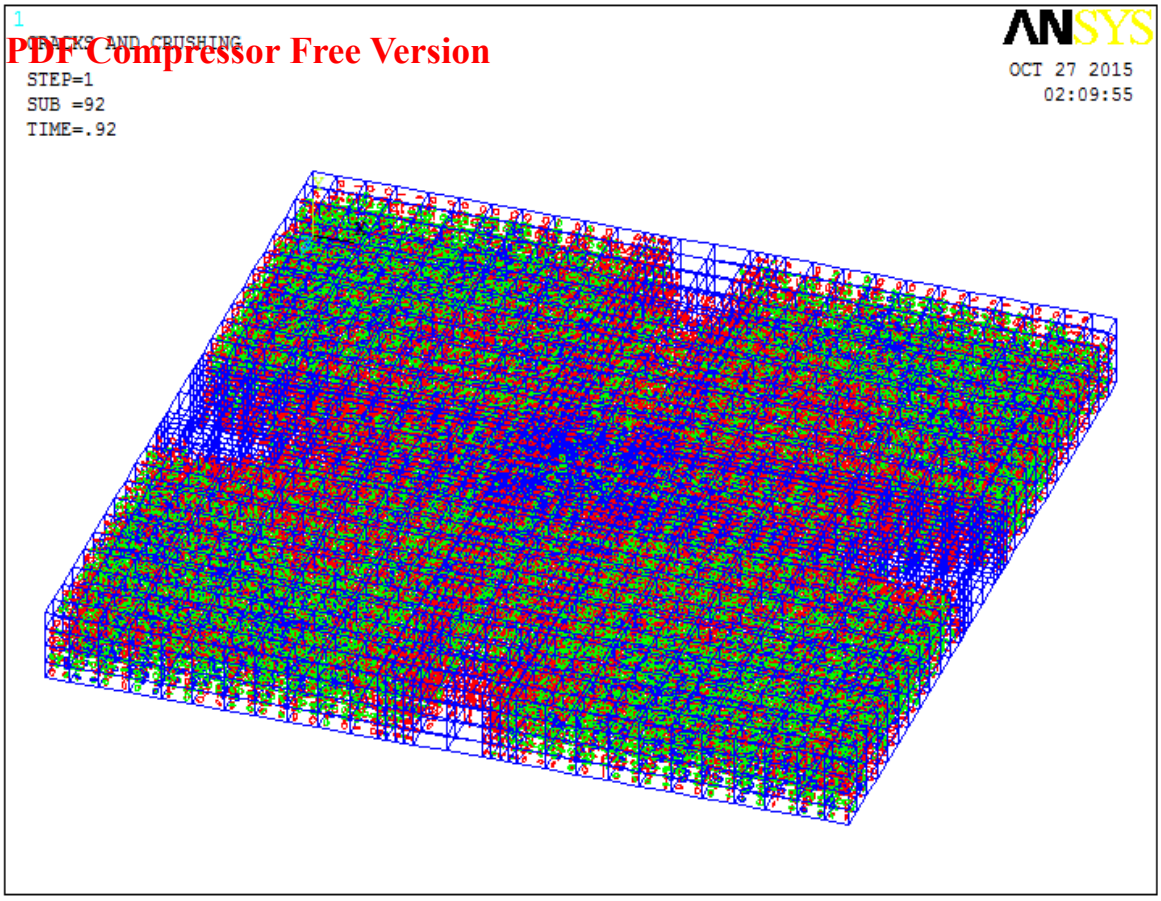

Fig.(6-15): crack pattern of S - A

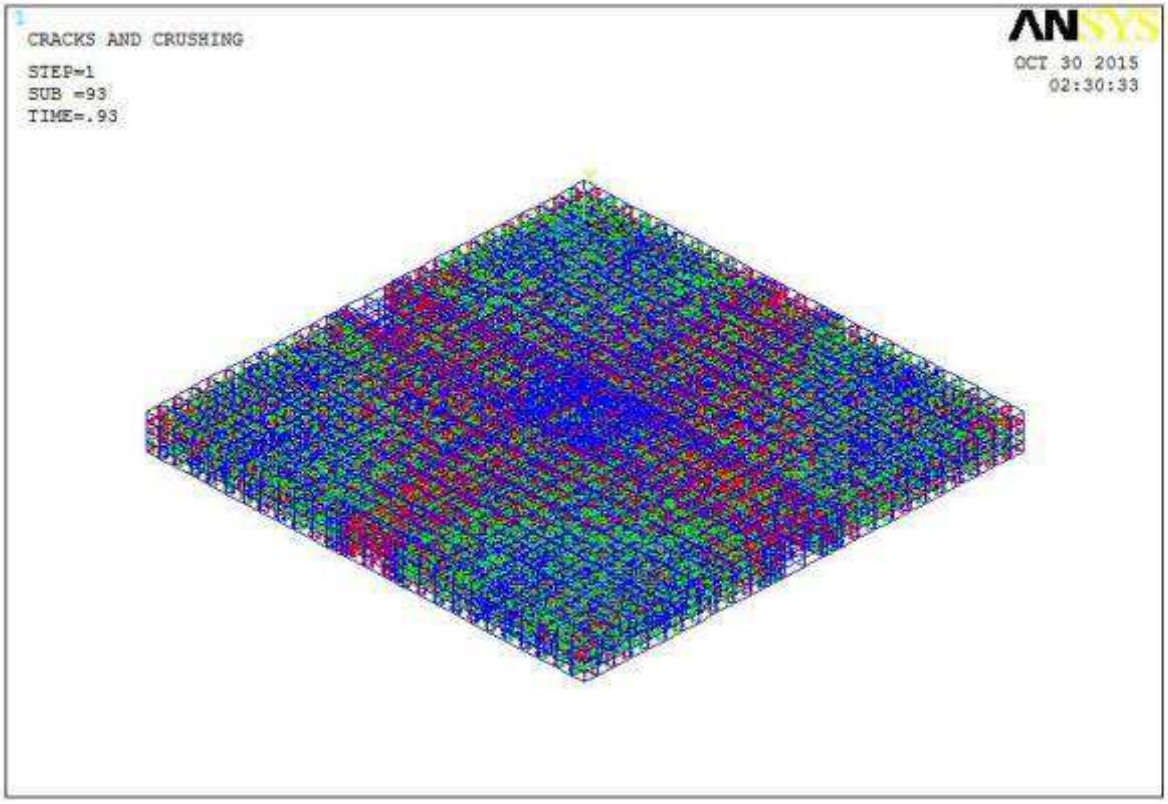

Fig.(6-16): crack pattern of S - B

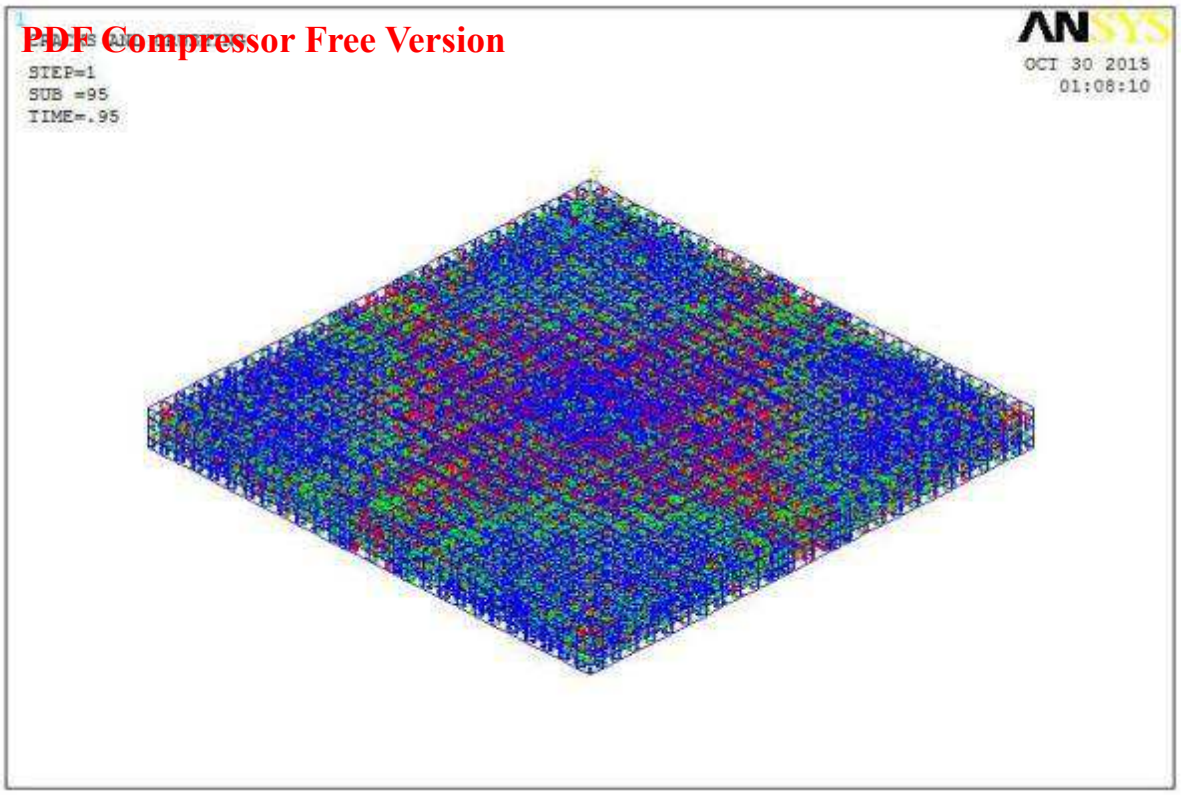

Fig.(6-17): crack pattern of S - C

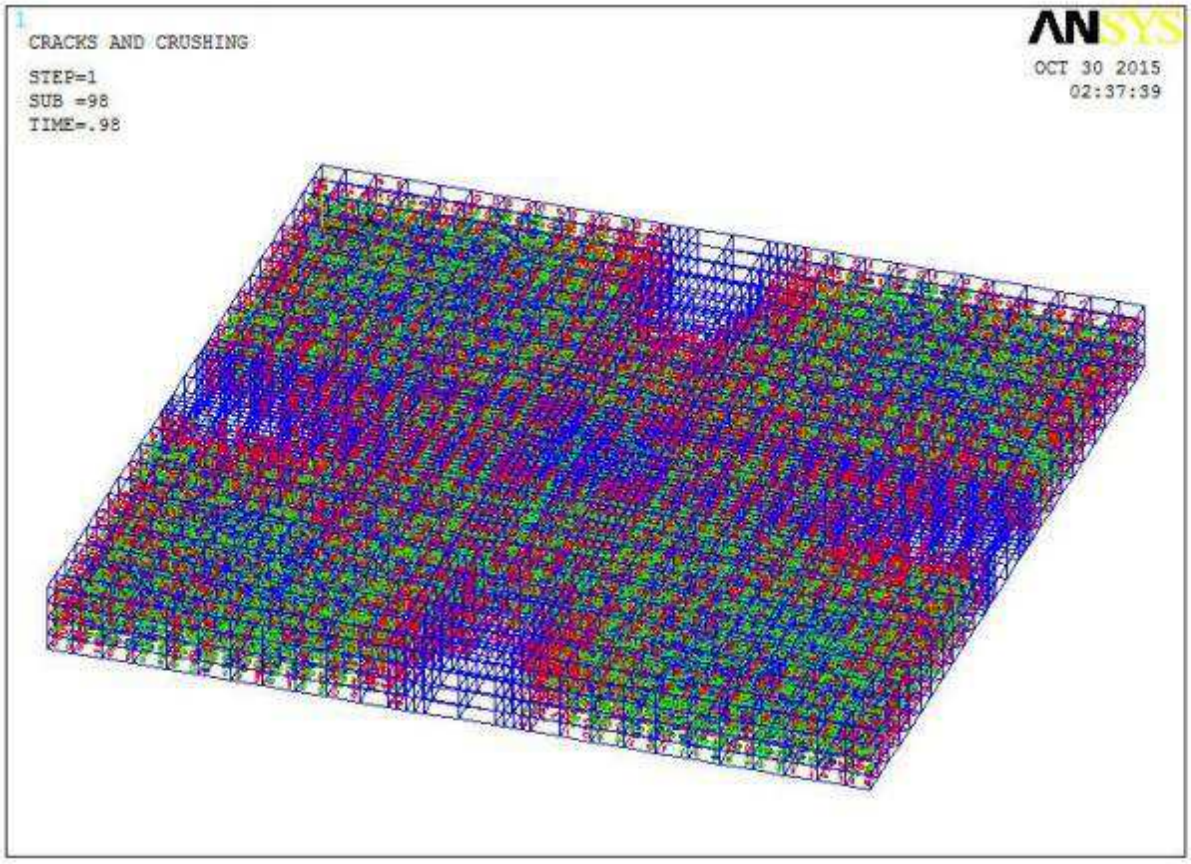

Fig.(6-18): crack pattern of S - D

Chapter Seven

Conclusions And Recommendations

7.1 General

Three sections of conclusions are presented in this chapter, the first includes material and mixing properties, the second concentrates on the experimental work and observations and the third deals with the theoretical analysis of RPC slab reinforced with CFRP bars. Also, recommendations for future research work are given.

7.2 Conclusions

Based on the experimental evidences and numerical analysis carried out in this research work, the following conclusions are obtained.

7.2.1 Experimental Work and Observations

1. Experimental tests of the fourteen RPC slabs reinforced by CFRP bars indicate that the first visible crack is observed at the tension face of the tested slab at load level equal to (21.54 – 55.56)% of ultimate load. Cracking on the tensile face began near the center and radiated towards the edges (semi- random phenomena).
2. By increasing the flexural reinforcement ratio (ρ_f) 8%, the ultimate punching shear strength by mean 18%.
3. The ultimate punching shear capacity is increased approximately 70% by increasing the thickness of RPC slab by 55%
4. by increasing the area of column about 20% the ultimate punching shear capacity of RPC slab is increased by average 14.5% because of the influence of distribution of stress in the slab – column connection area.
5. Treated the smooth CFRP bars by making steel codes coated by epoxy resin is very useful to prevent splitting of bar.

6. The proposed equation for punching shear strength of reactive powder concrete slab reinforced with CFRP bars according to experimental results with critical parameter 4(c+d/2) is

$$v_c = \frac{1}{K} \sqrt{f'c} \times 4\left(c + \frac{d}{2}\right) d \left(\frac{\rho_f}{100}\right)$$

7.2.2 Theoretical Analysis

1. Steel fibers in RPC slab can be represented as smeared layers within solid65 elements depending on the volume fraction in the mortar. Representation of steel fibers in more than one direction leads to crack pattern distribution in a larger area. Solutions obtained by representation of steel fibers as smeared layers were in better agreement of enhancement of mechanical properties of concrete by adding steel fibers.
2. Comparisons with experimental data indicate that the proposed expression properly estimates the punching shear strength of RPC slab reinforced by CFRP bars. This expression can be applied for a wide range of specimens with varying compressive strength (f'_c), reinforcement ratio and thickness of slab.
3. For tested slabs and at different load level, the crack pattern and shape failure from ANSYS Model and the actual slab agree well.
4. By increasing the compressive strength of RPC slab about 20% the ultimate punching shear capacity increased about 18.5% by average.
5. Appropriate ratio of numerical failure load to experimental failure load is ranging from 0.82 to 1.04

7.3 Recommendations

Further research can be suggested for better understanding the use of CFRP as a main reinforcement of RPC slab. Based on the present investigations and conclusions, the following suggestions can be put for future research:

1. Investigation of the behavior of RPC slab with CFRP as a main reinforcement under impact and seismic loads.
2. Study the structural behavior of lightweight concrete slabs reinforced by CFRP bars.
3. More applications with reinforced RPC slabs with CFRP bars having different sizes of opening or different values of compressive strength of concrete (f'_c).
4. Study the effect of the increasing of volume fraction of steel fiber on punching shear capacity of RPC slab without reinforcement.

References

REFERENCES

[1] Kyoros ,P. and Christiana, I., "***Verification of a Novel Punching Shear Reinforcement System for Flat Slabs***" International Workshop on Punching Shear Capacity on RC slabs-Stockholm,2000,PP.135.

[2] Allen, A.H., "***Reinforced Concrete Design to Cp110-simply explained***" 1976, (Cited by reference 102).

[3] Qi Zhang " ***The Punching strength of high strength flat slabs: experimental study***" M.Sc. Thesis, Memorial, University of Newfoundland, December, 2003. pp. 10-33.

[4] Hughes, B.P.,"***Limit State Theory for Reinforced Concrete Design***", 1976, (Cited by reference 102).

[5] Moe, J., "***Shearing Strength of Reinforced Concrete Slabs and Footing under Concentrated Load***" Portland Cement Association Research and Development Laboratories Bulletin D47, April 1961, PP. 130.

[6] Yitizaki, D., "***Punching Strength of Reinforced Concrete Slabs***", ACI Journal, May 1966, PP. 527-540.

[7] Tuan, N., "***Punching Shear Resistance of High Strength Concrete Slabs***", Electronic Journal of Structural Engineering, Department of Civil and Environmental Engineering ,The University of Melbourne, 2001, pp 52-59, www.Unimelb.Unilb.edu.au

[8] Morris, W.S., ***"Ultimate Strength of Reinforced Concrete Flat Plates"***, Journal of St. Div. Proc. ASCE, Vol. 90 ST4, August 1964.(Cited by Reference 14).

[9] Sujata Kulkarni (2002), ***"Calibration of Flexural Design of Concrete Members Reinforced with FRP Bars"***, M.Sc. Thesis, Louisiana State University..

[10] CNR-DT 203/2006,*" Guide for the Design and Construction of Concrete Structures Reinforced with Fiber-Reinforced Polymer Bars"*, Advisory Committee on Technical Recommendations for Construction, ROME.

[11] Wikipedia, the free encyclopedia (2012), http://en.wikipedia.org/wiki/ Carbon fiber reinforced polymer.

[12] Aurelio, M., "***Punching Shear Strength of Reinforced Concrete Slabs***" *ACI Structural Journal*, V. 105, No. 4, July-August 2008

[13] Osman,M., Marzouk,H. and Helmy,S."***Behavior of High-Strength Lightweight Concrete Slabs under Punching Loads***" ACI structural journals,V.97,No.3. May-June, 2000, PP.492.

[14] Al-Ani, M., A., R**.,** "***Influence of Steel Fibers on Punching Shear Resistance of Reinforced Concrete Slabs***" M.Sc. Thesis, Baghdad University, January 1985.

[15] Nilson, A. H. , Darwin, D. and Dolan, C. W. , "***Design of Concrete Structure***" McGraw-Hill Book Company 2004, Thirteen Edition, PP. 412.

[16] Johansen, K.W. ,Brudlinieteorier, Gjellerup, Copenhagen, 1943,189pp.(English Translation: ***Yield- Line Theory , Cement and Concrete Association, London, 1962***)

[17] Harris, D.K., "***Characterization of Punching Shear Capacity of Thin UHPC Plates*** ", M.Sc. Thesis, Virginia Polytechnic Institute and State University, December 2004.

[18] (Report Morsch, E., 1906) by Kevin Ka Loo Li, " ***Influence of Size on Punching Shear Strength of Concrete Slabs*** ", M.Sc. Thesis, McGill University, Department of Civil Engineering, Montreal.. Canada, March 2000.

[19] Talbot, A.N."***Reinforced Concrete Wall Footings and Column Footings***" Bulletin, No.67. University of Illinois, Engineering Experiment Station.. Urbana Ill. March, 1913. PP.114.

[20] Harris, D.K., "***Characterization of Punching Shear Capacity of Thin UHPC Plates*** ", M.Sc. Thesis, Virginia Polytechnic Institute and State University, December 2004.

[21] Graf, O. "***Tests of Reinforced Concrete Slabs Under Concentrated Loads Applied Near One Support***", (in German), Berlin, 1933, No. 73, PP.28.(Cited by Reference 21).

[22] Richart, F.E."***Reinforced Concrete Wall and Column Footings***", ACI Journal "October and November" , 1948, V. 45" No. 2 and 3" . (Cited by Reference 21).

[23] Elstner, R.C. and Hognestad, E., "***Shearing Strength of Reinforced Concrete Slabs***" ACI Journal, Vol. 53, No. 1, July 1956, PP. 29-58.

[24] Whitney. C.S. "***Ultimate Shear Strength of Reinforced Concrete Flat Slabs. Footings. Beams. and Frame Members Without Shear Reinforcement*** ", ACI Journal ,1957, V. 54. No. 4. October, pp. 265-298.

[25] Long, A.E. and Bond, D.,"***Punching Failure of Reinforced Concrete Slabs***" Proceeding, Institution of civil Engineers (London), Vol. 37, May 1967, pp. 109, 135.

[26] Herzog, M. "***A New Evaluation of Earlier punching Shear Test*** ", Concrete Journal, Vol. 4, No. 12, London, England, Dec. 1970, pp. 448-450.

[27] Long, A.E., " ***A Tow Phase Approach to the Prediction of the Punching Shear of Slabs***" ACI Journal, Proceedings, Vol.72, No.2, February, 1975, pp. 37-45.

[28] Hawkins, N.M and Mitchell, D. "***Progressive Collapse of Flat Plate Structures***", ACI Journal, Proceedings V.76, No. 7, July 1979, PP. 775-808.

[29] Regan, P. E., "***Behavior of Reinforced Concrete Flat Slabs***", CIRIA Report No. 89, Construction Industry Research and Information Association, London, 1981.

[30] Rankin, G. I.B.and Long,A.G.,"***Predicting the Punching Strength of Conventional Slab-Column Specimens***", Proc. Instr. Civ. Engrs., 82 , April 1987, PP. 327-346.

[31] Gardner, N. J., "***Relationship of the Punching Shear Capacity of Reinforced Concrete Slabs with Concrete Strength***", ACI Journal, February 1990, PP. 66-710.

[32] Alexander, S. D. B.and Simmonds S.H." ***Tests of Column-Flat Plate Connection"***, ACI Journal. September-October 1992, V.89,No. 5, PP.495-502.

[33] British Standard Institution (BS 8110), (1997) "***Code of Practice for Design and Construction***" British Standard Institution Part 1, London.Alexander,

[34] ACI Code (318-02) "***Building Code Requirement for Reinforced Concrete***" American Concrete Institute, Detroit, Mich., 2002.

[35] ACI Code (440.1R-06) "***Building Code Requirement for Reinforced Concrete***" American Concrete Institute, Detroit, Mich., 2004.

[36] S. El-Gamal ***"A New Punching Shear Equation for Two-Way Concrete Slabs Reinforced with FRP Bars"*** ACI journal. SP-230—50

[37] Ahmed, F.R. " ***Punching Shear Strength and Time – Dependent Deflection of High – Strength Reinforced Concrete Panels***" Ph.D. Thesis, University of Baghdad, November 2005. pp. 133.

[38] Muhammed N.J., "***Esidual Punching Strength of NSC,HSC and LWC Panels Exposed to High Temperatures***", M.Sc. Thesis, Univ. of Al-Mustansiriya, Coll. of Eng., May 2007.

[39] AS3600-2001"***Concrete Structure***", Australian Standards, 2001, PP. 175.

[40] Comite Euro-International Du Beton "***CEP-FIP Model Code 1990***" PP. 175.

[41] Regan, P. E. and Braesturp, M. W., "***Punching Shear in Reinforced Concrete***" Bulletin d, Information, CEP, Lusanne, 1985, PP. 232.

[42] Marzouk, H. and Hussein, A., "***Experimental Investigation on the Behavior of High-Strength Concrete Slabs*****,** ACI Structural Journal, Vol.88, No. 6, 1991, PP. 701-713.

[43] Hawkins, N. M, and Yamazaki, J. **"*Moment Transfer from Concrete Slabs to Columns*"**, ACI Structural Journal. Vol. 86, No. 6, 1989. pp. 705-716.

[44] Dao, V.N.T., Dux, P.F., O'Moore,L.**"*Punching Shear of Slab-Column Connection in Flat Plate Construction*"**, International Congress, "Global Construction: Ultimate Concrete Opportunities", University of Dundee, 2005, PP.183-190.

[45] Bazant, Z. P. and Cao, Z.," ***Size Effect in Punching Shear Failure of Slabs*"**. ACI Structural Journal. Vol. 84, No. 1, 1987. pp. 44-52.

[46] Ozbolt, J. and Vocke, H., ***"Size Effect in Punching of Flat Slabs"***, Jahresbericht/ Activities, 1998/99, PP.103-111.

[47] Kuang, J. S. and Morley, C. T., "***Punching Shear Behavior of Restrained Reinforced Concrete Slabs***", ACI Structural Journal, Vol. 89, No. 1,1992, PP.(13-19).

[48] El-Salakawy, E. F., Polak, M. A., and Soliman, M. H., "***Reinforced Concrete Slab-Column Edge Connections with Openings***" ACI Structural Journal, Vol. 96, No. 1, 1999, PP. 79-87.

[49] Lovrovich, J. S. and Mclean, D.I., "***Punching Shear Behavior of Slabs with Varying Span-Depth Ratio***", ACI Structural Journal, Vol. 87, No. 5, 1990, PP. 507-511.

[50] Ghali, A., and Hammil, N., "***Effectiveness of Shear Reinforcement in Slabs*** " Concrete International, Vol. 14, No. 1, 1992, PP. 60-66.

[51] Broms, C. E., "***Elimination of Flat Plate Punching Failure Mode*"** ACI Structural Journal, Vol. 97, No. 1, 2000, PP. 94-101.

[52] Ebead, U. and Marzouk, H., "***Strengthening of Two-Way Slabs Using Steel Plates*"** ACI Structural Journal, Vol. 99, No. 1, 2002, PP. 23-31.

[53] Ali H. N. " ***Investigation the Punching Shear Behavior of Reinforced Concrete Slab-Column Connection Using Carbon Fiber Reinforced Polymers*** " Al-Qadisiya Journal For Engineering Sciences, Vol. 8……No. 1 ….2015

[54] Nielsen, M.P., ***"Punching Shear Resistance According to the CEB Model Code"***, ACI-CEB-PCI-FIP Symposium, ACI Publication SP59-11, 1967, PP.193-210.

[55] Wey, E.H. and Durrani, A.J., ***"Seismic Response of Interior Slab-Column Connections With Shear Capitals"***, ACI Structural Journal, Vol.89, No.6, November-December, 1992, PP.682-691.

[56] Patrick, P. and Caroline, M., ***"Distribution of Moment in Reinforced Concrete Slabs With Continuous Drop Panels"***, Canadian Journal of Civil Engineering, 29, 2002, PP.119-124.

[57] Kaiss F. Sarsam, and Hassan F. Hassan" ***Punching Shear Failure Characteristics Of Flat Slabs Using Reactive And Modified Powder Concrete With Steel Fibers"*** Journal of Engineering and Development, Vol. 17, No.5, November 2013 , ISSN 1813- 7822

[58] Ali H. A., Shatha S. Kareem, Ban Sahib A., " ***Experimental Study For Punching Shear Behavior In RC Flat Plate With Hybrid High Strength Concrete"*** Journal of Engineering and Development, Vol. 17, No.3, August 2013, ISSN 1813- 7822

[59] Ghali, A., Sargious, M.A. and Huizer, A., ***"Vertical Prestressing of Flat Plate Around Columns"***, Shear in Reinforced Concrete, SP42-38, American Concrete Institute, 1974, PP.905-911

[60] Richard P, and Cheyrezy M, ***"Composition of Reactive Powder Concrete"***, Cement and Concrete Research, Vol. 25, No.7, (1995), pp. 1501 – 1511.

[61] Wasan I. Khalil ***"Some Properties of Modified Reactive Powder Concrete***" Journal of Engineering and Development, Vol. 16, No.4, Dec. 2012 ISSN 1813- 7822

[62] Nuha H. Al-Jubory *"**Mechanical Properties of Reactive Powder Concrete (RPC) with Mineral Admixture**"* Al-Rafidain Engineering Vol.28 No. 5 October 2013

[63] Bickley J. A, and Mitchell D, ***"A State-Of-The-Art Review Of High Performance Concrete Structures Built In Canada: 1990-2000"***, (2001), pp. 96 – 102.

[64] Aitcin P.C, ***"Cements of yesterday and today Concrete of tomorrow"***, Cement and Concrete Research, Vol. 30, (2000), pp 1349 - 1359.

[65] **المواصفات العراقية / رقم 5، "السمنت العراقي "، الجهاز المركزي للتقييس والسيطرة النوعية، بغداد 1984، ص 8.**

[66] **المواصفات العراقية / رقم45، "ركام المصادر الطبيعية المستعملة في الخرسانة والبناء"، الجهاز المركزي للتقييس والسيطرة النوعية، بغداد 1984.**

[67] American Specification for Testing and Materials" **Standard Specification for Steel Fibers for Fiber-Reinforced Concrete**" A820

[68] American Specification for Testing and Materials "**Standard Specification for Chemical Admixtures for Concrete**" C – 494.

[69] ***"Silica Fume User's Manual"***.

[70] American Specification for Testing and Materials ***"Standard Specification for Silica Fume Used in Cementitious Mixtures"*** C- 1240

[71] ANSYS V.11 help topics.

[72] Schnobrich, W. C., ***"Behavior of Reinforced Concrete Structures Predicted by the Finite Element Method"***, Computers & Structures Journal, Vol. (7), Pergaman Press, UK, 1977, PP. 365-376.

[73] Wolanski, B. S., ***"Flexural Behavior of Reinforced and Pre-Stressed Beams Using Finite Element Analysis"***, M.Sc. Thesis, Marquette University, May 2001, (73) p., (web Site).

[74] Yousifani, A. H., ***"Investigation of the Behavior of Reinforced Concrete Beams with Construction Joints Using Nonlinear Three-Dimensional Finite Elements"***, M.Sc. Thesis, University of Technology, April 2004, 123 pp.

[75] Owen, D. R., and Hinton, E., ***"Finite Elements in Plasticity: Theory and Practice"***, 1st Edition, Redwood Burn Limited, U.K 1980, 594 pp.

[76] Ghailan, D. B., ***"Shear-Transfer Strength and Behavior of Reactive Powder Concrete"***, PhD. Thesis, Al-Mustansiriya University, February 2013, Baghdad, 221 pp.

[77] Mahdi, B.S., ***"Properties of Self Compacted Reactive Powder Concrete Exposed to Saline Solution"***, PhD. Thesis, Building and Construction Engineering Department, University of Technology, Baghdad, 2009, 223 pp.

[78] Viet, T.V., Holger, S., Gert, S. and Deltef, S., ***"Bearing Capacity of Stub Columns Made of NSC, HSC and UHPC Confined By***

a Steel Tube", Proceedings of the International Symposium on Ultra High Performance Concrete, University of Kassel, Kassel, Germany, September 13-15, 2004, PP. 338-350.

[79] Yan, P.Y. and Feng, J.W., ***"Mechanical Behavior of UHPC and UHPC Filled Steel Tubular S UHPC Filled Steel Tubular Stub Columns"***, Proceedings of Second International Symposium on Ultra High Performance Concrete, University of Kassel, Kassel, Germany, March 5-7, 2008, PP. 355-364.

[80] ***"ANSYS Manual"***, Version (13.0), USA, 2012.

[81] Nie, J., Fan, J., and Cai, C. S., ***"Stiffness and Deflection of Steel-Concrete Composite Beams under Negative Bending"***, ASCE-Journal of Structural Engineering, Vol. (130), No. (11), November 2004, PP. 1824-1851.

Appendixes

Appendix

Slab Designation	***Thickness of slab h (mm)***	***Column* side length C(mm)**	***CFRP ratio*** %	$k = (10.4)\times4(c+d/2)\times d\times\rho_f\% /$ Pu
S – 1	100	150	0.3686	1.66
S – 2	100	150	0.3993	1.53
S – 3	100	150	0.43	1.6
S – 4	100	150	0.4607	1.66
S – 5	80	150	0.368	1.8
S – 6	100	150	0.4607	1.66
S – 7	120	150	0.44217	2.3
S – 8	150	150	0.453	1.75
S – 9	100	100	0.3686	1.32
S – 10	100	125	0.3686	1.5
S – 11	100	150	0.3686	1.66
S – 12	100	175	0.3686	1.55
S – 13	100	150	0.276	1.34
S – 14	100	150	0.3378	1.64
S – 15	100	150	0.3378	1.42
S – 16	100	150	0.3378	1.334
				$K_{ave.} = 1.6$

MEYCO® MS610

meyco ms610 UGC 0897

Densified microsilica

Master Builders Technologies

Description of product

MEYCO® MS610 is a concrete additive for top quality concretes. MEYCO® MS610 changes the porous structure of the concrete in a definitive manner and makes it denser and more resistant to any type of external influence. MEYCO MS610 must be used in combination with a plasticizer or a superplasticizer.
MEYCO® MS610 is a special high quality microsilica, approved as a concrete additive according to the ASTM standard.

Fields of application

MEYCO® MS610 is used to produce long-life, durable concretes.

- All types of wet-mix sprayed concrete applications
- Cast concrete
- Pumped concrete
- High strength concrete
- Underwater concrete
- Concrete with low cement content
- Tunnel grouting (backfilling)

Features and Benefits

- Increased strengths
- Substantially improved resistance to chemical and mechanical attack
- Prevents bleeding and segregation in fresh concrete
- Reduced dosages of activators/accelerators
- Larger layer thicknesses sprayable

Combination

The use of Pozzolith® plasticizers or Rheobuild® superplasticizers is recommended for any microsilica concrete. For frost resistant concrete, an additional air-entraining agent (Pozzolith® Micro-Air) has to be added. Combinations with Delvo®Crete Stabilizer or Delvo®Crete Activator are

Packaging

MEYCO® MS610 is supplied in 20 kg bags, big bags or in bulk.

Technical data

Form	powder
Colour	grey
Density	0.55–0.7 kg/l
Chloride content	<0.1%

Application procedure

Mixing
MEYCO® MS610 is added to the concrete during batching. Minimum mixing time is 90 seconds.

Consumption
The dosage of MEYCO® MS610 is 5–15% of the cement weight.

Storage

If stored dry and in tightly closed original bags, MEYCO® MS610 has a shelf life of at least 12 months.

Safety precautions

Avoid contact with eyes and prolonged contact with skin. If contact occurs, wash thoroughly with water and seek medical advice.
For further information refer to product Material Safety Data Sheet.

* SIA = Swiss Association of Engineers and Architects

Construction

Product Data Sheet
Edition 02, 2015
Version no. 12.2014

Sika ViscoCrete® -5930

High Performance Superplasticiser Concrete Admixture

Product Description

Sika ViscoCrete® -5930 is a third generation super plasticizer for concrete and mortar. It meets the requirements for super plasticizer according to ASTM-C- 494 Types G and F and BS EN 934 part 2: 2001.

Uses

Sika ViscoCrete® -5930 is suitable for the production of concrete.

Sika ViscoCrete® -5930 facilitates extreme water reduction, excellent flowability at the same time optimal cohesion and highest self compacting behaviour.

Sika ViscoCrete® -5930 is used for the following types of concrete:

- Precast concrete.
- Ready Mix Concretes.
- Concrete with highest water reduction (up to 30%).
- High strength concrete.
- Hot weather Concrete.
- Self compacting concretes.

High water reduction, excellent flowability, coupled with high early strengths, have a positive influence on the above mentioned applications.

Advantages

Sika ViscoCrete® -5930 acts by different mechanisms. Through surfaces adsorption and sterical separation effect on the cement particles, in parallel to the hydration process, the following properties are obtained:

- Strong self compacting behaviour. Therefore suitable for the production of self compacting concrete.
- Extremely high water reduction (resulting in high density and strengths).
- Excellent flowability (resulting in highly reduced placing - and compacting efforts)
- Increase high early strengths development.
- Improved shrinkage- and creep behaviour.
- Reduced rate of carbonation of the concrete.
- Improved Water impermeability.

Sika ViscoCrete® -5930 does not contain chloride or other, steel corrosion promoting ingredients, it may therefore be used without any restrictions for reinforced and prestressed concrete construction.

Technical Data

Basis	Aqueous solution of modified Polycarboxylate
Appearance	Turbid liquid
Density	1.095 kg/lt. (ASTM C494)
Packaging	5 Kg, 20 Kg pails 200 kg drums Bulk Tanks are available upon request.
Storage/ Shelf Life	In unopened, undamaged original container, protected from direct sunlight and frost at temperatures between + 5 °C and + 35°C. Shelf life at least 12 months from date of production.

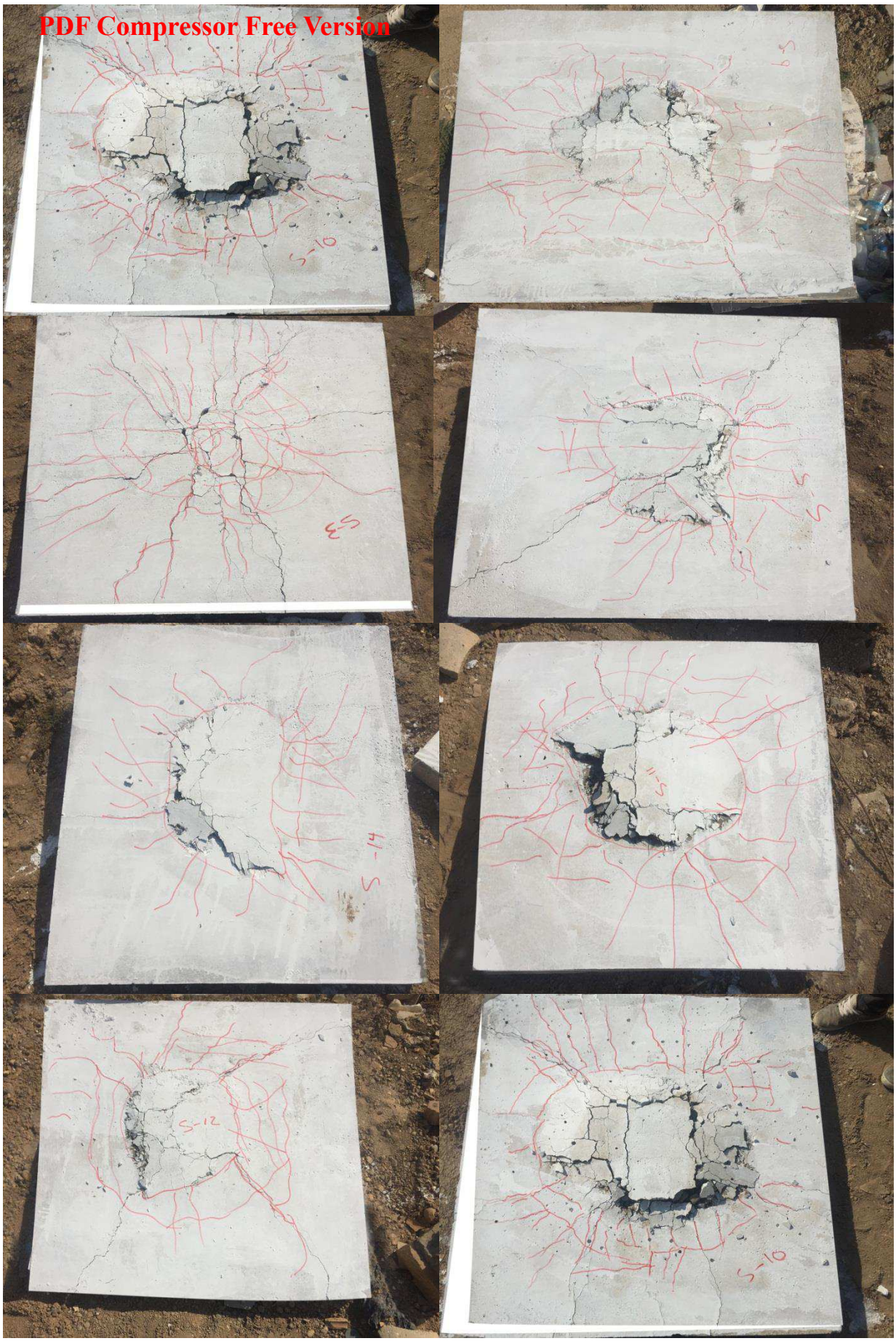

*Shapes of failure of slab specimen

\

مقاومة القص الثاقب لسقوف خرسانة المساحيق الفعاله المسلحه بواسطة قضبان الياف الكاربون البوليمريه

اطروحه مقدمة الى

قسم الهندسة المدنية في كلية الهندسة / جامعة بغداد

كجزء من متطلبات نيل درجة دكتوراه فلسفة في الهندسة المدنية –(الأنشاءات)

من قبل:

سامر محمد جاسب الموسوي

(بكالوريوس هندسة مدنية /الجامعة المستنصرية / 2006)

(ماجستير هندسة انشائية / جامعةالبصرة / 2010)

2016

الخلاصه

في هذا البحث استعمل نوع جديد من التسليح (قضبان الياف الكاربون البوليميرية) مع ماده عالية المقاومة وذات خصائص فيزيائية متقدمة (خرسانة المساحيق الفعالة). تمتاز خرسانة المساحيق الفعالة بمقاومتها العالية ونفاذيتها الواطئة حيث انها متكونة من نسبه عالية من السمنت ومسحوق السيلكا والياف الحديد.

البحث المقدم يمكن تقسيمه الى جزئين كما مبين:

الجزء الاول لدراسة مقاومة القص الثاقب لسقوف خرسانة المساحيق الفعالة والمسلحة بواسطة قضبان الياف الكاربون البوليمرية. تم اختبار اربعة عشر نموذجاً لسقف خرسانة المساحيق الفعالة والمسلحة بقضبان الياف الكاربون البوليمرية . تم دراسة تأثير نسبة حديد التسليح، سمك السقف، مساحة العمود الذي يمثل منطقة الحمل وشكل توزيع حديد التسليح في السقف على مقاومة القص الثاقب. لهذه العوامل المذكورة تم بيان قيم الهطول للسقف في كل مرحلة تحميل وكذلك قياس الانفعال في الخرسانة وزاوية الفشل اضافة الى مقاومة القص. وجد انه بزيادة نسبة التسليح 8% فان مقاومة القص الثاقب تزداد بنسبة 18 % كذلك ان زياده مساحة التحميل بمعدل 20% يؤدي الى زيادة مقاومة القص بمعدل 14.4 %.

الجزء الثاني :

تم تحليل بعض النماذج التي اختبرت عمليا بواسطة برنامج ANSYS V.11. باستخدام التحليل اللا خطي بواسطة العناصر

المحـــددة، وقـــد تـــم تمثيـــل الخرســـانة بواســـطة عنصـــر (solid-65) والليـــاف الحديـــد مثلـــت كنســـبه حجميـــه داخـــل هـــذه ال العناصـــر وتمثيـــل اليـــاف الكـــاربون البولمريـــة بعنصـــر احـــادي (link–180). وجـــد ان نســـبة حمـــل الفشـــل العملـــي الـــى نســـبة حمـــل الفشـــل المحســـوب نظريـــا تتـــراوح (0,82- 1,04) ونســـبة الهطـــول المحســـوب نظريـــا الـــى الهطـــول المحســـوب نظريـــا هـــي 1,178 . وقـــد وجـــد ان هنـــاك تقاربـــا كبيـــرا بـــين النتـــائج المختبريـــة والنتـــائج المحللـــة نظريـــاً لـــذا تـــم دراســـة زيـــادة مقاومـــة الانضغاط للخرسانة على بعض النماذج ودراسة تأثيرها نظرياً.